

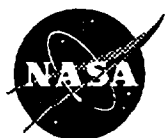
NASA Contractor Report 198496

Wave Rotor Demonstrator Engine Assessment

Philip H. Snyder
Allison Engine Company, Inc.
Indianapolis, Indiana

June 1996

Prepared for
Lewis Research Center
Under Contract NAS3-25950



National Aeronautics and
Space Administration

CONTENTS

	<u>Page</u>
1.0 SUMMARY	1
2.0 INTRODUCTION	1
2.1 Program Structure.	1
2.2 The Wave Rotor Concept.	2
3.0 RESULTS AND DISCUSSION	3
3.1 Subtask A - Viability Assessment.	3
3.2 Subtask B - Design Point Study.	4
3.3 Subtask C - Off Design Analysis.....	5
3.4 Subtask D - Preliminary Design.	6
3.4.1 Mechanical Components	6
3.4.2 Demonstrator Engine Configuration Study.	6
3.4.3 Wave Rotor Port Ducting.	6
3.4.4 Combustor Design	8
3.4.5 Alternate Port 5 Design: Reduction of Burner Inlet Temperature.	8
3.4.6 List of Engine Hardware Required For the Demonstrator Engine.	8
3.5 Subtask E - Fabrication and Test Cost And Schedule Estimate.	8
4.0 CONCLUSIONS	9
5.0 REFERENCES	9
6.0 NOMENCLATURE	10

LIST OF TABLES

Table I. Partial Allison Engine Company Model 250 Product Line Data.	11
Table II. Wave Rotor Cycle Selection Trade Study Results.	11
Table III. Wave Rotor Design Summary.	12
Table IV. Estimated Fabrication and Program Costs.	13

LIST OF FIGURES

Figure 1. Allison 250-C30 Turbo-Shaft Engine.	14
Figure 2. Schematic of Wave Rotor Configuration.	15
Figure 3. Wave Rotor With Through Flow Used As A Gas Turbine Topping Cycle.	15
Figure 4. Wave Diagram Of The Selected Four-Port Through-Flow Wave Rotor Cycle.	16
Figure 5. Wave Diagrams Of The Engine Topping Cycle, Pressure, Density, and Velocity Contours.	17
Figure 6. Pressure ratio across wave rotor as a function of temperature ratio across it from reference1.	18
Figure 7. Wave Diagram Comparison Of The Through-Flow And Reverse-Flow Cycles.	19
Figure 8. Reverse-Flow Rotor With Alternately Right And Left Porting.	20
Figure 9. Performance Of Rotor Designed For Use In Demonstrator Engine, Pressure Gain.	21
Figure 10. Performance Of Rotor Designed For Use In Demonstrator Engine, Mass Flow.	22
Figure 11. Demonstrator Engine Design Point, Through Flow Cycle Conditions.	23
Figure 12. Comparison of Off Design Performance To Baseline Engine Performance.	23
Figure 13. Placement Of Operating Points On Freewheeling Wave Rotor Performance Map.	24
Figure 14. Cycle Pressure Ratios Of The Wave Rotor Topped Demonstrator Engine.	25
Figure 15. Overall Wave Rotor Pressure Gain For The Demonstrator Engine.	26
Figure 16. Drop In Gas Temperature From Burner Exit To Turbine Inlet.	27
Figure 17. Gas Path Temperatures In The Topping Cycle.	28
Figure 18. Burner Inlet Temperature Comparison.	29
Figure 19. Comparison Of Rotational Speed Of Gasifier Spool and Wave Rotor.	30
Figure 20. Wave Rotor Design, Wave Diagram and Rotor Dimensions.	31
Figure 21. Wave Rotor Design, Rotor End View.	32
Figure 22. Wave Rotor Design, End Plate Port Location.	33
Figure 23. Allison Model 250-C30 Engine Cutaway Schematic.	34
Figure 24. Allison Model 250-C28C Engine Cutaway Schematic.	35
Figure 25. Turbine Cooling And Balance Air Schematic.	36
Figure 26. An Early Engine Layout Concept.	37
Figure 27. Proposed Demonstrator Engine Arrangement Using the Allison Model 250.	38
Figure 28. Port 1 Preliminary Design.	39

LIST OF FIGURES continued

	<u>Page</u>
Figure 29. Port 2 Unwrapped Mean Line Section.	40
Figure 30. Port 2 Side And End Views.	41
Figure 31. Port 3 Unwrapped Mean Line Section.	42
Figure 32. Port 3 Side And End Views.	43
Figure 33. Port 5 Preliminary Design.	44
Figure 34. Cutaway View Of Wave Rotor Module Preliminary Design, Side View.	45
Figure 35. Cutaway View Of Wave Rotor Module Preliminary Design, End View.	46
Figure 36. Production Model 250 R20 Combustor.	47
Figure 37. Port 5 Stagnation Temperature Distribution.	47
Figure 38. Through-Flow Split Port 5 Demonstrator Engine Design Concept.	48
Figure 39. Model 250 Wave Rotor Demonstrator Engine Program Schedule Estimate.	49
 APPENDIX A. NASA Generated Wave Rotor Design.	 50
DISTRIBUTION LIST	

1. SUMMARY

The wave rotor topped gas turbine has shown significant promise for engine performance enhancement in both previous^(1,2) and ongoing analytical studies. One of the important next steps for moving this technology toward implementation in a commercial application is the demonstration of this technology in an engine. The assembly of a successful wave rotor demonstrator gas turbine engine is a necessary and logical step in the maturing of wave rotor technology and the assessment of the benefits of its integration into propulsion and power generation devices. A successful demonstration can greatly enhance the understanding and acceptance of wave rotor technology. In this way the potential for incorporation of wave rotors into commercial gas turbine engines may be more accurately assessed.

The objectives of the program were to establish the viability of assembly of a demonstrator wave rotor engine using the Allison model 250 turboshaft engine as a basis. Design point and off design operation of the engine was assessed. A preliminary design of the engine was performed. Cost and schedule for detailed design, fabrication and test of the engine were estimated.

Results of the program show how a successful wave rotor topped demonstrator engine may be assembled using existing hardware. The engine has the potential of demonstrating excellent design and off design performance. The wave rotor demonstrator engine has a predicted 733 hp power output at design point, a 11.4% increase relative to the production version baseline engine. SFC improves substantially also with a 22% decrease relative to the baseline. The design of the burner represents the greatest challenges due to high burner inlet temperatures.

2. INTRODUCTION

This program is designed to be part of a larger study at NASA LeRC, both analytical and experimental, developing the four port wave rotor concepts in a multi-phase program. Planned additional phases target the experimental evaluation of a rotor capable of being installed in a demonstrator engine. The program reported here performs the engine analysis need to identify existing engine hardware capable of being assembled into a successful demonstrator engine program.

A potentially successful demonstrator engine program is perceived as one which can:

1. Demonstrate a meaningful degree of improved engine performance.
2. Aggressively incorporate wave rotor technology.

3. Use current materials and technology.
4. Utilize existing engine hardware to a high degree.
5. Impose minimal mechanical complexities on the engine.

The first of the requirements stated above sets the goal substantially higher than that of assembling an engine able to merely achieve self-sustaining operation or attain levels of performance routinely found in production engines. In fact, assembling an engine accomplishing these lesser goals would, in itself, be a significant step forward in wave rotor engines, but insufficient, the author believes, to show the concept's true merit. Certainly meeting requirement 1 will necessitate the use of requirement 2. The wave rotor concept must be employed to the best of its present potential in order to demonstrate full merit. With regards to number 3, the focused development of a single new technology both enhances the opportunity of a successful outcome and clarifies the source of any noted engine performance. Requirement 4 allows program funding to be dedicated to the wave rotor components and avoids development effort being diverted away from the stated goal. Finally, the opportunity for success of any program is enhanced where simplicity can be maintained. In addition, credibility as to future product potential is boosted as simplicity in implementation is demonstrated.

As a basis for the effort, the Allison 250 (military classification T63) turboshaft engine series was selected as a candidate for use in the demonstrator. A typical 250 engine is depicted in Figure 1. Basis for this selection is derived from its low cost, low corrected flow, relatively low cycle pressure ratio, engine layout, and the numerous models of varying design point air flow from which to select components. Table I summarizes relevant data for this engine line. Previous studies had identified major gains available to engines of low cycle pressure ratio with application of the wave rotor concept.

2.1 Program Structure.

The work reported here was accomplished in 6 subtasks. Under subtask A, a viability assessment evaluated the probable success of formulating a suitable wave rotor demonstrator engine utilizing the Allison 250 engine. There are several wave rotor cycles that may be suited to a turbine engine application. Candidate wave rotor topping cycles were considered and a screening process used to indicate a preferred cycle. An engine cycle study performed indicated that from a performance and flow capacity standpoint, improved engine performance could be realized. A preliminary selection of basic engine components allowed the key design parameters of the wave rotor to be established. Using this data, candidate wave rotor design point flow size, pressures and temperatures were

established. NASA then designed the wave rotor and prepared maps of its performance. Rotor inlet area, rotor size (diameter, length) and rotational speed were established.

Subtask B performed a design point study using a detailed cycle analysis employing these wave rotor maps. Determined in the study were final values of wave rotor flow, inlet area, and rotor rotational speed. Engine design point temperatures, pressures, and burner design conditions were generated. A range of engine hardware suitable for use in the demonstrator engine was considered with a final selection based on minimal alterations to production engine hardware. A criterion carefully adhered to in the design was the replication of the production engine's compressor surge margin.

Subtask C extended the design point cycle work to an off design point analysis. The cycle study determined part power performance including idle.

Under subtask D, a preliminary engine design resulted in an engine layout. A list of engine hardware to be modified and new hardware to be procured was assembled. Also addressed was the effect of wave rotor output pressure pulse on turbine design.

In subtask E an estimate of engine build and test cost was made. A schedule for accomplishing same was also established.

Subtask F included the reporting effort.

2.2 The Wave Rotor Concept.

The wave rotor concept is based upon the use of transient fluid dynamic processes occurring within flow passages mounted on the circumference of a rotating drum as depicted in Figure 2. In general, the term wave rotor does not define a specific device but rather a broad classification of devices. In this particular application, pressure and expansion waves together with direct hot-to-cold gas flows are made to perform functions commonly reserved for steady state processes in conventional gas turbine equipment. The transient processes are made compatible with steady flow devices (compressor and turbine), ahead of and behind the device by making the transient processes cyclic within the passage and utilizing a series of tubes with staggered phases of the transient process occurring in adjacent passages.

In considering the wave rotor and its unique transient based operation, the gas turbine specialist may have to overcome a number of potential pitfalls in thought hindering his understanding. The following list is intended to address common misconceptions:

- The pressure waves in the rotor passages are not standing waves but instead travel the length of the tube.

- Whereas the flow within a rotor passage is unsteady, the flows entering and exiting the rotor through the ports are steady with some amount of pulsating component.
- The rotor turns to provide opening and closing of the passage end points, not to provide change in angular momentum of the entering and exiting flow streams.
- The wave speeds are sonic or greater but the gas speeds are everywhere subsonic.
- The device is not a partial admission turbine and compressor combination.

Figure 3 illustrates how a wave rotor device may be used to top a gas turbine engine cycle. A properly designed wave rotor can act as a high technology topping spool to a gas turbine engine. It increases the effective pressure ratio of the engine as well as increases the effective turbine inlet temperature. In contrast to a conventionally configured topping spool, the wave rotor offers the following advantages:

- Mechanically simple.
- Low rotational speed.
- One unit accomplishes both compression and turbine functions.
- Self Cooled.
- Conducive to application at low corrected flows.

The self cooled feature of the rotor is derived by the exposure of the rotor walls to alternatively hot then cold flow in rapid succession, thus bringing the wall to an average temperature which is well below the peak cycle temperature. Fluctuations in wall temperature are modulated by the thermal inertia of the wall.

Design of a wave rotor to successfully augment a gas turbine engine is not a straight forward process. Basically, the design of a wave rotor enhanced engine starts with the design of the cycle of wave processes on board the rotor. The cycle design is accomplished through innovation using an understanding of the transient flow processes. A successful design utilizes the transient processes to the best advantage of the gas turbine within the limits of inherently imposed constraints.

3. RESULTS AND DISCUSSION

3.1 Subtask A - VIABILITY ASSESSMENT.

The gas processes occurring within the wave rotor are depicted in Figure 4, the wave diagram of the through-flow (TF) wave rotor cycle. This particular cycle is explained in detail in reference 2, where it is explained along with the other competing candidate, the reverse-

flow (RF) cycle. The diagram describes the processes in the rotor by tracing the "trajectories" of the waves and gas interfaces within the rotor. Shock waves trajectories are shown here as broad solid lines, and expansion waves (actually fans) are shown as light dashed lines. Hot-to-cold gas interfaces are shown as heavier dashed lines. Individual passages and wave fronts are not generally shown in the diagram as was done in Figure 3 for instructive purposes. In many ways an understanding of a wave diagram is as basic to the understanding of a wave rotor as the understanding of a velocity diagram is to that of a conventional turbine or compressor.

Numerical methods validated by experimental results are now available to perform the determination of the wave processes occurring on board the wave rotor.^{3,4,5} Wave diagrams produced by such methods are shown in Figure 5 and are presented in terms of contour plots of pressure, density and velocity. Pressure plots show shock and expansion waves and the density plot very clearly shows the placement of hot-to-cold gas interfaces.

Two basic wave rotor cycle designs were considered in the study, these having been selected from a broader group of candidate cycles studied in previous work. The two cycles are termed the four-port through-flow (TF) and four-port reverse-flow (RF) cycles. Each is identical in its overall performance but they differ substantially in their internal layout. A comparison of the positive and negative characteristics of each cycle is detailed later in this section. Due to the identical nature of the performance of the two candidates, the viability study could be carried out without regard to cycle type. Overall performance characteristics used in the viability study were taken from reference 1 and are shown in Figure 6.

To appropriately guide the application of a wave rotor to an existing engine the inherent characteristics of the wave rotor cycle must dictate several important decisions. In general engine SFC improvements are realized through cycle pressure ratio increases. The wave rotor topping cycle achieves this in an expedient manner and the maximum levels of topping cycle pressure gain are realized by attaining a maximum temperature ratio across the device as shown in Figure 6. These characteristics show that as T_4/T_1 increases, P_4/P_1 increases. The overall pressure rise across the topping cycle is thus set by the ratio of the turbine inlet temperature to the compressor discharge temperature. The pursuit of maximum performance improvement thus results in an engine cycle fully utilizing the turbine inlet temperature capabilities of the baseline engine.

In retrofitting a wave rotor into an engine design, it is most important to avoid compromising the component performance by poor operating point selection. This

dictates that the compressor operate at or near its design flow and pressure ratio, generally near the rated power point of the baseline engine. Similarly the requirement to maintain compressor surge margin in the demonstrator engine at baseline levels constrains the design operating point to near baseline engine levels.

With the compressor operating near its design pressure ratio and flow and the turbine operating at its design inlet temperature, the pressure at the turbine inlet in the demonstrator engine will of necessity be higher than that of the baseline engine. The end result is that a change in the turbine hardware is required to accommodate the reduced turbine inlet corrected flow due to the higher turbine inlet pressure, while maintaining appropriate efficiency and work extraction in the turbine section. An apparent conflict thus arises between the use of existing engine hardware and the need to reduce the turbine section flow capacity.

Considering the 250 model line in particular, the need to modify turbine flow capacity may be accommodated by a "mix and match" strategy combining compressor and turbine section from two of the multiplicity of different engine models available. Engines in this product line range in mass flow at design point from 3 to 7 lbm/sec.

The cycle analysis carried out in this phase of the program identified a favorable engine selection using the compressor of the 250 C30 engine together with the turbine section of the 250 C28C engine. With the turbine inlet temperature (TIT) maintained at 1930 F in the topped engine, a topping cycle pressure ratio of 3.0 was achieved through addition of the wave rotor. The pressure of the gas entering the turbine was increased by a factor of 1.2 as a result. Performance improvements were dramatic with an increase of 20% in specific shaft horsepower (SP) and decreases in specific fuel consumption (SFC) of 22% indicated. Improvements of this magnitude together with favorable results regarding component selection essentially proved concept viability.

As described above, analysis conducted to this point is equally applicable to both the TF and RF cycles. Subsequent tasks objectives, however, required selection of a particular cycle. Wave diagrams of the two cycles side by side in Figure 7. The TF and RF cycles differ in direction of flow into and out of the wave rotor. The TF routes all gasses through the rotor left to right. The RF brings cold gas into and out of the same side of the rotor. This is also true of the hot gas flow. Thus the RF cycle does not inherently have a self cooled rotor. In order to achieve a self cooled RF design, a two cycle per revolution design of the RF configuration must be constructed which orients the cycle alternately right and left on the rotor as illustrated in Figure 8. A number of the positive and negative

characteristics of each cycle are presented in Table II. The TF cycle appeared to be a more advantageous selection for purposes of a demonstrator engine. Essentially, demonstration of self cooled rotor capability, with a mechanically simple arrangement, was judged highly desirable. The result of the selection process, due to its limited scope and narrowly defined objective, is not intended to be a definitive indicator of absolute merit of either candidate in the topping of gas turbine engines in general. Selection in individual applications will require careful examination of all competing concepts.

3.2 Subtask B, DESIGN POINT ANALYSIS

Prediction of the performance of the wave rotor was accomplished through the use of a detailed map of the wave rotor cycle performance generated over a broad range of operating parameters. Design of the rotor and preparation of the performance maps used in this study are the accomplishment of Jack Wilson and Dan Paxson of NYMA, Inc. and NASA Lewis Research Center respectively and were based on their work^{1,2,4}. Effects of fluid friction, heat transfer, and leakage are included in this analysis. One representation of the resulting map is shown in Figure 9 and 10. Mass flow and heat addition are represented in terms of dimensionless corrected parameters in these maps but were generated for a specific set of design variables as defined below:

$$Q_{\text{corr}} = \left(\frac{Q}{A_1 P_1 \sqrt{RT_1 g_c}} \right)$$

and

$$m_{\text{corr}} = \left(\frac{m_1}{AP_1} \right) \sqrt{\frac{RT_1}{g_c}}$$

A summary of the wave rotor design is shown in Table III and details of the wave rotor design and its performance are documented in Appendix A.

A detailed cycle analysis was used to model engine operation. Maps of compressor, gasifier and power turbines, and wave rotor performance were utilized for a number of component selection sceneries. The study was constrained by the following:

- retain production engine compressor surge margin.
- scale turbine flow capacity less than 5%.
- avoid the use of compressor bleed to achieve surge margin.
- scale the wave rotor flow capacity less than 10%.

Scaling of the turbine hardware over a limited range is applicable when utilizing existing hardware. The employment of modification techniques commonly used in engine development programs, but feasible for use on production engine parts makes this possible. These modifications leave turbine efficiency essentially unchanged while altering flow capacity over a narrow range.

The use of compressor bleed to control surge margin was ruled out because of its severe impact on engine performance. Although the influence of the bleed flow could be accounted for and the engine performance analytically compensated to remove this penalty, this approach was rejected in favor of a more defensible demonstration of performance improvement.

Results of the study indicated that the selection of a 250 model C30 compressor joined to a C28C turbine section downstream of the wave rotor, resulted in a demonstrator engine having the greatest performance increases possible using existing hardware. Flow capacity of the turbine hardware was increased by 1.4% for both the gasifier and power turbine. The flow capacity of the basis wave rotor design was increased by 6%. The revised dimensions are identified in Table III for the wave rotor design as matched for use in the demonstrator engine.

The baseline engine becomes the 250 C30 engine producing a nominal 650 shaft horsepower at maximum continuous rating with an SFC of 0.59. The demonstrator engine has a predicted 733 shaft horsepower with an SFC of 0.45. Comparative design point results are quoted with both engines operating at a turbine inlet temperature of 1930 F. Application of the wave rotor thus yields a 11.4% increase in shaft horsepower, a 20.0% increase in SP, and a 22% decrease in SFC. These improvements are very impressive and show the potential for a very successful demonstrator engine test.

Design point operating conditions within the demonstrator engine are detailed in Figure 11. Comparing station 4 with station 1 shows a 1.24 pressure gain across the wave rotor section. The burner inlet operates at a pressure ratio of 3.37 higher than the compressor discharge. Turbine inlet temperature is held to the production engine levels (1930 F) while burner exit temperature is at the 2605 F level. Gas expansion within the wave rotor thus realizes a 675 degree reduction in gas temperature before the turbine inlet station is reached.

Note that the burner inlet temperature is elevated significantly above that expected for a conventional cycle. This is due to an inherent feature of the TF wave rotor cycle which recirculates through the burner loop a mass flow 60% larger than that entering the wave rotor

from the compressor. This impacts the burner design significantly, as will be discussed in section 3.4.

3.3 Subtask C. OFF DESIGN OPERATION.

The cycle model of the engine was exercised over a 6 point set of power settings ranging from idle to take off power. Figure 12 compares SP and SFC for the topped and baseline engines as a percent improvement for the off design points. Both comparisons show exceptional performance improvements by the demonstrator engine with increasing gains as power output is reduced. Idle performance was improved with a 19% increase in SP and a 32% decrease in SFC. For each point, compressor surge margin was maintained at production engine levels. With respect to compressor operation, one consequence of using existing components was noted in the speed of the gas generator. The design speed match point of the topped engine is 6% below that of the production engine. This results in a somewhat over sized compressor and turbine system compared to the production engine.

A closer examination of the workings of the wave rotor is shown in Figure 13 with the engine operating points placed on the wave rotor operating map. Design point operation falls near the knee of the curve at the design heat addition level. As power output is decreased, the operating point moves to a curve of lower level of heat addition. The operating point remains near the knee of the curve in each case. This characteristic is maintained over the operating range including the idle points. It can be noted that a number of idle points were run over a range of power turbine speeds to assess sensitivity. Engine operation was acceptable at each point examined.

Also shown in Figure 13 is the P5/P1 pressure ratio characteristics of the wave rotor and the placement of the operating points on this map. It is noted that the operating points fall upon a locus of points representing a maximum in P5/P1 as corrected heat addition is altered. P5 represents the burner inlet pressure, which appears to be maximized in this operating point selection.

Further examination of the pressures within the engine cycles are provided in Figure 14. Most notable is a comparison of the overall pressure ratios of the topped and un-topped engines. At design point operation, the topped engine approaches a pressure ratio of 23:1. Baseline engine levels are near 9:1. Over the operating range, the wave rotor contributes a nearly constant 3:1 compression. It should be noted that in the demonstrator engine, the shaft compressor operates at a lower pressure ratio than that of the identical compressor in the baseline engine. This is due to the above mentioned less than optimal component

matching resulting in gasifier shaft speeds averaging 6% below design.

Figure 15 examines the pressure gain contribution of the wave rotor in an alternate way. The pressure gain from compressor discharge to turbine inlet represents, in a simplified way, the contribution of the wave rotor to the cycle. This ratio approaches 1.24 at the high power settings and lowers to 1.09 at the idle conditions.

A second way of examining the overall contribution of the wave rotor is to compare burner exit temperatures to turbine inlet temperatures across the range of power settings. Figure 16 indicated that the difference in these temperatures remains nearly a constant 600 degree level with some additional gain shown at the highest power setting.

Gas path temperatures throughout the cycle are shown in Figure 17. It can be noted that at equal shaft horsepower points for the two engines, production engine rotor inlet temperatures are 60 to 75 degrees higher than those in the wave rotor topped engine.

One disadvantage of the topped engine relative to the production engine is clearly noted when examining the burner inlet temperature concern mentioned earlier, this time across the range of power settings. Figure 18 indicates that due to the combined effect of higher compression ratio and hot gas recirculation, the burner inlet temperatures operate from 600 to 1000 degrees higher for the demonstrator engine when compared to the baseline engine. This moves the design of the burner to a significantly higher level of technology than that existing in the baseline engine today.

As described above, wave rotor speed is self determining due to the free wheeling design selected for use in this study. A comparison of the speeds of the wave rotor and gasifier shaft in the demonstrator engine is shown in Figure 19. The wave rotor speed is approximately a constant 1/3 of the gasifier speed for all power points, with the ratio approaching 1/4 at the idle power setting. The feature that at power, the rotational speed of the wave rotor remains a near constant fraction of the gas generator speed indicates a favorable result if some type of mechanical lashing of the gas generator and wave rotor shafts should become necessary as the concept is examined and tested in further work.

The wave rotor design upon which these performance characteristics were based is outlined in Figures 20, 21 and 22. The wave rotor employs a 2 wave rotor cycles per revolution design in order to accomplish a more advantageous design package. The rationale for this will be discussed in the following section.

3.4 Subtask D. PRELIMINARY DESIGN

The preliminary design engine layout addressed the following issues:

1. Mechanical aspects of component re-match.
2. Component configuration selection.
3. Wave rotor port ducting design.
4. Combustor design.
5. Wave rotor and adaptive engine parts required.

3.4.1 Mechanical Components

Figures 23 and 24 show cutaway schematics of the Allison 250-C30 and C28C engines respectively. As can be readily noted, these engines share a high degree of commonality. In addressing mechanical hardware aspects, the key issues were:

- Shaft thrust bearing implications.
- Supply of cooling air for the gasifier turbine.
- Compatibility of the gearboxes.
- Potential for forced turbine vibration.

The layout of the 250 engine minimizes the impact of increased thrust on component bearing due to a basic feature of the engine; compressor, and individual turbine thrusts are carried on separate bearings. This implies that a boost in turbine inlet pressure yields a simple increase in thrust with no change in thrust direction or large load increase at a low design thrust bearing system such as is common in other engine configurations.

Cooling air for the gasifier turbine is supplied at approximately 4.5% above turbine inlet pressure. Mass flow required is 2.2% of the compressor discharge flow. Cooling air at the design point is 665 F. A diagram of the turbine air cooling scheme is shown in Figure 25. This air performs a number of tasks and the temperature level at which it normally arrives plays a key function. Although the burner inlet air pressure far exceeds the required pressure, so does its temperature at 1767 F (+1102 F). For this particular wave cycle, an alternate source of air must be created. Some additional cooling air may also be required to cool the ducting to and from the wave rotor. It is likely that cooling air can be made available at the wave rotor cycle level. However, the generation of an alternate source of cooling air was not investigated as such was outside the scope of this effort.

With respect to gearbox compatibility of the C30 and C28C models it has been found that the two are compatible. Interconnecting shafting is common between the models and a direct bolt up of components is anticipated.

The potential for gas pressure pulses emanating from the wave rotor port 4 flow, entering the gasifier turbine and exciting critical vibration modes in the turbine hardware was examined. The wave rotor gas pulse

frequency was calculated to be between 10,000 and 13,900 Hz for operation between idle and design point. A first stage turbine blade first bending mode was found to exist at 12,500 Hz. It was recommended that the frequency of excitation be moved lower to a maximum of 11,000 Hz. Latitude in selection of wave rotor passage number indicates that it may be accomplished without significant performance impact.

3.4.2 Demonstrator Engine Configuration Study.

A highly important consideration in design of the demonstrator engine is the proposed layout of the baseline engine. The wave rotor section is to be introduced in the flow path at the point normally held by the combustor. Downstream of the wave rotor, the conventional flow path picks up again at the turbine inlet. The burner in the wave rotor concept is connected to the wave rotor both at the inlet and the exit. Due to the additional length occupied by the wave rotor, the ability to stretch the length of the portion of the flow path in the baseline engine between the compressor discharge and the turbine inlet may be highly desirable.

Several unique aspects of the 250 engine series are relevant to the selection of this engine for wave rotor topping. The turbine inlet is directly accessible without required engine gas generator or power turbine shafting changes. The dual transfer tube feature at the exit of the compressor is also useful in coupling the engine with a two cycle per revolution wave rotor layout.

An early engine layout concept is shown in Figure 26. The layout accomplished direct transfer of the gas flow from the wave rotor to the turbine and used the two transfer tubes from the compressor to feed the wave rotor. However, with the burner placed along side and below the wave rotor, the ducting to the wave rotor from the combustor is long, hot, and complex in shape. Shortening of this duct lead to the final engine layout concept as shown in Figure 27. In addition, the engine components are placed on a common center line allowing the engine case to be fully utilized in the structure of the engine back through the combustor module.

3.4.3 Wave Rotor Port Ducting.

Design of the wave rotor ducting is critical to the successful application of the wave rotor concept. Using the results of the previous subtasks, an engine layout was carried to the preliminary design level by using the following port ducting design study analysis.

The engine ducting must conform to the allowable losses of their individual gas flows. The cycle analysis of subtasks B and C assumed:

1. Compressor to wave rotor losses are unchanged from the production engine.

2. Burner to wave rotor losses are determined by the wave rotor internal cycle matching.
3. Wave rotor to turbine losses are assumed to be 3.25%.
4. Wave rotor to burner losses are determined by the wave rotor internal cycle matching.

Total of losses in 2 and 4 above is 8.9% so as to achieve wave rotor cycle matching.

The results of the cycle work now allow the reexamination of these assumptions. Design strategy for each duct has been broken down into a statement of the challenge, followed by a preferred approach to meet that challenge. In each case, the approach has been judged to be capable of meeting the levels initially assumed appropriate.

1. Port 1: Compressor to wave rotor.

Challenge: Create a low loss transition from transfer tube at 0.15 Mach number to a value of 0.41 Mach number in the port, then execute a 153 degree turn.

Approach: Accelerate the flow slightly in the turn then rapidly accelerate the flow in a converging duct to the port. This is a straight forward duct design with acceleration helping to keep the losses low in the turn. Preliminary design is shown in Figure 28.

2. Port 2: Burner to wave rotor:

Challenge: With flow from combustor at low velocity, using a short duct, accelerate the flow to 0.35 Mach number into the port while turning the flow 23 degrees.

Approach: Using existing combustor transition to form an annulus, divide the annulus into two ducts, then accelerate the flow in a convergent duct with a simultaneous turn. Figures 29, and 30 illustrate the design.

3. Port 4: Wave rotor to turbine:

Challenge: Create a compact design with low loss. The production engine turbine inlet geometry is designed for very low axial velocity into the nozzle row, hence the ducting plus nozzle row has a pressure loss much less than the 3.35% goal targeted here. Wave rotor turbine flow exits at 0.49 Mach number. Warning: a design with diffusion followed by acceleration will result in very high losses exceeding the 3.25% goal and thus must be avoided.

Approach: By eliminating the 1st stage turbine nozzle row and utilizing a transition duct from wave rotor to turn the flow into the turbine,

diffusion followed by acceleration is avoided. This change mandates changes to the existing engine hardware including the rear turbine bearing support (RTBS). Careful design is required to reduce the duct length experiencing high velocity flow. The preliminary design includes a turning vane to properly guide the flow. The throat is set at the trailing edge of the turning vane. Figure 31 and 32 present the preliminary design. Proper design of this section requires CFD analysis to minimize both heat transfer area and flow losses while assuring proper flow into the blade row.

4. Port 5: Wave rotor to burner:

Challenges:

- a. Receive flow from the wave rotor at 0.33 Mach number, turn 152 degrees and diffuse to 0.15 Mach number. Pressure loss requirement set by wave rotor matching. Total loss from wave rotor exit at 5 to inlet at 2 is 8.9% .

The loss breakdown is:

- burner liner, 4.9%, the production engine liner level.
- burner to wave rotor, 1.0% estimated based on above port 2 design.
- wave rotor to burner, 3.0% goal.

- b. A strong temperature gradient exists across the flow in this duct, 3100R to 1690R, with a 2227R average.

Approach: Turn the flow at port Mach number (0.33) and diffuse to 0.15 Mach number in straight duct. Use high temperature materials in duct until temperature mixing is attained. Turning will aid mixing of the hot and cold flows. Figure 33 shows the resulting duct design.

The resulting engine wave rotor module is illustrated in Figures 34 and 35 showing the side and end views. High radius air bearings are selected for the wave rotor handling both radial and axial loads. The high radius feature lightens the device and its high temperature capability enhances its applicability. Figure 35 clearly shows the dual nature of the compressor to wave rotor inlet and burner inlet external ducting.

3.4.4 Combustor Design

Analysis indicates that a burner design based on a modified production 250 R20 burner (Figure 36) will result in a combustor of superior design. However, the predicted liner wall temperature is 2500F for a film cooled production design since the burner inlet temperature is 1767 F. The standard liner material, AMS 5521, is unacceptable since 2500F is above this material's limits. In fact this temperature is impractical

for any liner material except ceramic. For a demonstrator engine, a ceramic liner is deemed too expensive and has an excessively long lead time for procurement.

Alternately, the predicted liner wall temperature is 1915F for a Lamilloy liner design. The preferred material for this temperature range is HA188 with a 3 ply Lamilloy. It is anticipated that peak temperatures can be reduced an additional 20 degrees with optimization of the liner. Such a liner is predicted to have a life suitable for demonstrator test series.

Thus analysis indicates that through the use of a effusion cooled liner and a careful selection of non exotic burner liner materials, a demonstrator engine burner may be developed based on a production 250 burner.

3.4.5 Alternate Port 5 Design: Reduction of Burner Inlet Temperature.

The burner inlet temperature may be reduced in the through-flow cycle by splitting of the port 5 flow into 2 gas streams. As shown in Figure 4, flow exiting port 5 is composed of a hot and cold streams which mix together downstream of the port. Initial gas is hot gas not exhausted to the turbine, followed by gas previously arriving from the compressor and compressed within the wave rotor. Figure 37 quantifies the temperature levels of the two gas streams. (Note that the predictions shown are those for the subtask A viability study design point with the average value deviating slightly from the subtask B predictions.) Hot gases at 3100 R are directed directly to the wave rotor port 2 entrance (burner exit) since temperature levels there are near identical. Cold gas at 1600R is routed to the burner inlet, lowering the burner inlet temperature from 1767F to 1140F. This allows conventional materials to be used in the combustion liner and reduces gas mass flow rate to the burner, allowing a significant burner size reduction.

Figure 38 presents a design concept for the split port 5 ducting. The use of internal ducting for the hot gas reduces heat loss and isolates hot ducting from the exterior of the engine. A feasibility analysis has indicted that the gas streams have appropriate levels of total pressure to allow the required ducting design.

3.4.6 List of Engine Hardware Required For the Demonstrator Engine.

Adaptive engine parts required:

- A1. Gasifier turbine rear bearing support
- A2. Nozzle assembly- gasifier turbine 1st stage
- A3. Shield - gasifier turbine bearing sump
- A4. Combustor case
- A5. Combustor liner
- A6. Misc. exterior pipes and wiring

- A7. Spacer- turbine containment ring
- A8. Turbine nozzle mounting flange and support
- A9. Engine mount
- A10. Misc. parts in gasifier turbine sump

Wave Rotor Components required:

1. Rotor
2. Forward end plate
3. Rear end plate
4. Air bearing journal shaft
5. Outer wave rotor assembly case
6. Inner case tube
7. Air bearing components
8. Transition ducts - compressor to port 1
9. Transition case - combustor to wave rotor
10. Combustor center body
11. Support for combustor center body
12. Duct from combustor outlet annulus to port 2
13. Duct from port 5 to combustor case inlet
14. Intermediate flange - liner support at combustor flange

3.5 Subtask E Demonstrator Engine Design, Fabrication and Test Cost and Schedule Estimates.

Estimates of costs include:

- Component Design/Analysis
- Pattern procurement
- Fabrication and/or casting
- Machining

Costs presented in Table IV are based on fabrication of 3 sets of hardware to be used in the testing phase. Rapid prototype parts are assumed based on computer aided design.

Schedule estimate for this effort is presented in Figure 39.

4. CONCLUSIONS

As substantiated by the viability study results, the design point analysis predicts that the wave rotor topped 250 engine produces 11.4% more shaft horsepower (+20% specific power) with a 22% decrease in engine SFC at a 100% power setting (1930 F turbine inlet temperature). The re-match of components can be accomplished using existing engine hardware with a minimum of changes. At off design operation, the improvements in SP and SFC are similarly improved at part power and idle. Surge margin of the topped engine is equivalent to that of the production engine. The wave rotor delivers a near constant 3:1 cycle pressure ratio boost realizing a 1.24 overall wave rotor system pressure rise. Burner inlet

pressure runs at 3.3 to 3.2 X the compressor discharge pressure for the power points. Burner size remains at current level due to the 60% gas recirculation and the 600 degree higher burner outlet temperature.

For the components selected, the turbine inlet temperature of the topped engine runs between 59 and 74 degrees below that of the production engine for equal power output. The wave rotor is free wheeling and spins at $1/3$ the N_g + or - 3% (15369 at design point). The burner pressure loss is between 8.8% and 7.9% for the power points with corrected burner inlet flow going from 0.95 to 0.90 respectively. N_g for the topped engine is 94% that of the production engine resulting in reduced flow and pressure ratio on the compressor.

The preliminary design has verified that re-match of engine components can be accommodated with existing engine hardware. A stacked component configuration works well with two cycle per revolution wave rotor and the 250 engine layout. The allowable duct pressure losses and goal pressure losses appear achievable. Difficulties for further effort include identifying a source for turbine cooling air supply and the high burner inlet temperatures. High temperatures result in heat loss concerns for the two external ducts plus material selection concerns. In addition, burner liner material selection and liner design are made more difficult. A simple change in rotor passage number will eliminate the wave rotor pulsations coinciding with the 1st bend mode of the turbine blades. A careful study is required to optimize the transition duct to the turbine to achieve near conventional engine nozzle row performance.

It is instructive to evaluate the status of the demonstrator engine design relative to the criteria for success established at the start of the program. The degree to which each was met may be evaluated using a score card approach:

A SUCCESSFUL WAVE ROTOR DEMONSTRATOR ENGINE PROGRAM WILL:

1. Demonstrate a meaningful degree of engine performance improvement.
 - 11.4% SHAFT HORSEPOWER increase, 22% SFC improvement, even more at part power.
 - Score: A+
2. Aggressively incorporate wave rotor technology.
 - The best cycle available was utilized. The potential exists for improvement by using the split port 5 or other yet undetermined cycle changes.
 - Score: A
3. Utilize current materials and mechanical technology.

- Current material limits pushed in combustor liner and port 2 transfer duct. Air bearings are selected for wave rotor. Rotor is of conventional materials.
 - Score: C
4. Utilize existing engine hardware to a high degree.
 - All existing hardware used except combustor and 1st nozzle row.
 - Score: A
 5. Impose minimal mechanical complexities on the engine.
 - External transfer tubes used for ducting to combustor.
 - Score: B

Summarizing, a successful wave rotor topped demonstrator engine may be assembled using existing hardware. The engine has the potential of showing excellent design and off design performance. The design of the burner represents the greatest challenges due to high burner inlet temperatures.

5. REFERENCES

1. Wilson, J. and Paxson, D. E. "Jet Engine Performance Enhancement Through Use of a Wave-Rotor Topping Cycle", NASA TM 4486, October 1993.
2. Wilson, J. and Paxson, D. E. "Optimization of Wave Rotors for Use As Gas Turbine Engine Topping Cycles", SAE paper 951411, May 1995.
3. Paxson, D. E., "A General Numerical Model for Wave Rotor Analysis", NASA TM 105740, July 1992.
4. Paxson, D. E. and Wilson, J., "An Improved Numerical Model for Wave Rotor Design and Analysis", AIAA 93-0482, January 1993.
5. Paxson, D. E., "Comparison Between Numerically Modeled and Experimentally Measured Wave-Rotor Loss Mechanisms", Journal of Propulsion and Power, Vol. 11, No. 5, September-October 1995, p. 908, 914.

6. NOMENCLATURE

symbol	definition	units, if applicable
Q_{corr}	heat addition rate.	dimensionless
m_{corr}	mass flow rate	dimensionless
A	port flow area	
P	total pressure	
T	total temperature	
R	gas constant	
x	distance in rotor passage	
L	length of rotor passage	
SFC	specific fuel consumption	lbm/hp/hr
SP	specific power	hp sec/lbm
N	mechanical shaft speed	rpm

Subscripts

1	port 1 conditions
2	port 2 conditions
3	port 3 conditions
4	port 4 conditions
corr or c	corrected dimensionless
design or d	design conditions
gg	gas generator
WR	wave rotor

Table I. Partial Allison Engine Company Model 250 Product Line Data.

Model		Weight	Pressure ratio	Take Off Power	SFC
Series I					
T63-A-5	C18	141	6.2	317	0.697
Series II					
T63-A-700	C20	158	7.2	400	0.630
C20B		158	7.2	420	0.650
Series III					
C28B		228	8.6	500	0.606
C28C		222	8.6	500	0.590
Series IV					
C30		240	8.6	650	0.592

Table II. Wave Rotor Cycle Selection Study Results.

Cycle Type	Positives	Negatives
TF	Inherently self cooled design. Walls see hot/cold flow at 530 Hz.	Combustor inlet temperature is 600+ degrees higher than RF cycle. Pressure in combustor is 1% higher than RF cycle. Pressure loss of 6.5% in combustor loop requires carefully designed ducting. Mass flow in combustor loop is 60% higher than RF cycle requiring larger ducting and combustor.
RF single cycle	Simple compact combustor loop due to ample pressure drop allowable.	1250+F temperature difference from end to end of rotor. Average temperature of hot end at 2140F, 310F higher than TF cycle. Rotor inlet and exit ducting at opposing angles on the same end of rotor complicating mechanical arrangement.
RF two cycle	Average rotor temperature is 200 F lower than TF cycle Inherently self cooled design. Walls see hot/cold flow at 265 Hz.	Rotor inlet and exit ducting at opposing angles on the same end of rotor complicating mechanical arrangement. Ports to and from combustor are on opposite ends of rotor for the two cycles complicating ducting to and from rotor. Turbine ports are on opposite ends of rotor for the two cycles complicating ducting from rotor to turbine.

Table III. Wave Rotor Design Summary.

Rotor Dimensions As Designed:

Inlet Port Area, A_1 ,	4.3 sq in.
Mean Radius	3.21 in.
Passage Height	0.8792 in.
Rotor Length	6.0 in.

Design Point Parameters:

cycles per revolution	2
rotor speed	16800 rpm
passages	52
ratio of specific heats	1.353
viscosity	2.734×10^{-5} lbm/ft/sec
mean Prandlt no.	0.75
P_4/P_1	1.219
T_4/T_1	2.210
mass flow	4.785 lbm/sec
Q_{corr}	2.155
m_{corr}	0.465

Rotor Dimensions As Scaled To Achieve Matched Flow Capacity:

Inlet Port Area, A_1 ,	4.595 sq in.
Mean Radius	3.21 in.
Passage Height	0.9294 in.
Rotor Length	6.0 in.

Match Point Operating Parameters

cycles per revolution	2
rotor speed	16067 rpm
passages	52
ratio of specific heats	1.353
viscosity	2.734×10^{-5} lbm/ft/sec
mean Prandlt no.	0.75
P_4/P_1	1.237
T_4/T_1	2.245
mass flow	4.827 lbm/sec
Q_{corr}	2.149
m_{corr}	0.450

Table IV. Estimated Fabrication and Program Costs.

Adaptive engine parts required, 3 assemblies:		Cost (\$)
A1.	Gasifier turbine rear bearing support	122100
A2.	Nozzle assembly- gasifier turbine 1st stage	57800
A3.	Shield - gasifier turbine bearing sump	40900
A4.	Combustor case	27800
A5.	Combustor liner	36900
A6.	Misc. exterior pipes and wiring	6100
A7.	Spacer- turbine containment ring	4100
A8.	Turbine nozzle mounting flange and support	11600
A9.	Engine mount	8600
A10.	Misc. parts in gasifier turbine sump	6100
Total adaptive engine parts		\$ 322,000
Wave Rotor Components required, 3 assemblies:		Cost (\$)
1.	Rotor	73400
2.	Forward end plate	45300
3.	Rear end plate	45300
4.	Air bearing journal shaft	8700
5.	Outer wave rotor assembly case	21100
6.	Inner case tube	4400
7.	Air bearing components	33600
8.	Transition ducts - compressor to port 1	93100
9.	Transition case - combustor to wave rotor	57700
10.	Combustor center body	15300
11.	Support for combustor center body	5100
12.	Duct from combustor outlet annulus to port 2	57000
13.	Duct from port 5 to combustor case inlet	116300
14.	Intermediate flange - liner support at combustor flange	5100
Total Wave Rotor Components		\$581,000
Total Program Cost		
Program Management		\$246,000
General Layout Design and Analysis		\$153,000
Total adaptive engine parts		\$322,000
Total Wave Rotor Components		\$581,400
Basic Conventional Engine Components		\$236,000
Engine Assembly, 10 builds		\$28,100
Test Costs		\$48,800
Misc.		\$161,500
Total Cost		\$1,776,800

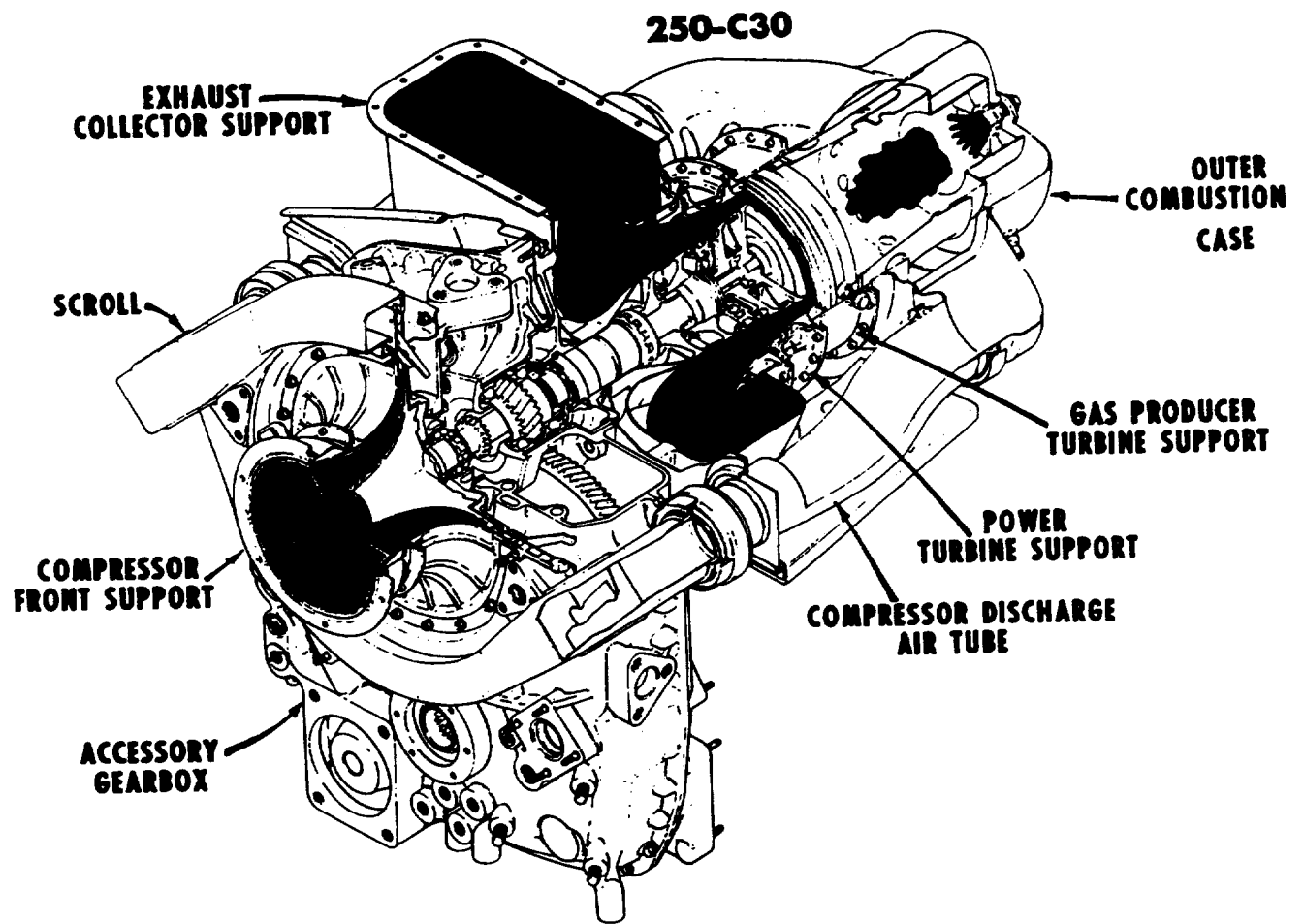


Figure 1. Allison 250-C30 Turbo-Shaft Engine.

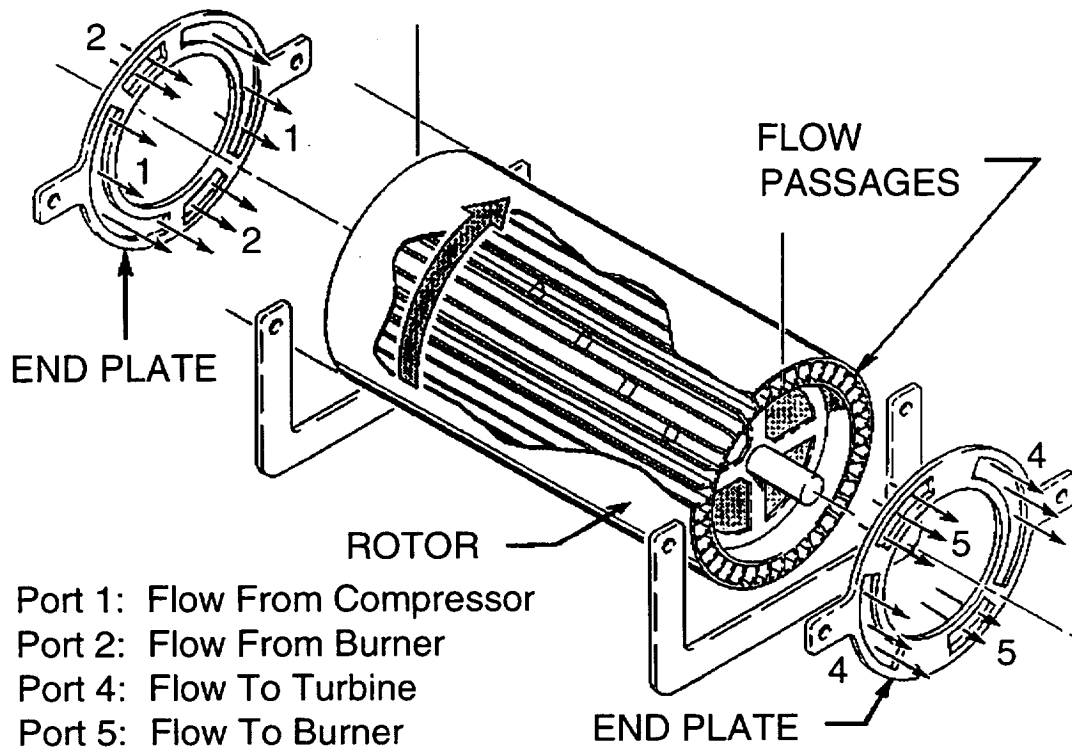


Figure 2. Schematic of Wave Rotor Configuration.

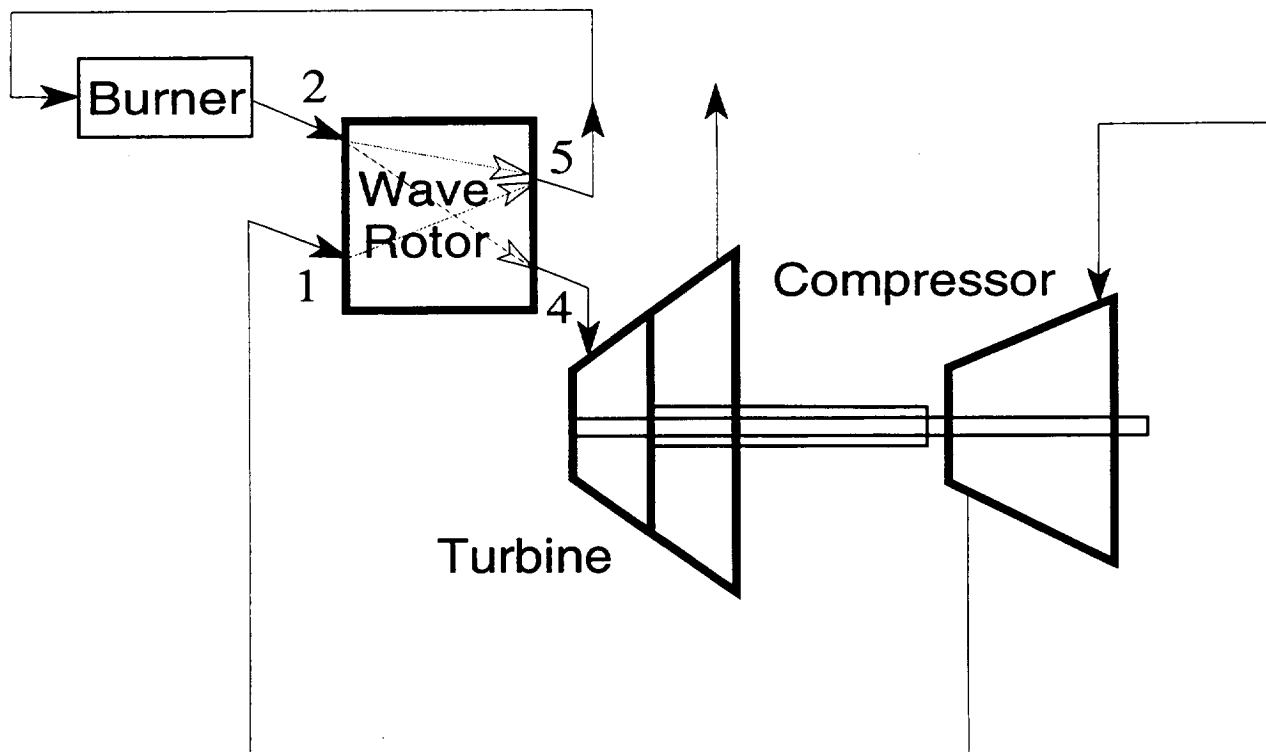


Figure 3. Wave Rotor With Through Flow Cycle Used As A Gas Turbine Topping Cycle.

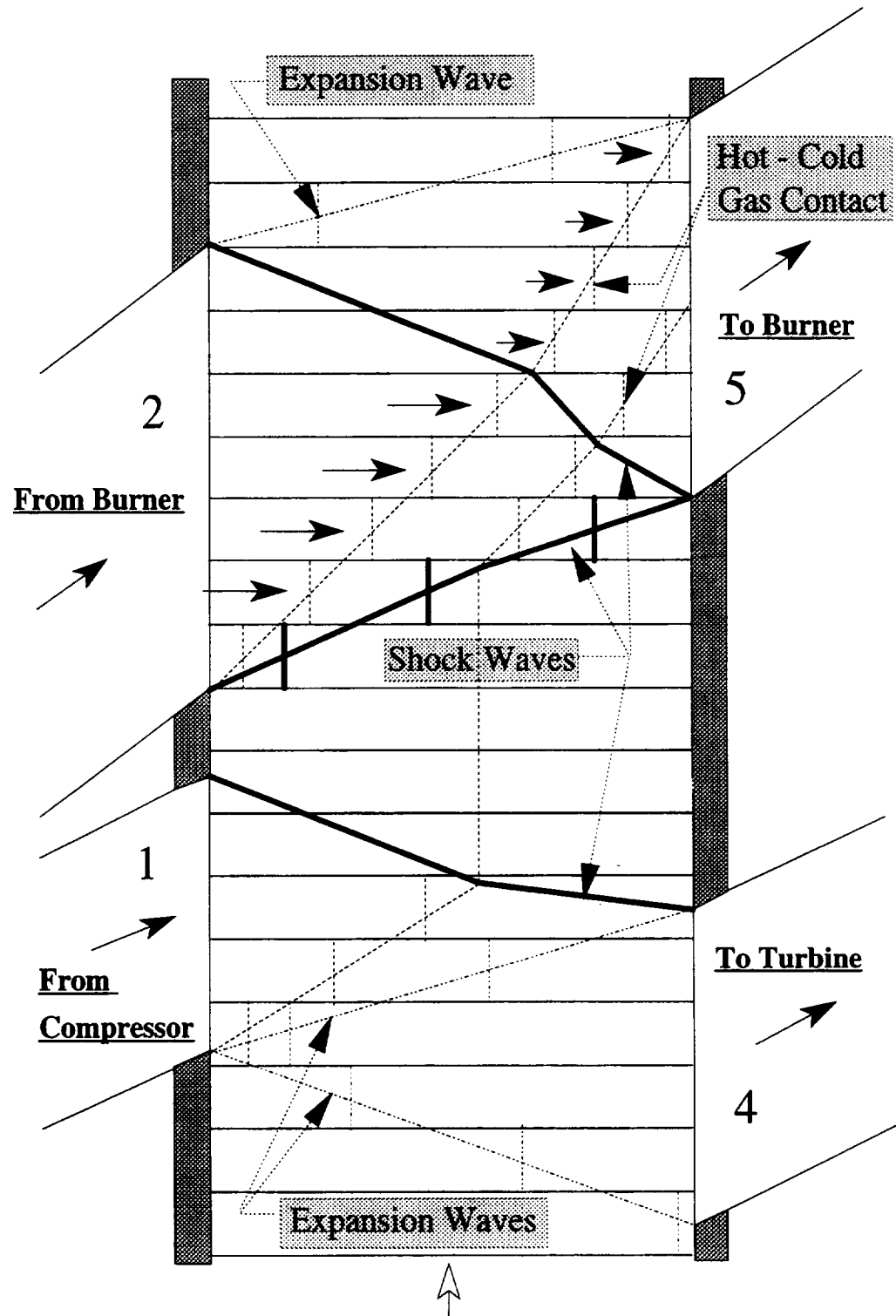


Figure 4. Wave Diagram Of The Selected Four-Port Through-Flow Wave Rotor Cycle.

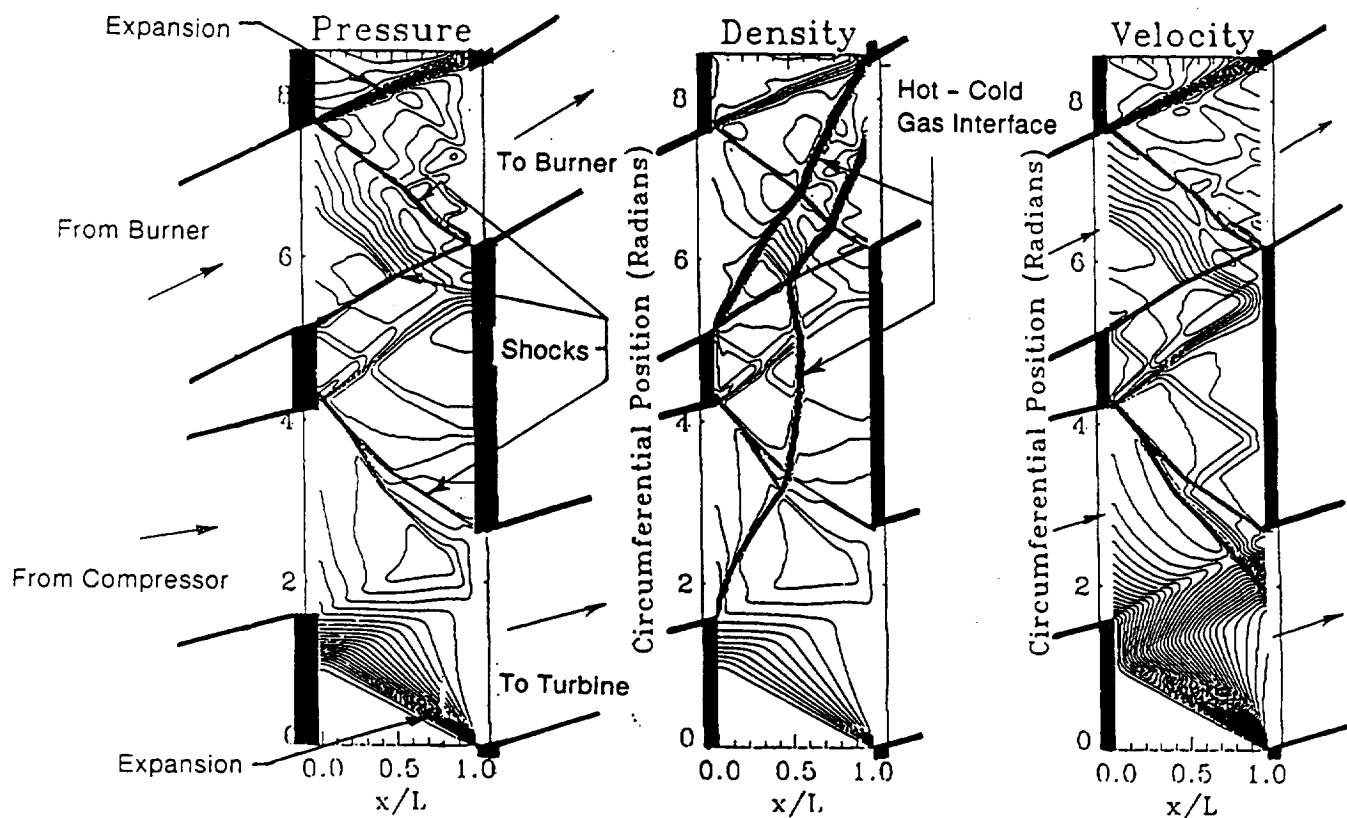


Figure 5. Wave Diagrams Of The Engine Topping Cycle, Pressure, Density, and Velocity Contours.

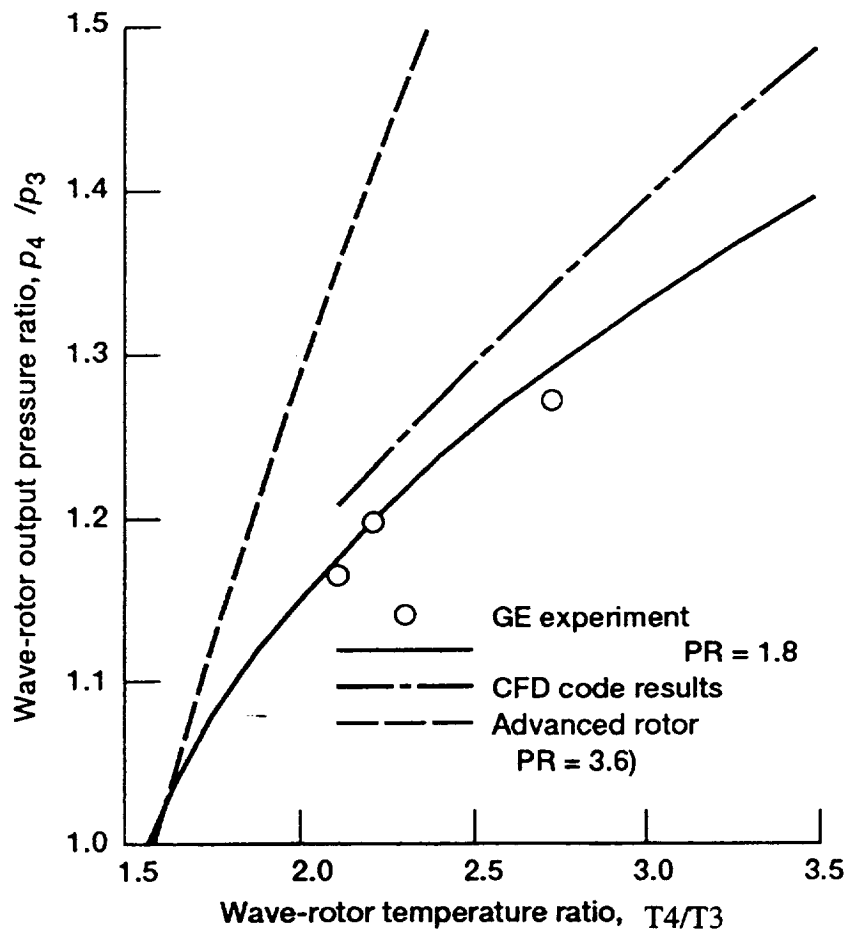
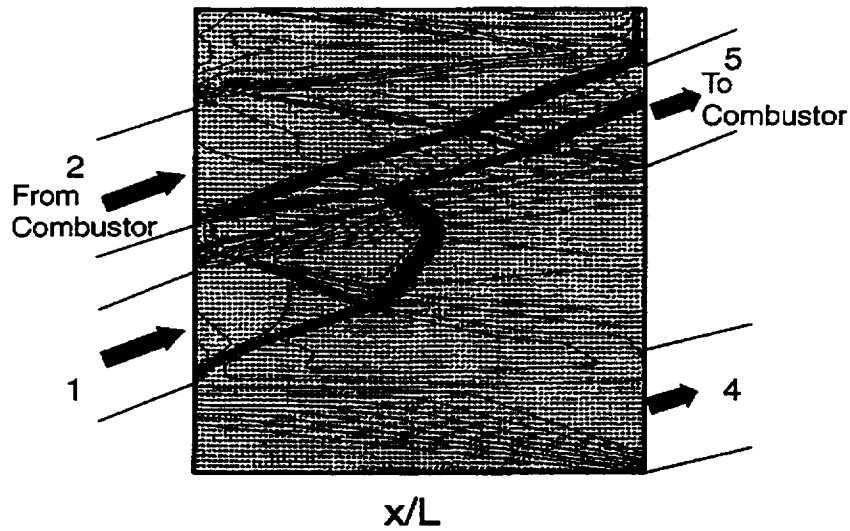


Figure 6. Pressure ratio across wave rotor as a function of temperature ratio across it from reference 1. Solid line characteristic used.

Through Flow Rotor



Reverse Flow Rotor

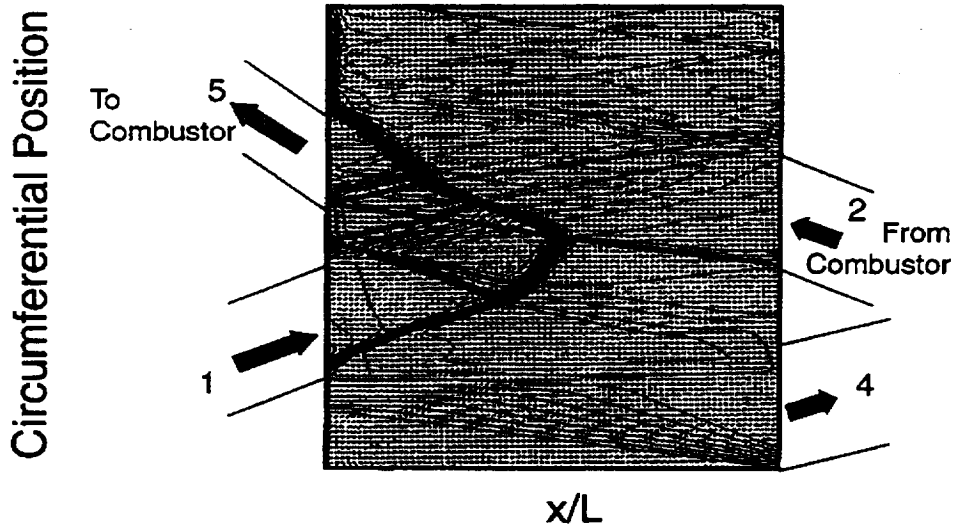


Figure 7. Wave Diagram Comparison Of The Through-Flow And Reverse-Flow Cycles.

Reverse Flow Rotor

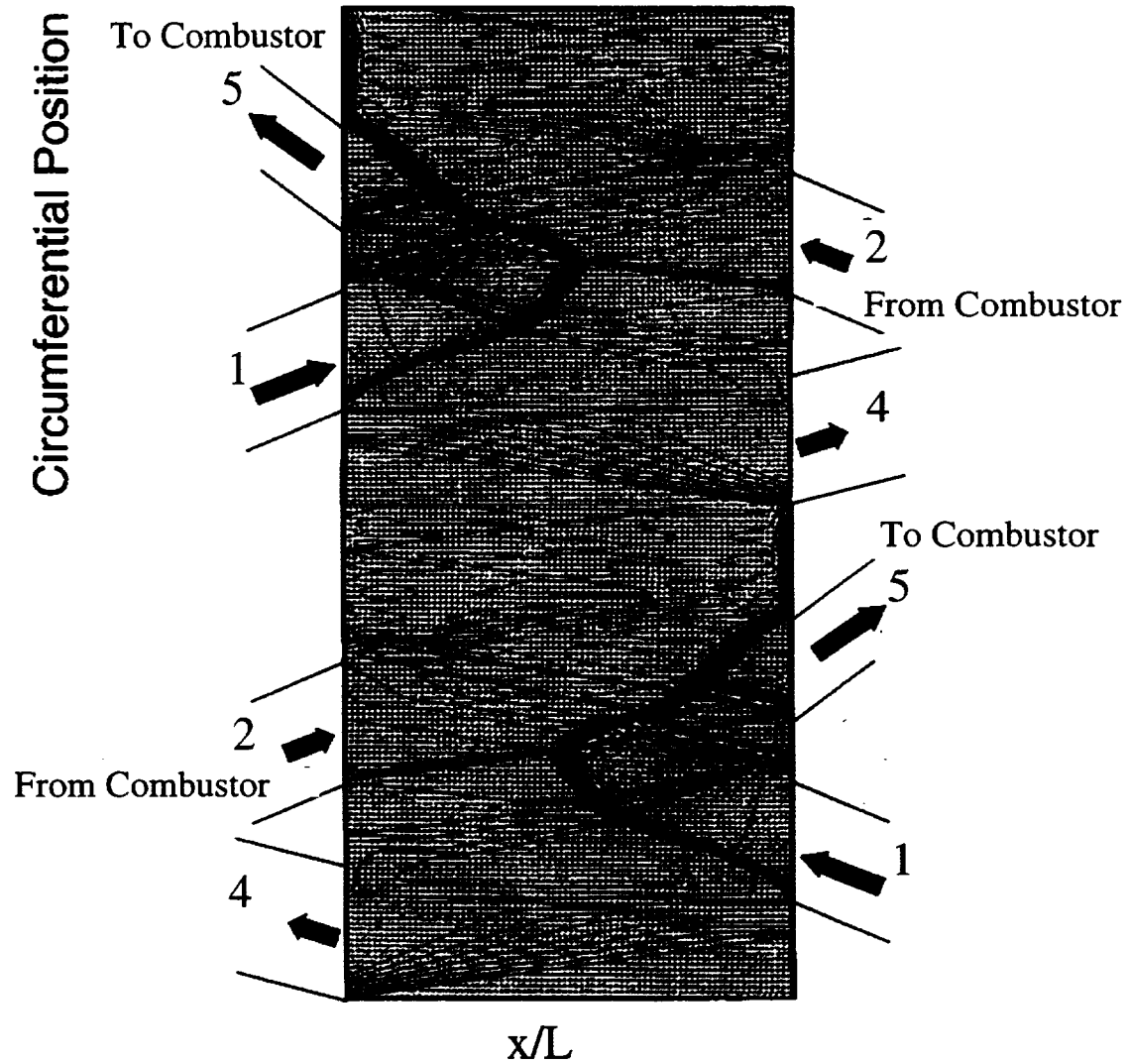
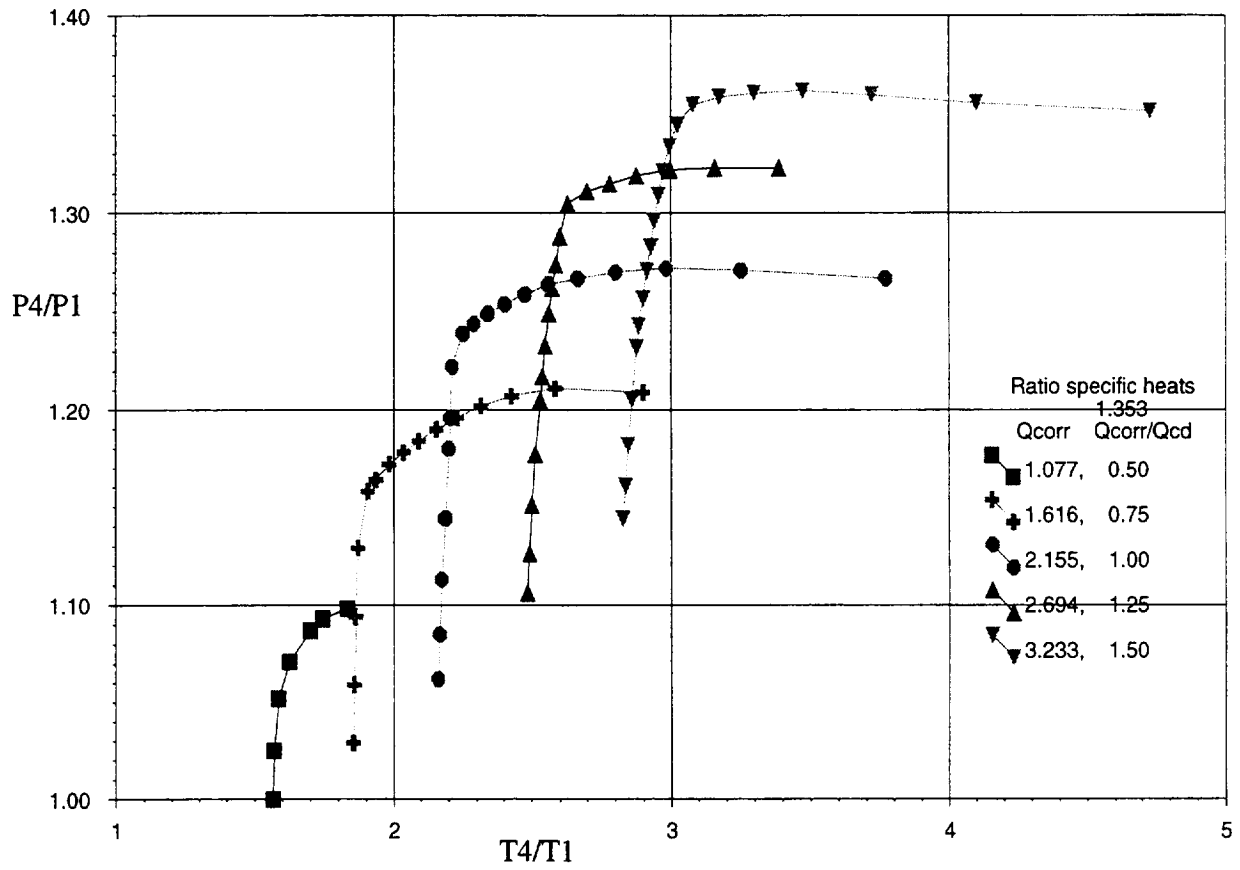


Figure 8. Reverse-Flow Rotor With Alternately Right And Left Porting.

Freewheeling Wave Rotor

Model 250 Demonstrator



Data from D. Paxson 2/24/95

Figure 9. Performance Of Rotor Designed For Use In Demonstrator Engine, Pressure Gain.

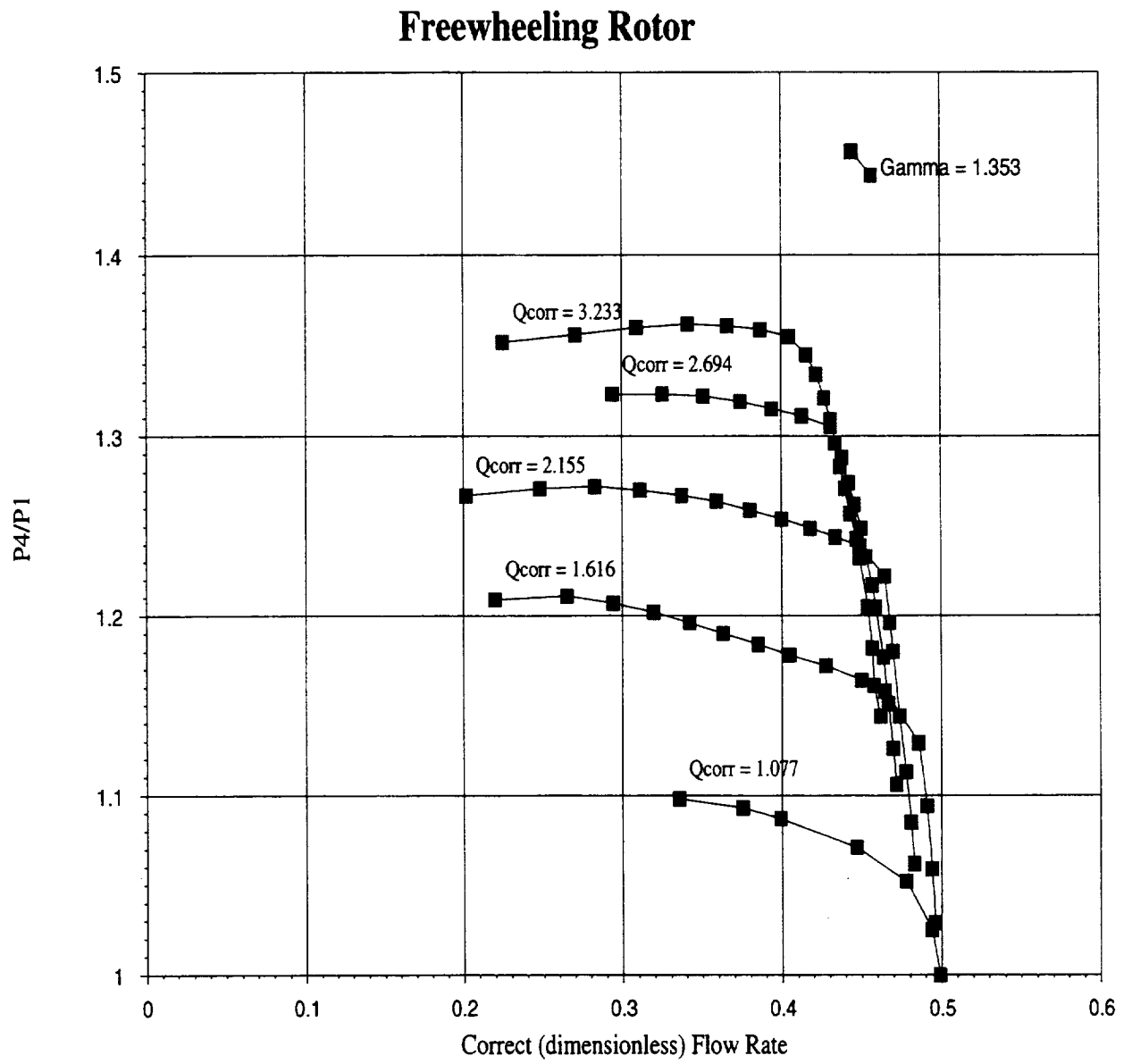


Figure 10. Performance Of Rotor Designed For Use In Demonstrator Engine, Mass Flow.

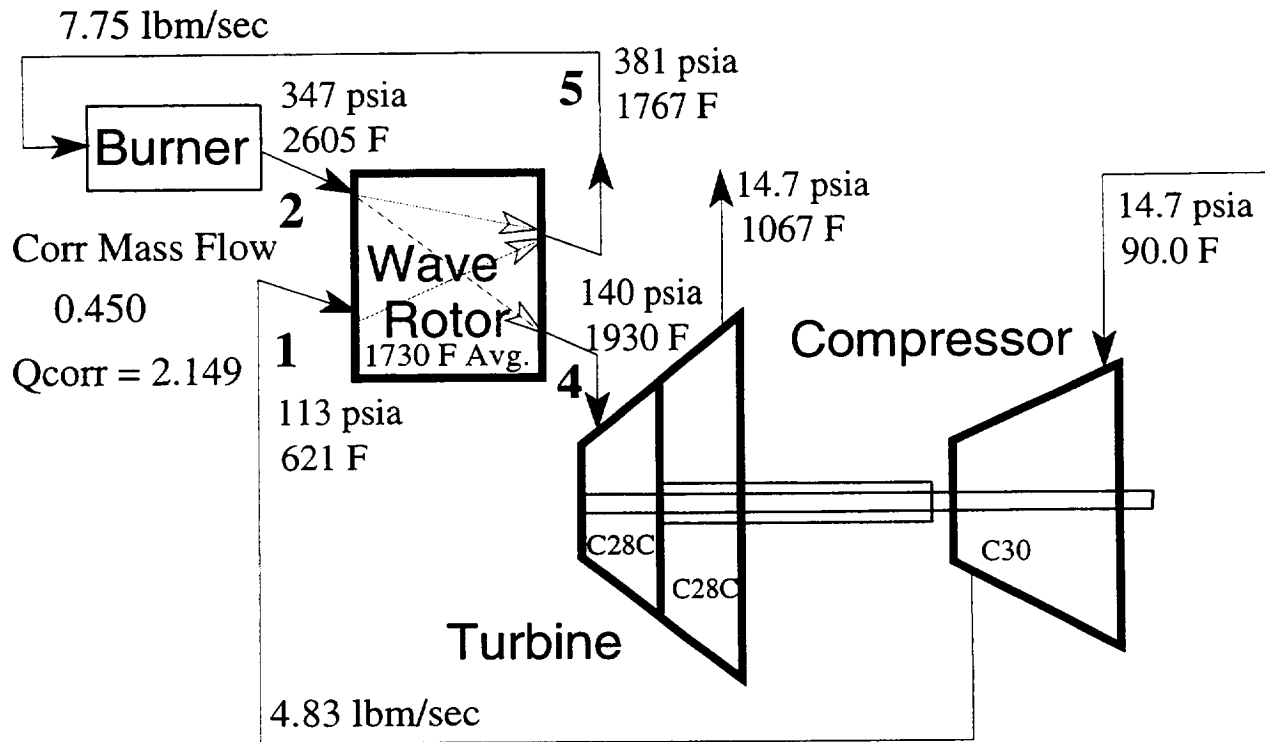


Figure 11. Demonstrator Engine Design Point, Through Flow Cycle Conditions.

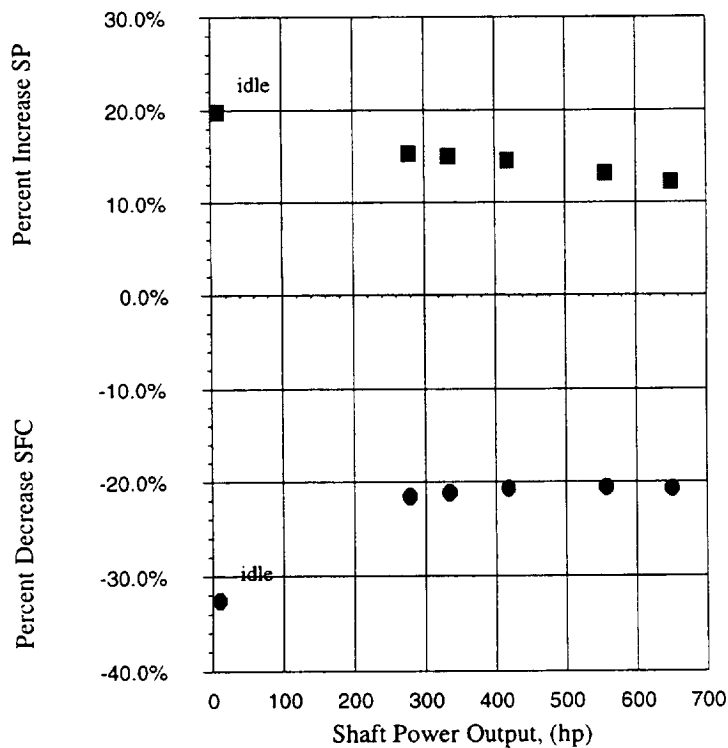


Figure 12. Comparison of Off Design Performance To Baseline Engine Performance.

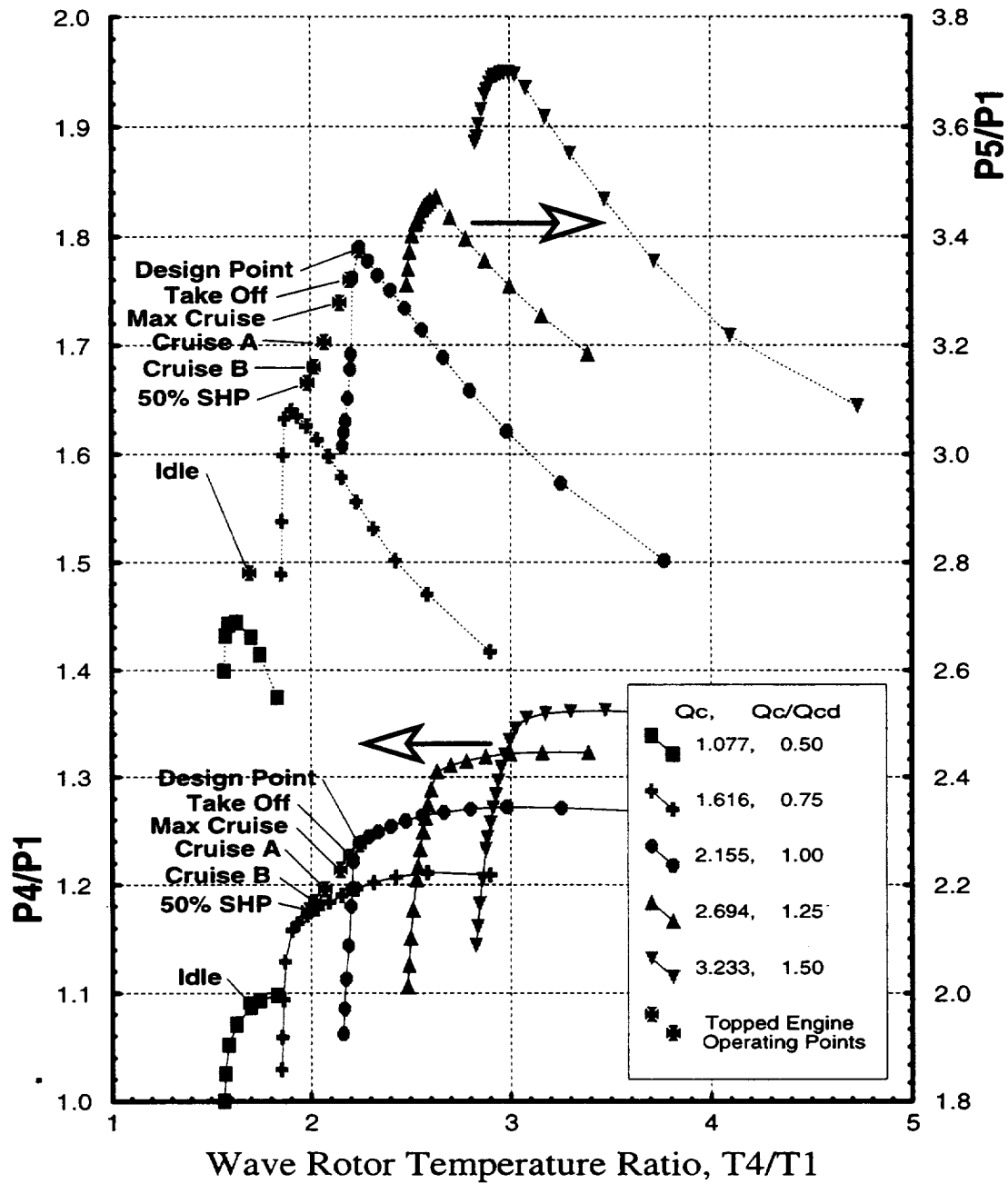


Figure 13. Placement Of Operating Points On Freewheeling Wave Rotor Performance Map.

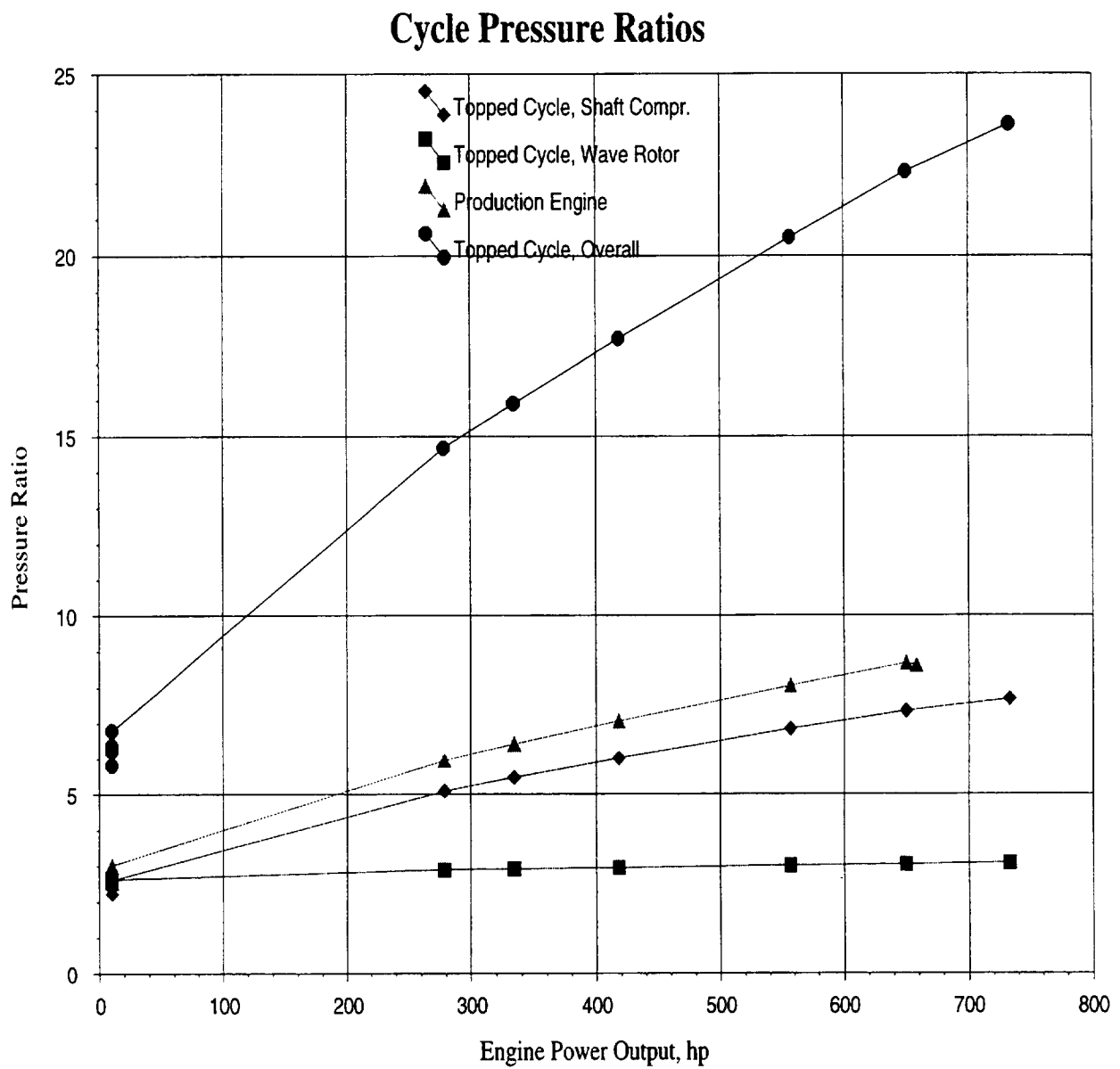


Figure 14. Cycle Pressure Ratios Of The Wave Rotor Topped Demonstrator Engine.

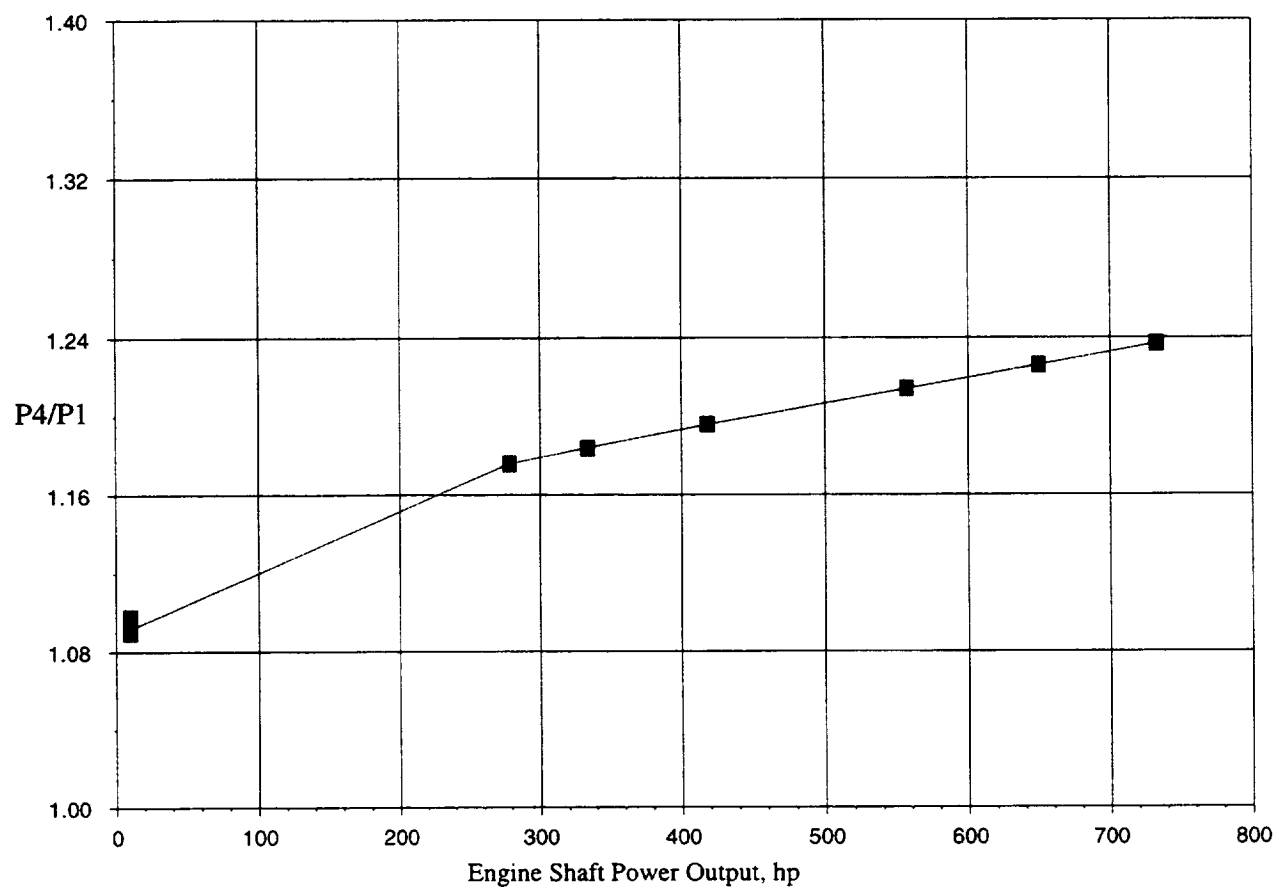


Figure 15. Overall Wave Rotor Pressure Gain For The Demonstrator Engine.

Hot Gas Expansion Within Wave Rotor

Temperature Reduction

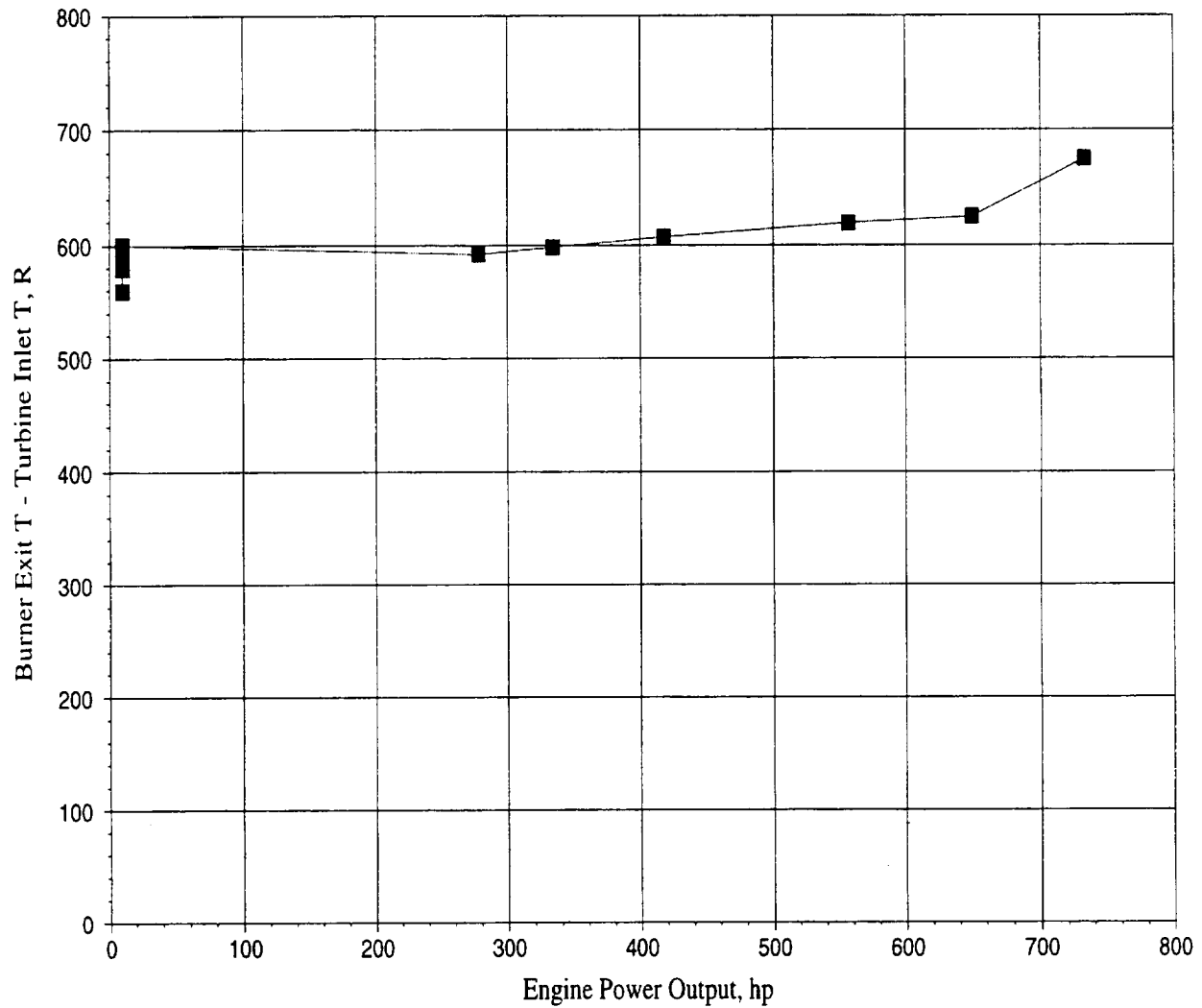


Figure 16. Drop In Gas Temperature From Burner Exit To Turbine Inlet.

Wave Rotor Gas Temperatures Compared With Production Engine Gas Temperatures

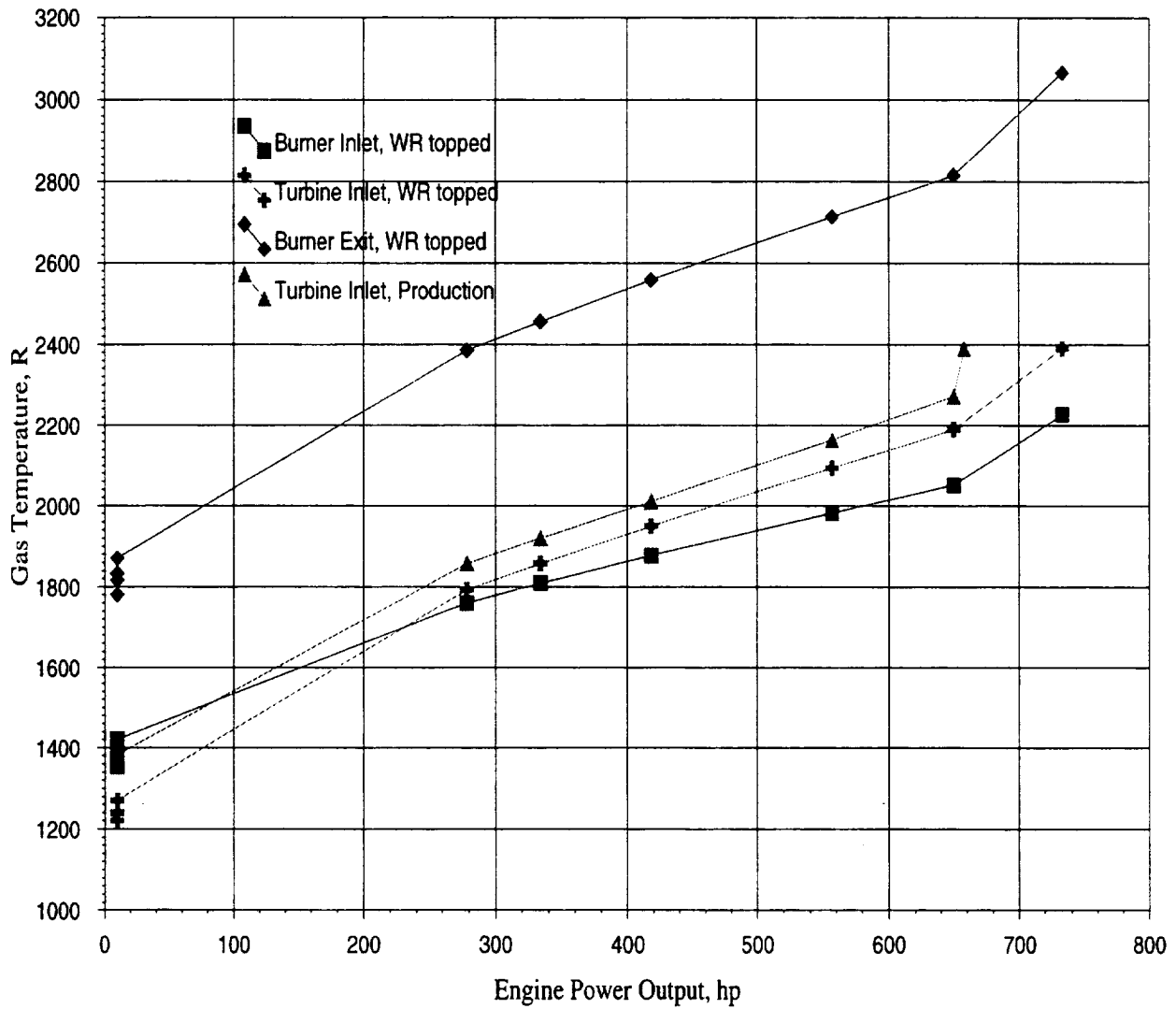


Figure 17. Gas Path Temperatures In The Topping Cycle.

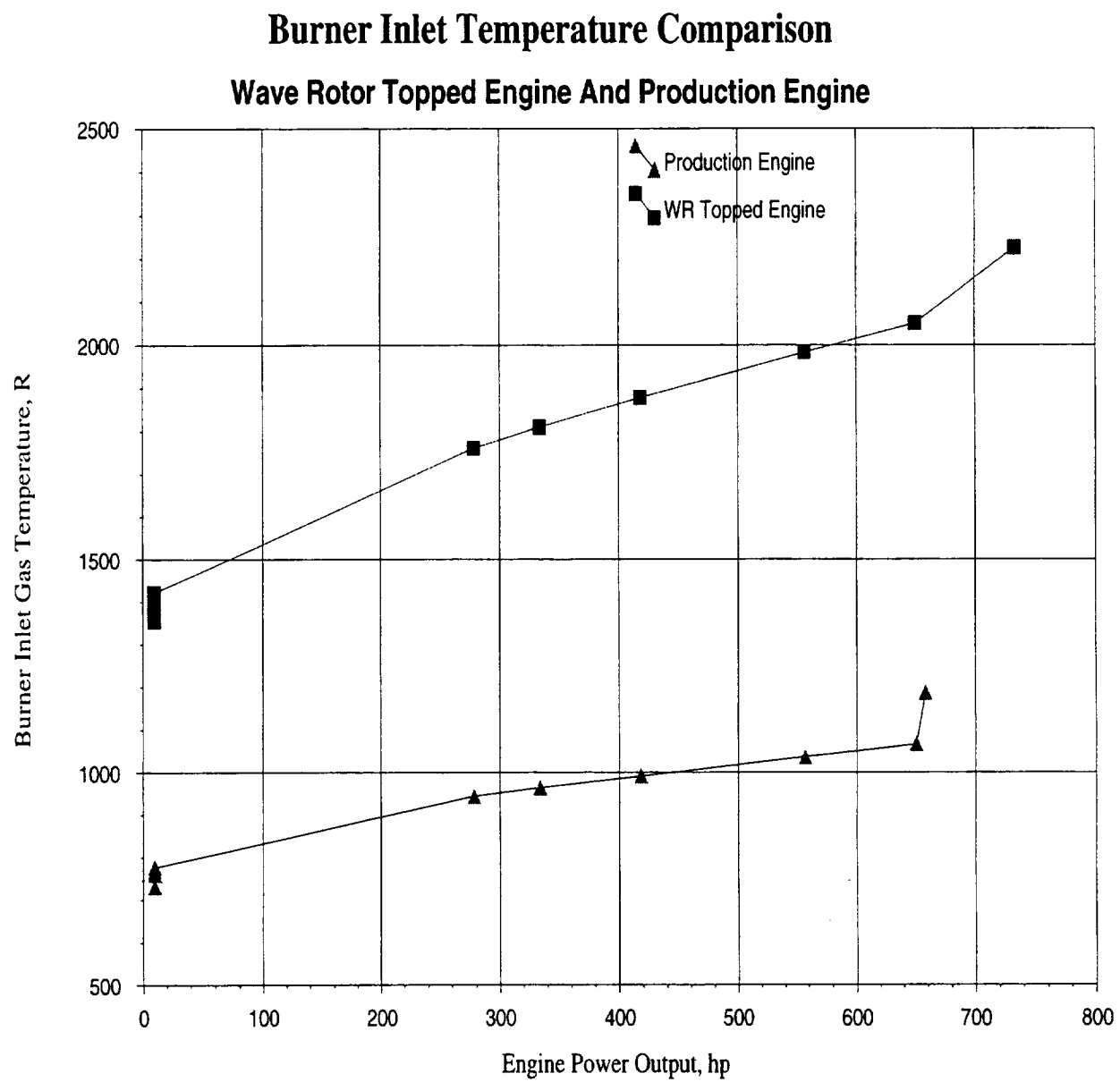


Figure 18. Burner Inlet Temperature Comparison.

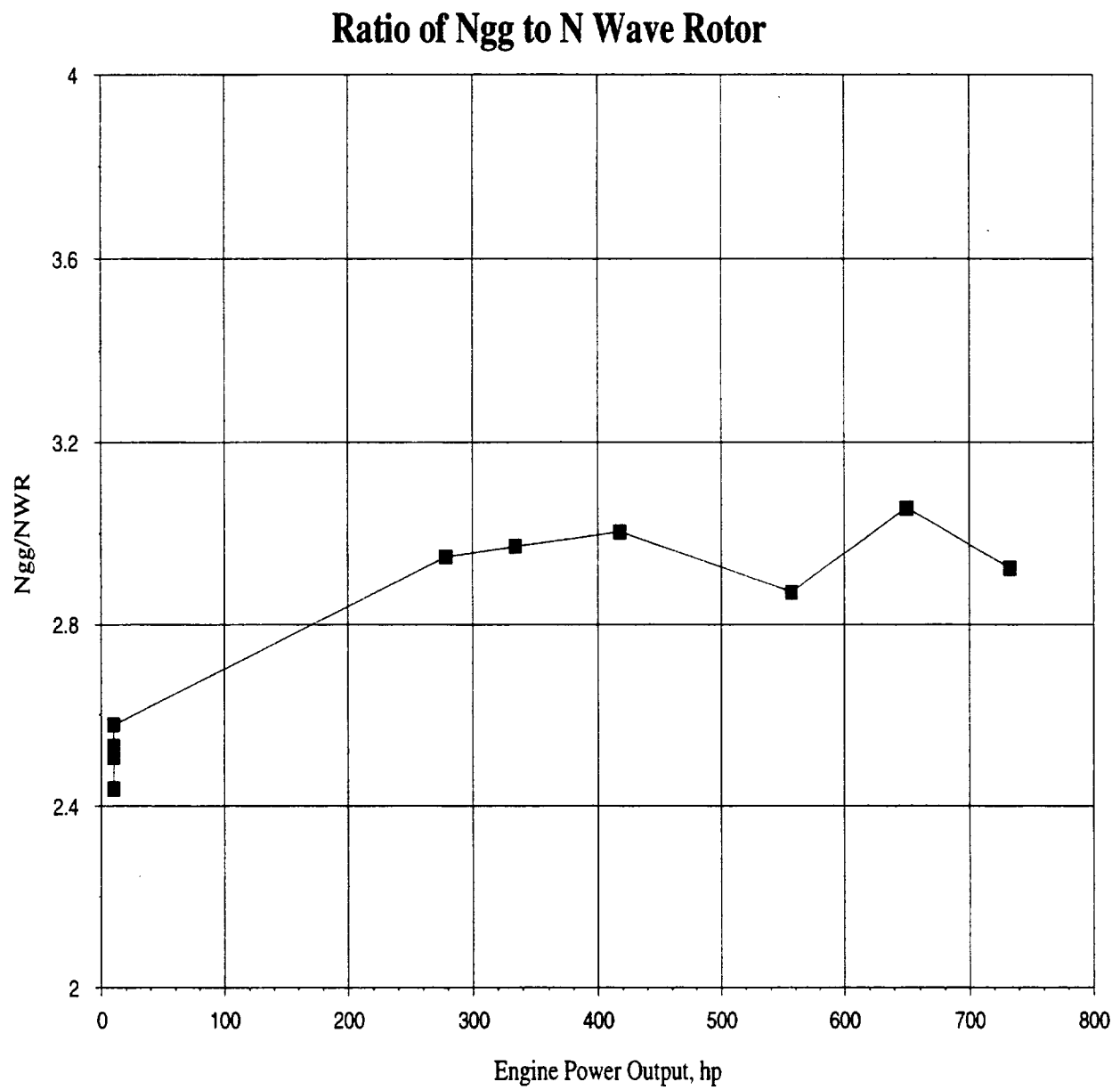


Figure 19. Comparison Of Rotational Speed Of Gasifier Spool and Wave Rotor.

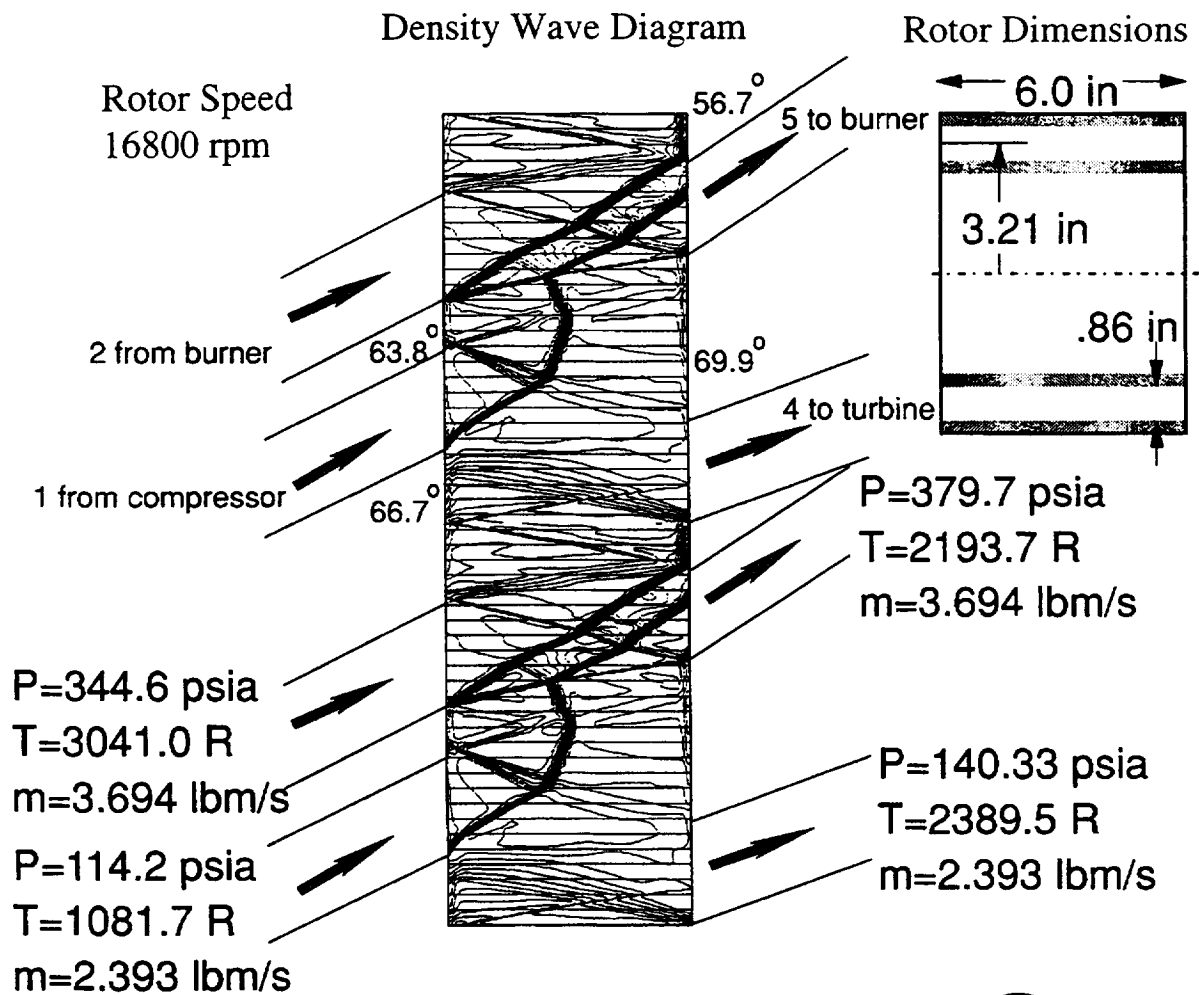


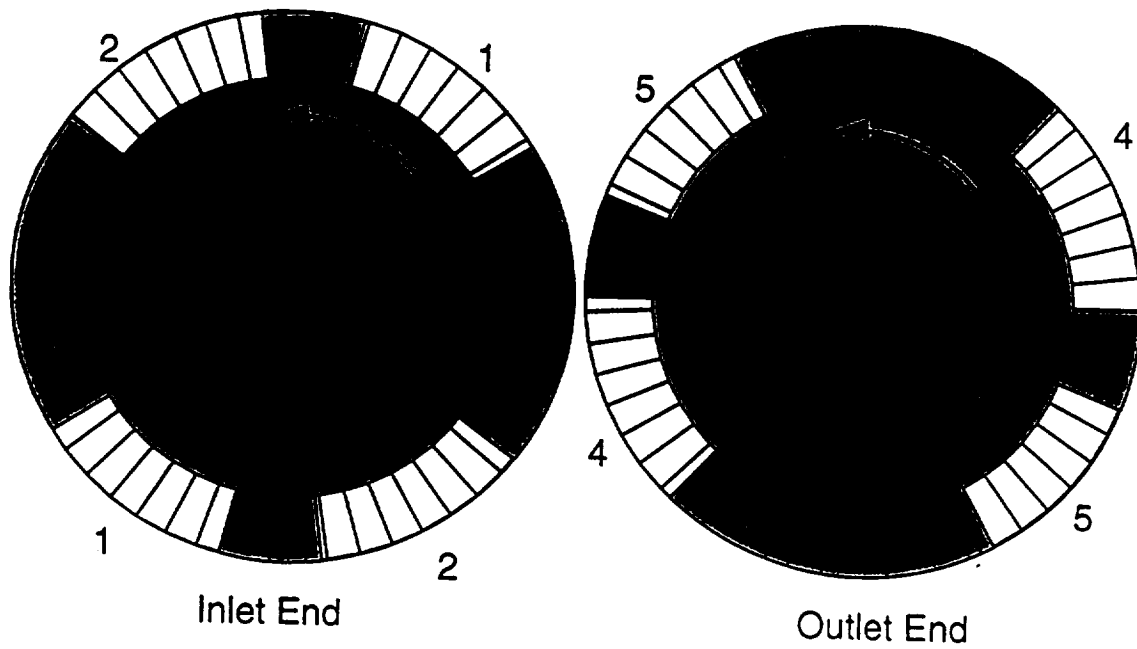
Figure 20. Wave Rotor Design, Wave Diagram and Rotor Dimensions:



Rotor Designed For Use In
Allison 250 Wave Rotor Demonstrator Engine



End Plate
Port Spacing



1 from compressor
2 from burner
4 to turbine
5 to burner

Figure 21. Wave Rotor Design, Rotor End View.

Rotor Designed For Use In
Allison 250 Wave Rotor Demonstrator Engine



End View of Rotor

52 passages
12% Blockage
due to Passage Walls

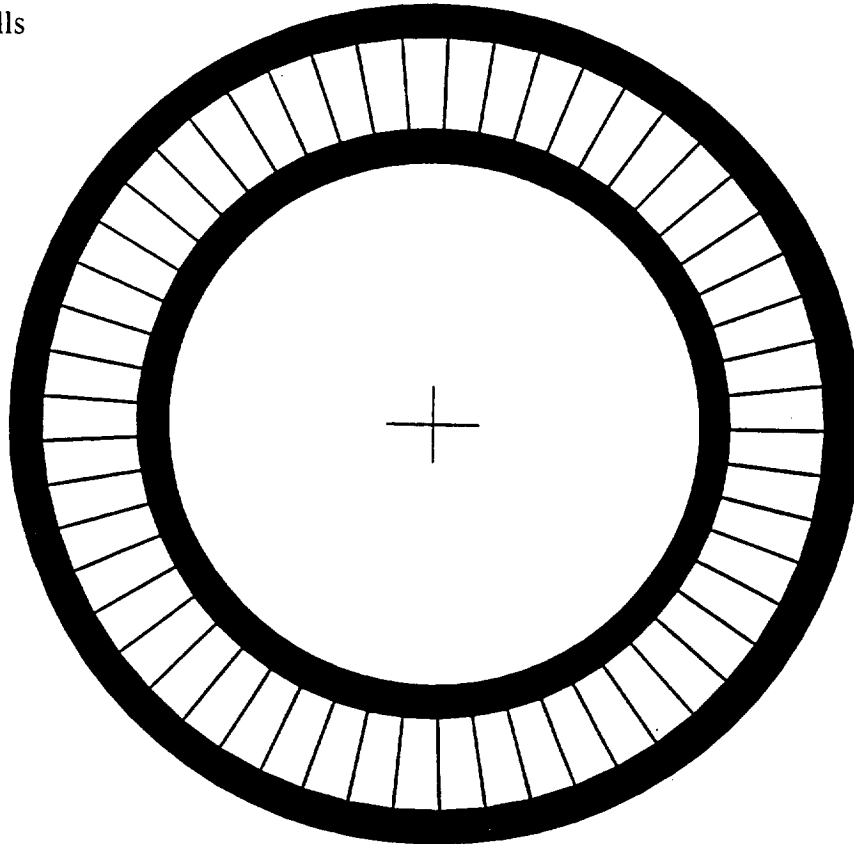


Figure 22. Wave Rotor Design, End Plate Port Location.

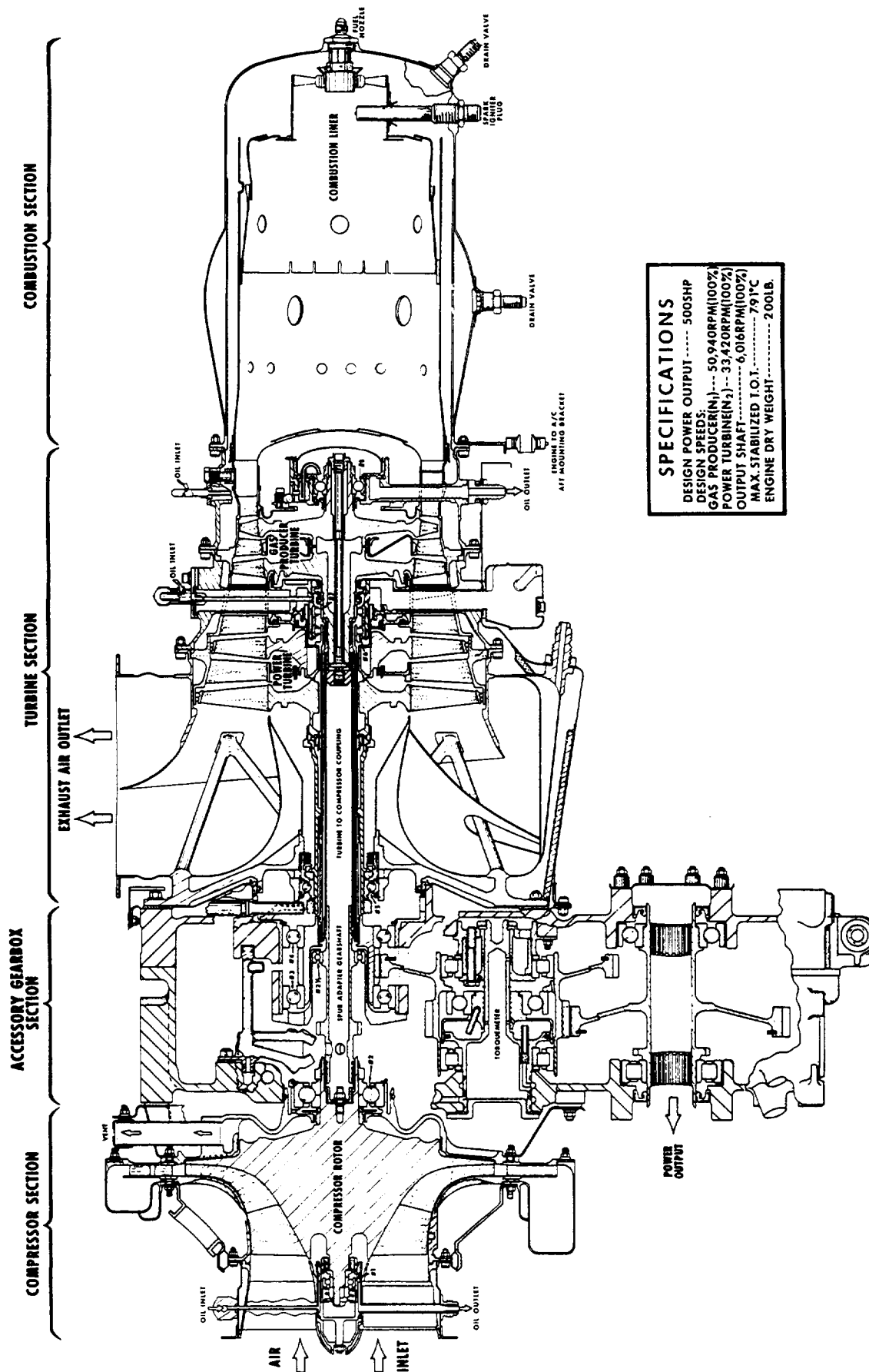


Figure 24. Allison Model 250-C28C Engine Cutaway Schematic.

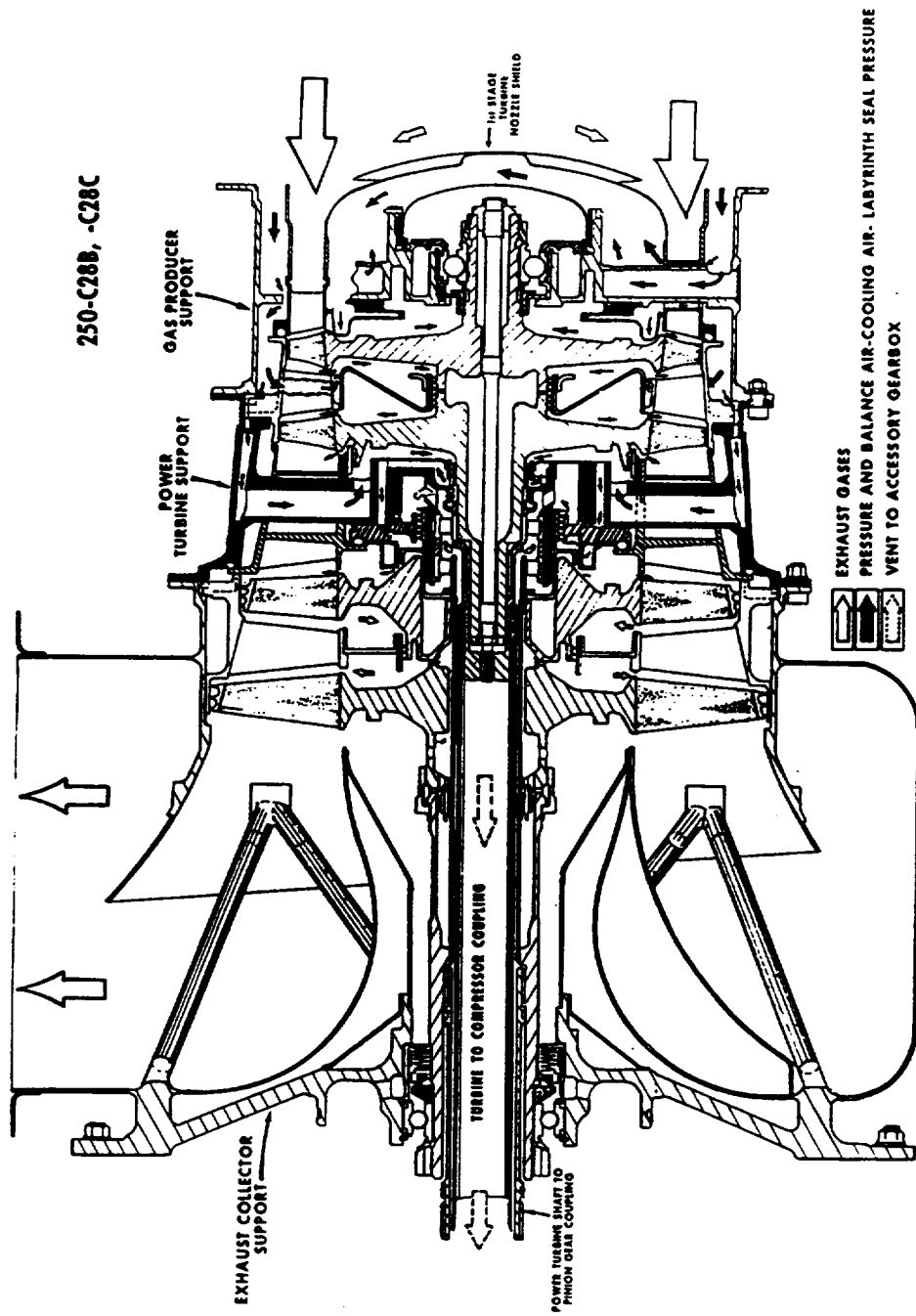


Figure 25. Turbine Cooling And Balance Air Schematic.

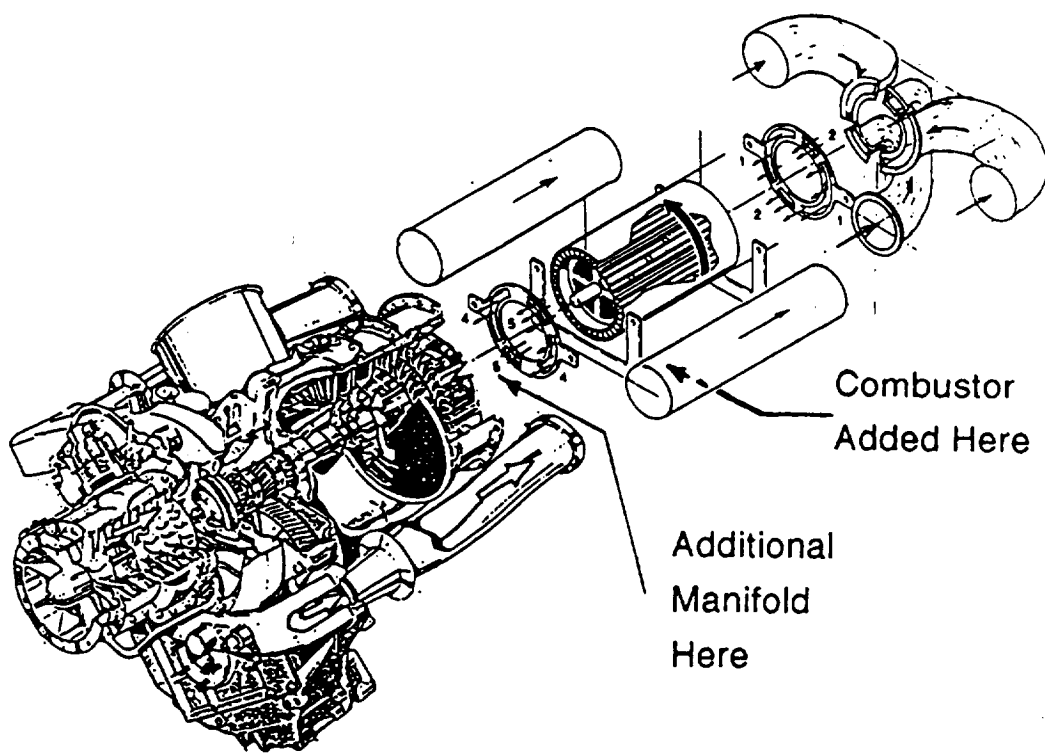


Figure 26. An Early Engine Layout Concept

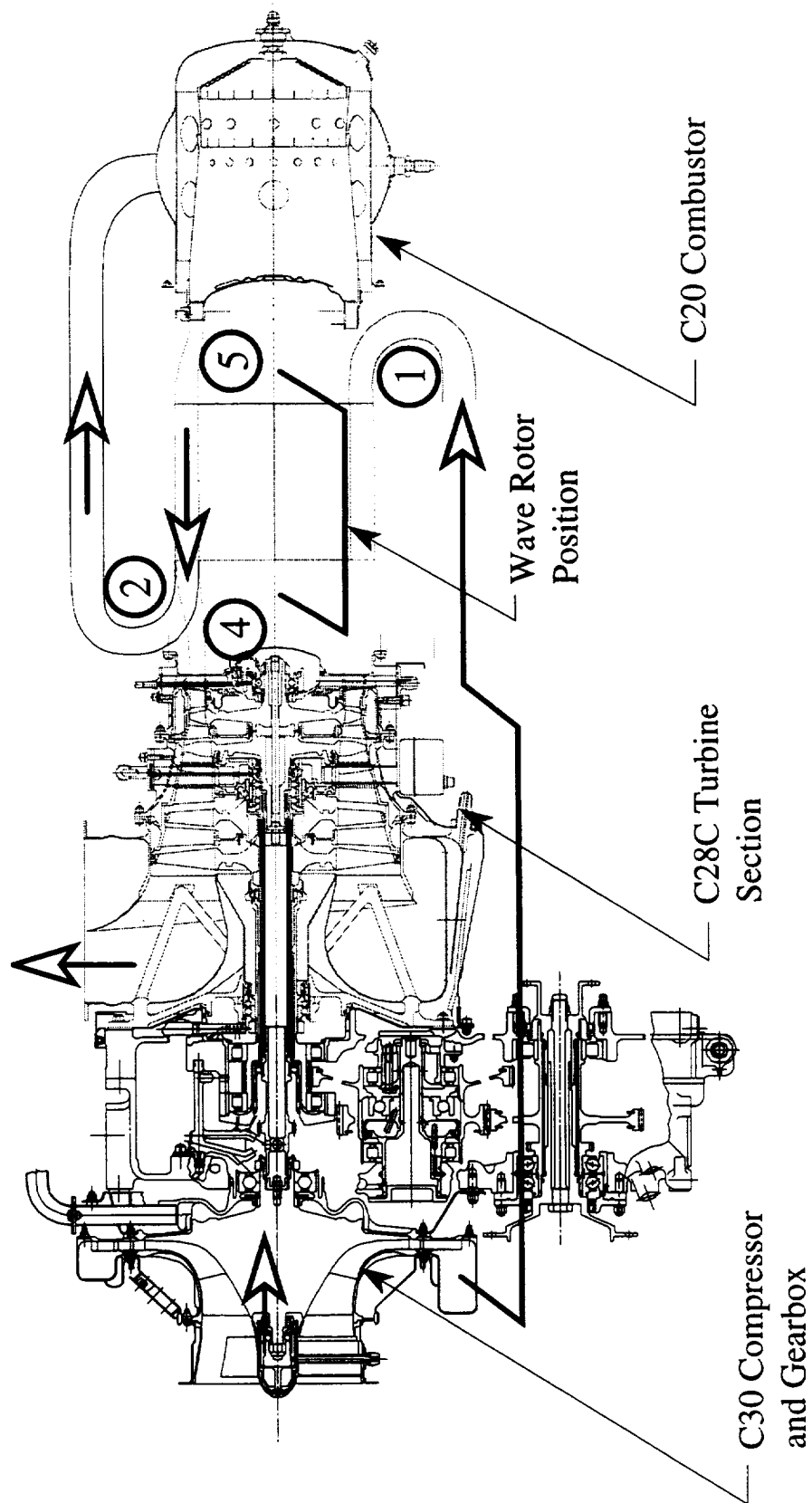


Figure 27. Proposed Demonstrator Engine Arrangement Using the Allison Model 250.

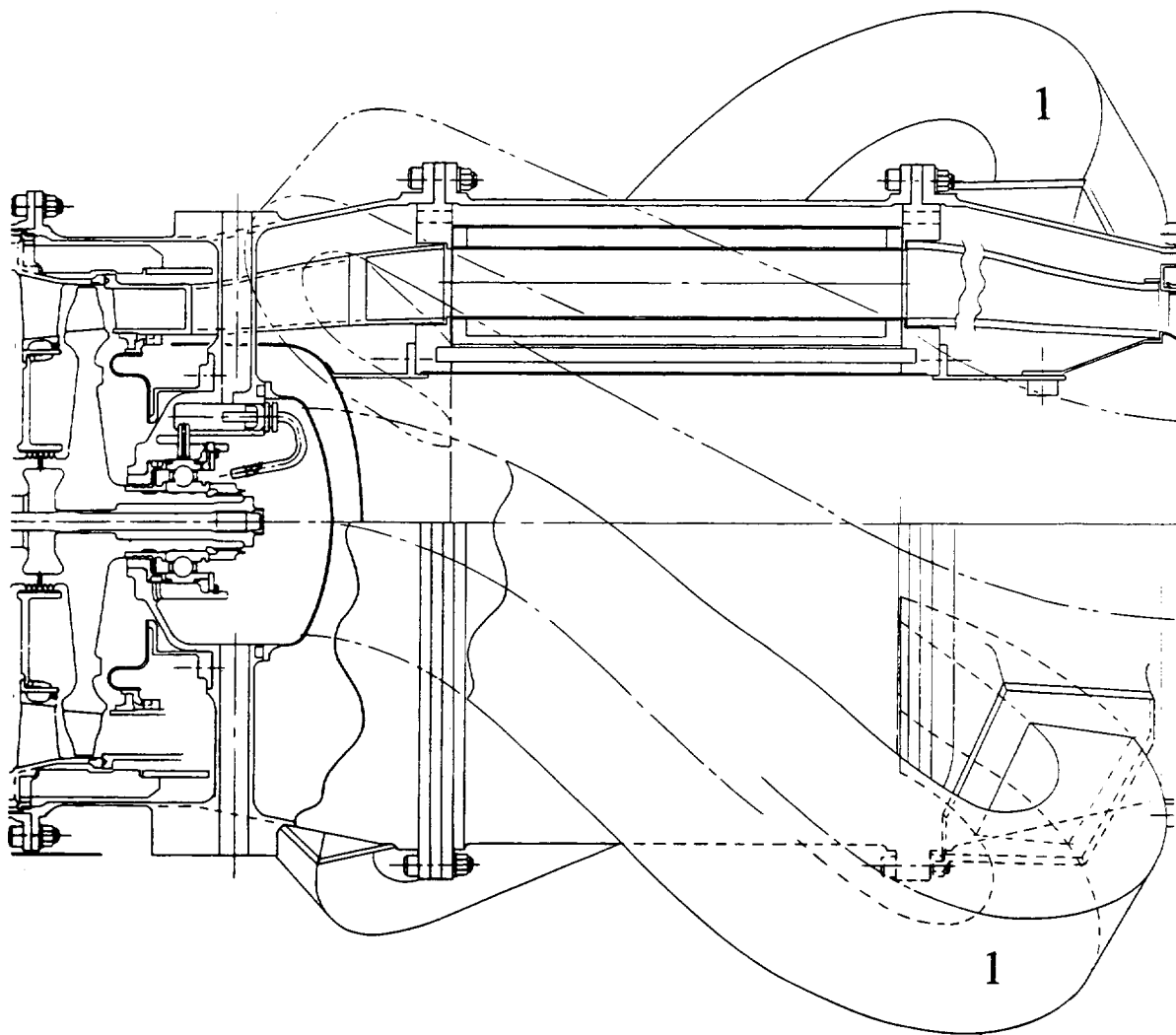


Figure 28. Port 1 Preliminary Design.

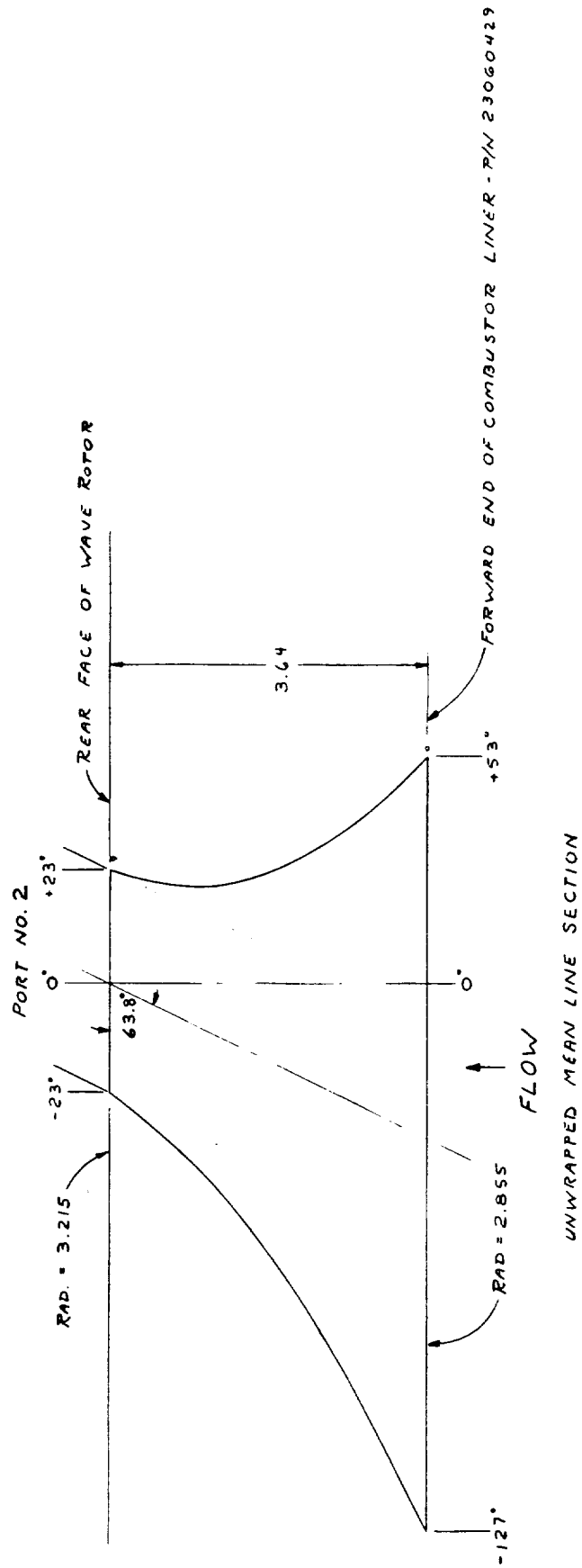


Figure 29. Port 2 Unwrapped Mean Line Section

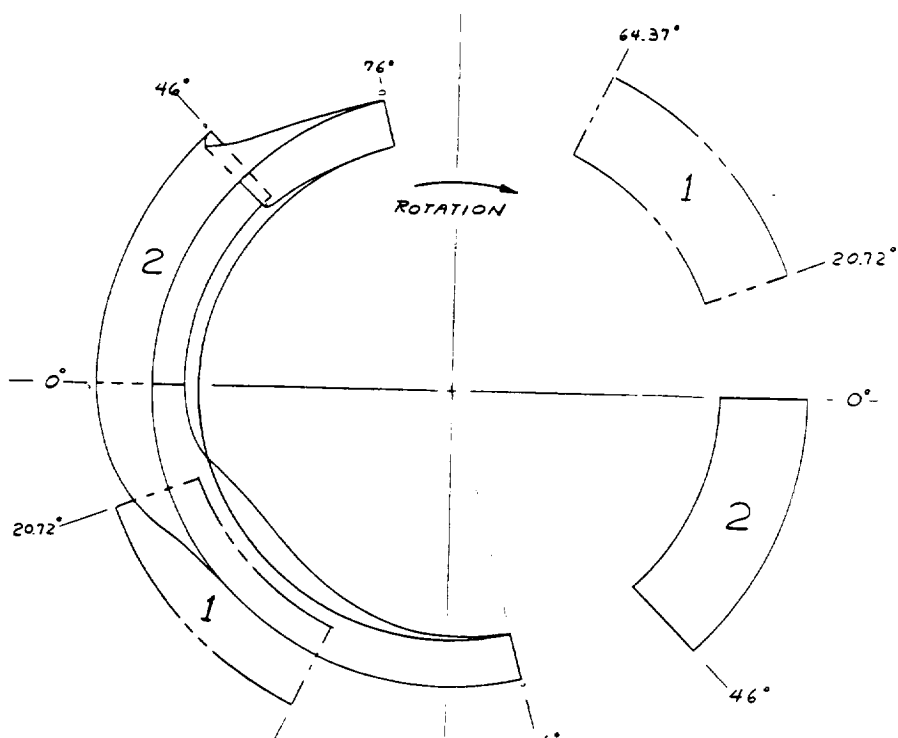
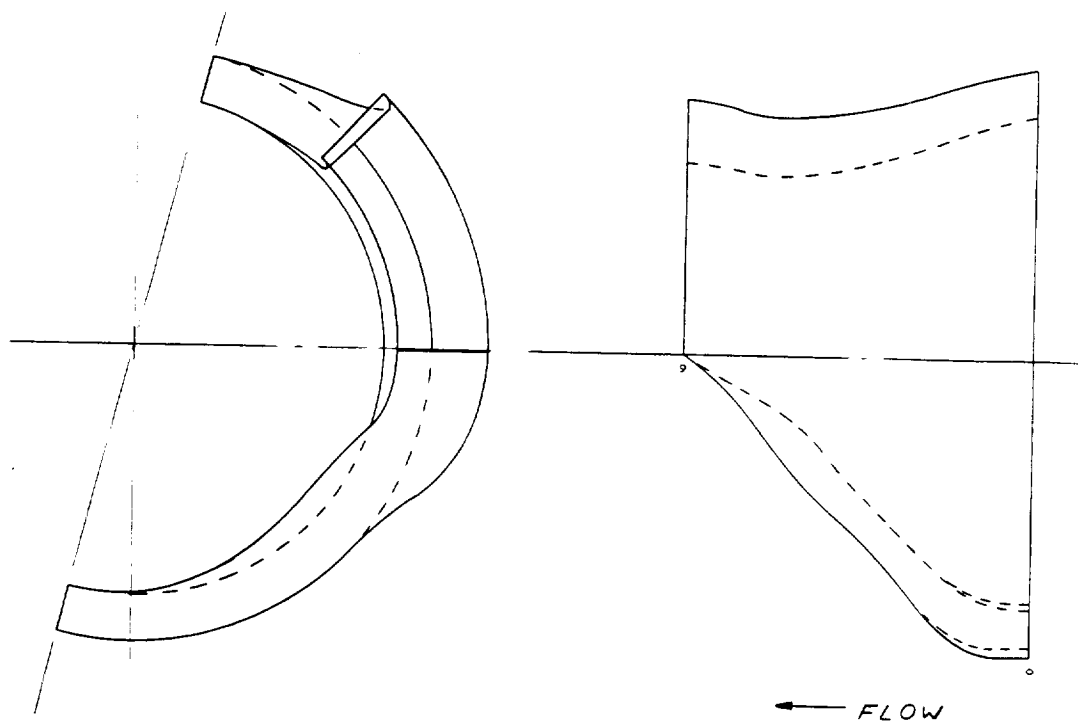
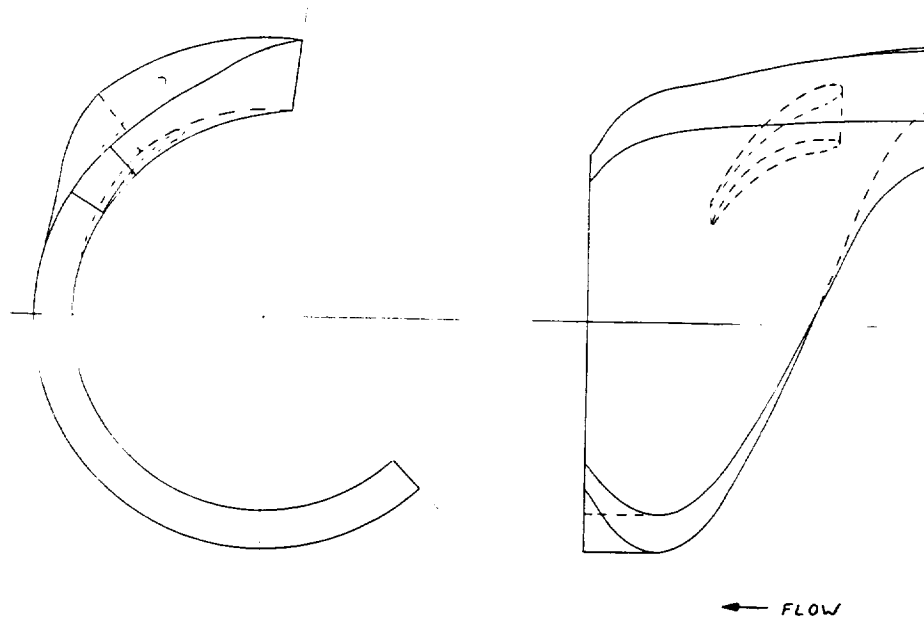


Figure 30. Port 2 Side And End Views.



NOTE: DUCT FLOW PATH CONTOUR SHOWN
ADD MATERIAL THICKNESS TO OUTSIDE OF FLOW PATH

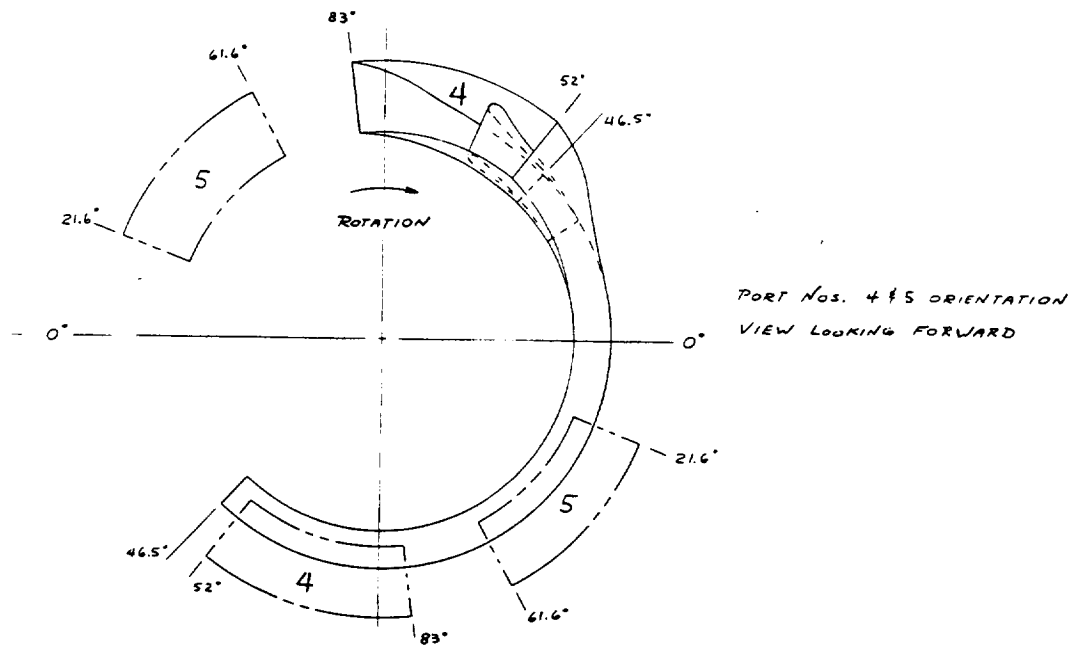


Figure 32. Port 3 Side And End Views.

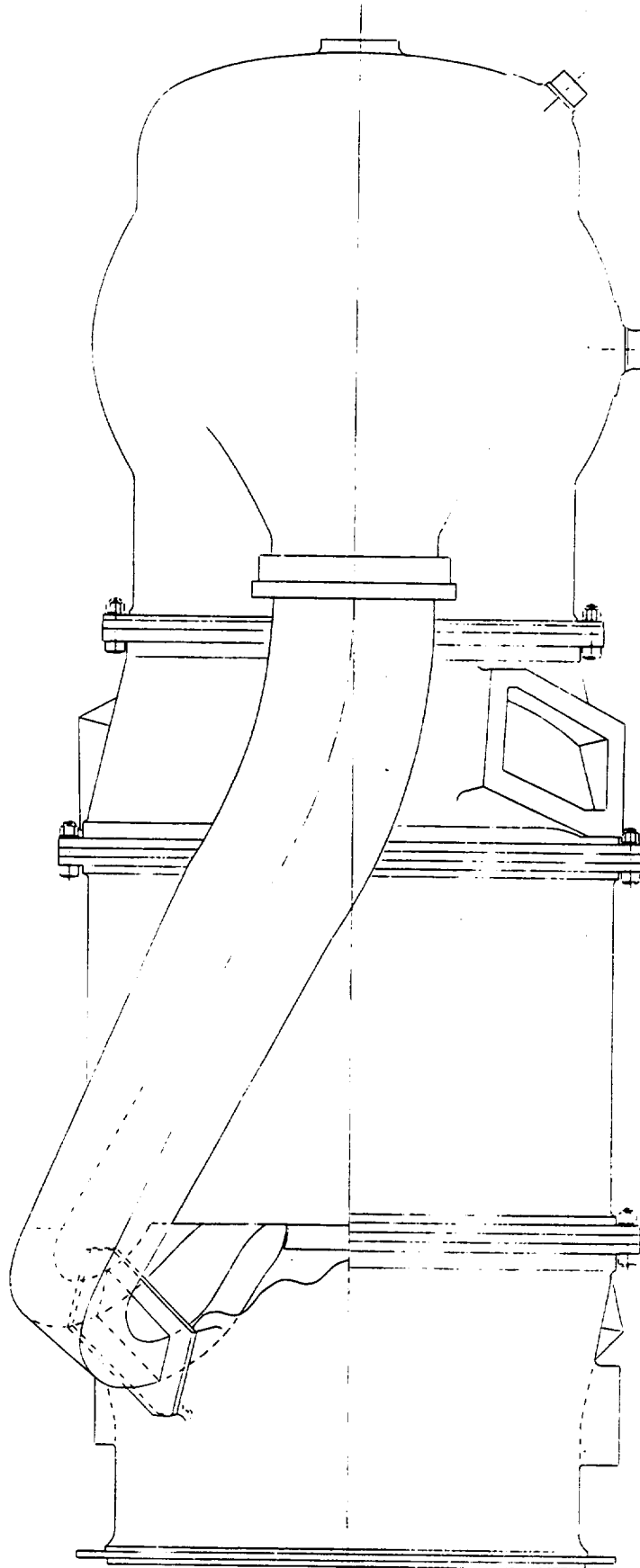


Figure 33. Port 5 Preliminary Design.

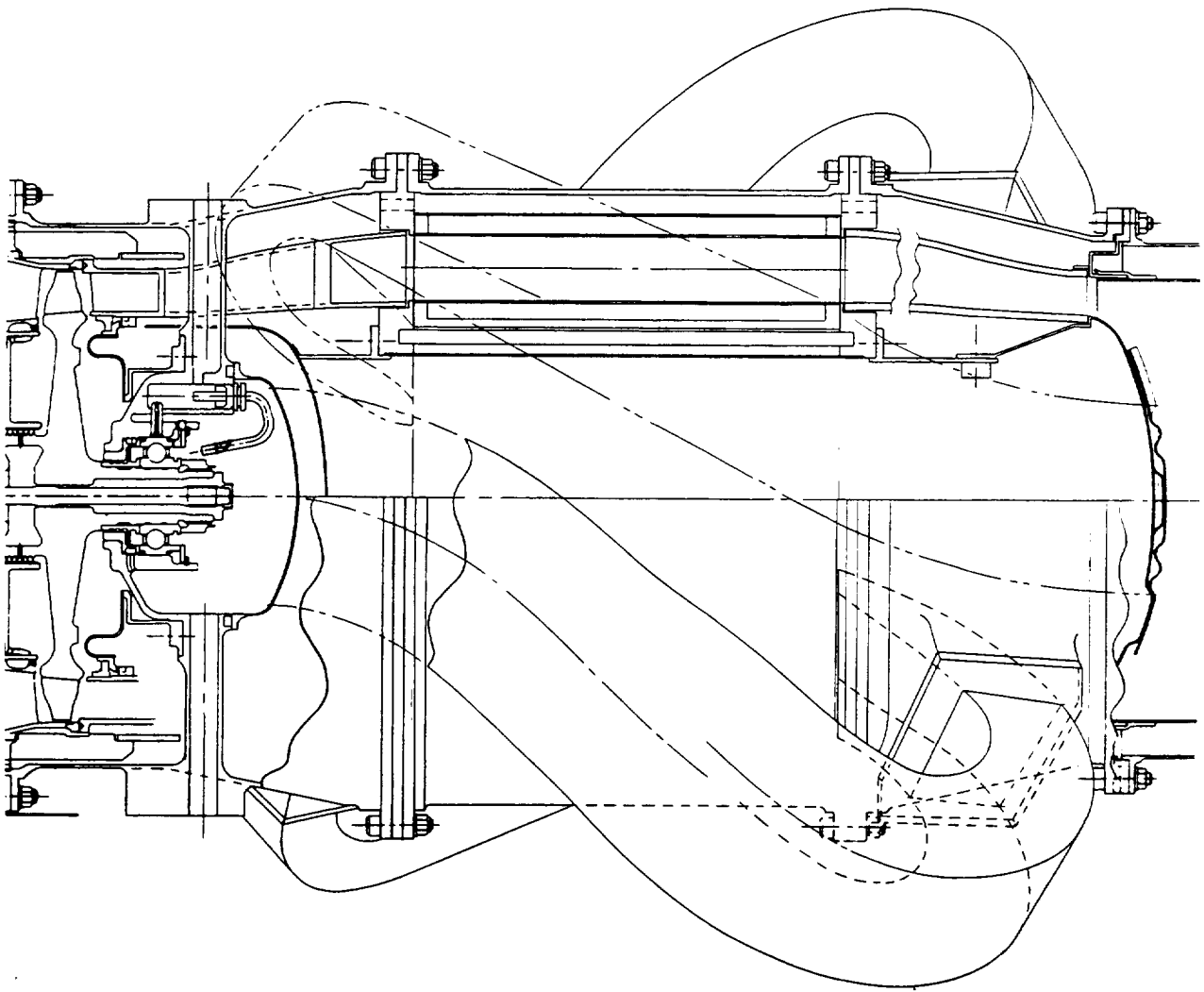


Figure 34. Cutaway View Of Wave Rotor Module Preliminary Design, Side View.

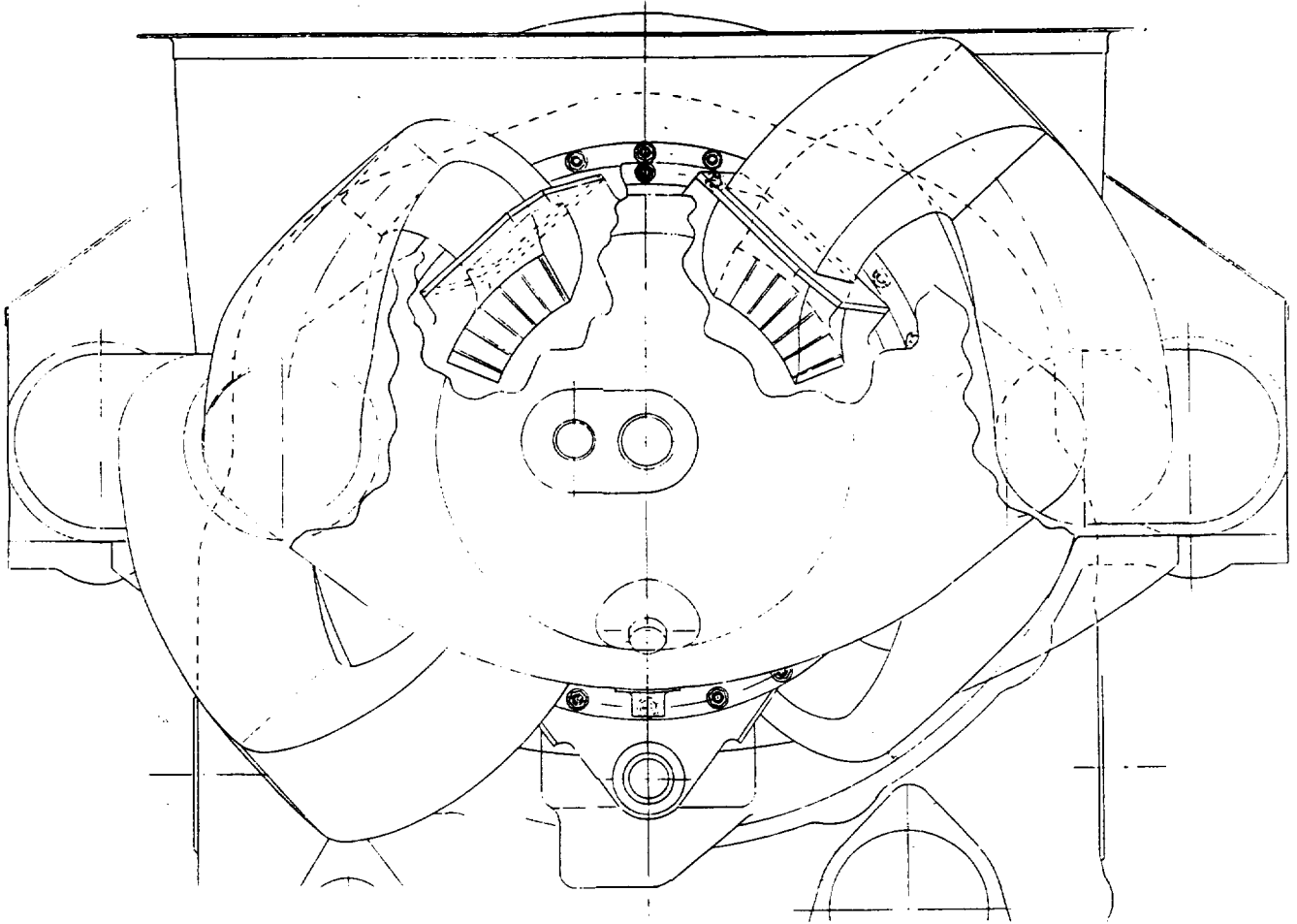


Figure 35. Cutaway View Of Wave Rotor Module Preliminary Design, End View.

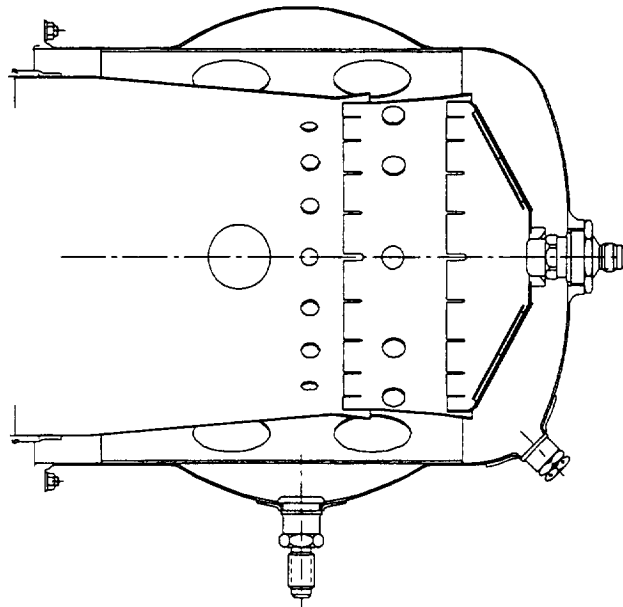


Figure 36. Production Model 250 R20 Combustor.

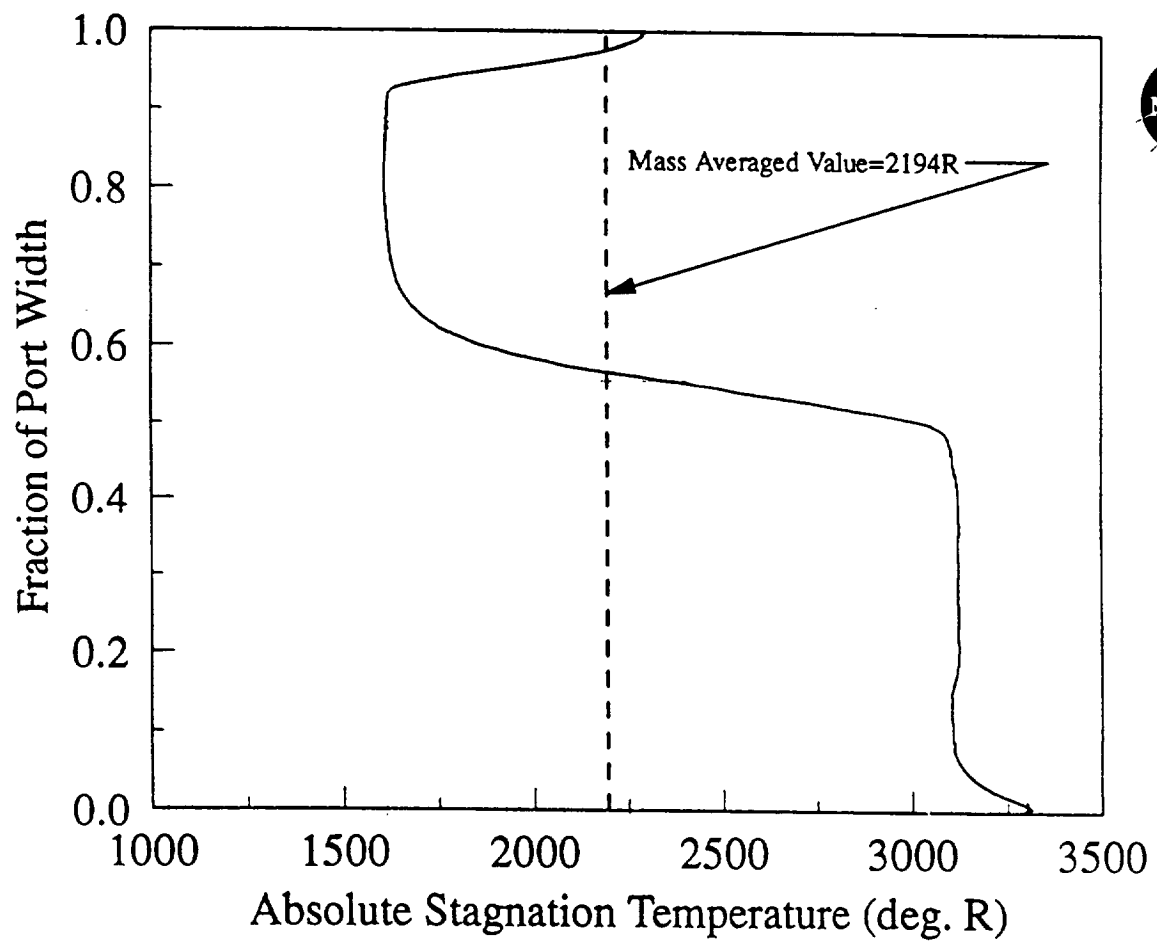


Figure 37. Port 5 Stagnation Temperature Distribution.

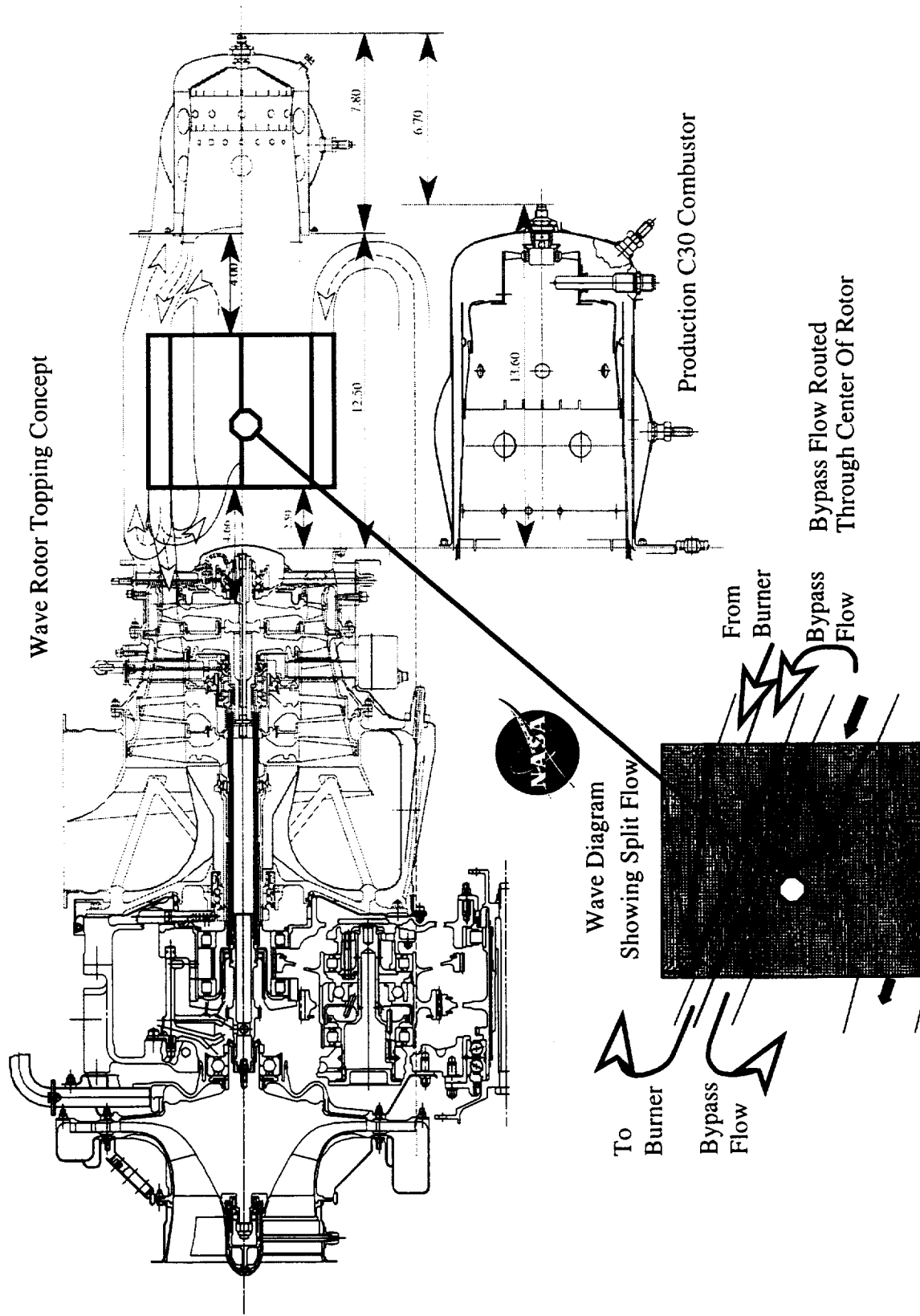


Figure 38. Through-Flow Split Port 5 Demonstrator Engine Design Concept.

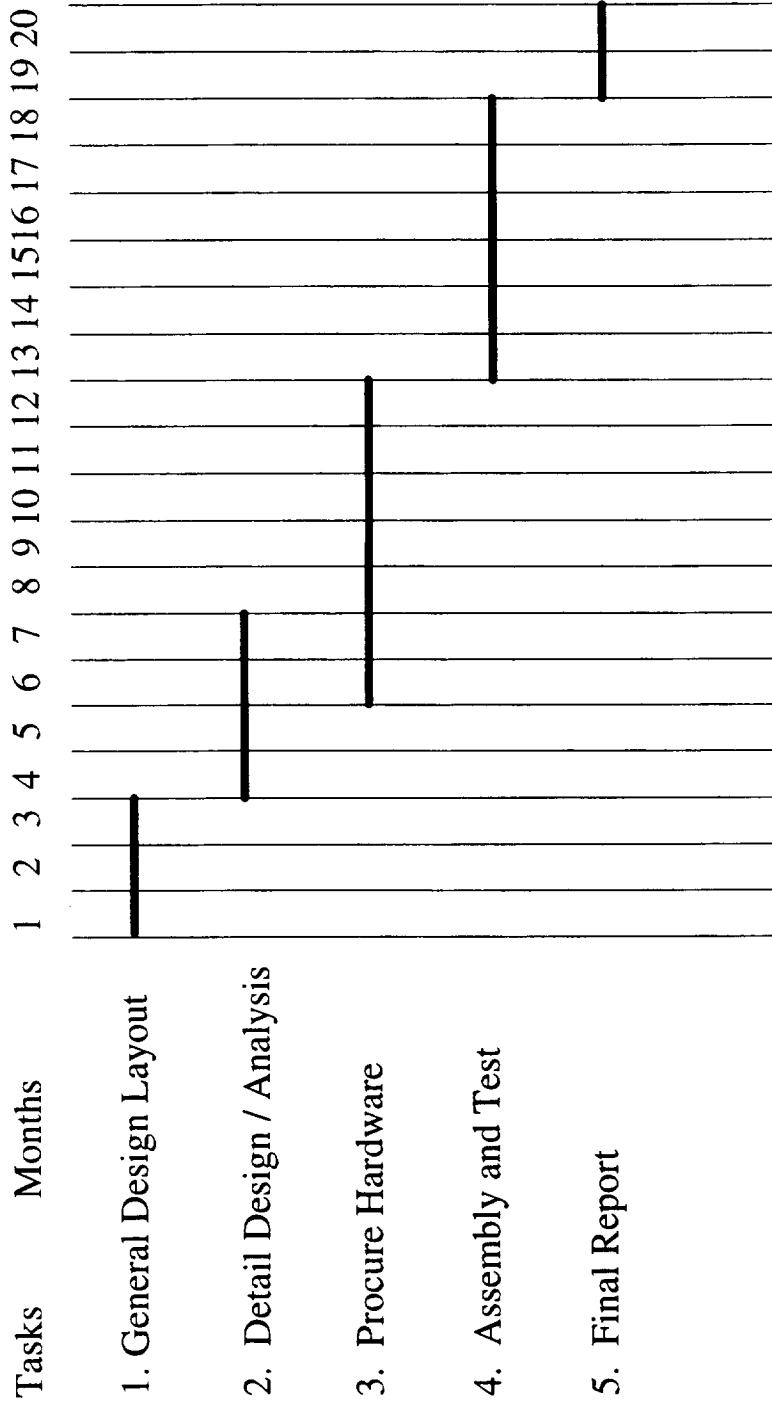


Figure 39. Model 250 Wave Rotor Demonstrator Engine Program Schedule Estimate.

Appendix A. NASA Generated Wave Rotor Design.

Optimized 250 Wave Rotor

An optimization procedure was performed for an Allison 250 based, 4-port, through-flow wave rotor (originally designed for approximately 4.0 lbm/s). Little performance difference was found between one and two cycle per rotor revolution designs. The two cycle design was selected because a) it commensurate with the ducting from the 250 compressor and b) it maintains the option of a reverse flow design if further investigation shows that cycle to be superior. The relevant geometry and design point information are presented below and shown in Figures 1-3.

radius=3.21 in.
 length=6.0 in.
 cycles per revolution=2
 omega=16800 rpm
 passage height=0.86490 in
 mass flow=4.785 lbm/s
 passages=52
 passage width= 0.3445 in
 web thickness=0.0434 in
 ratio of specific heats=1.353
 $P_{inlet}^o=114.2$ psia (reference pressure)
 $T_{inlet}^o=1081.7$ R (reference temperature)
 $T_{exhaust}^o=2390$ R
 $P_4/P_1=1.229$
 $T_4/T_1=2.209$
 viscosity= 2.734×10^{-5} lbm/ft/s (based on mean of inlet and exhaust)
 mean Pandtl #=.750
 web blockage=12.6%
 inlet port area=4.23 sq. in.

Below is sample output of the supplementary data for the design point.

QCORR	MFFRAC	MFC	PR	TR	OMEGA	P02	T02	P05	T05	WDOTIN	EPSLON
2.188	1.544	0.472	1.229	2.209	0.550	3.017	2.811	3.325	2.028	0.000	0.405

All of the data has been normalized by the inlet state shown above. The first column is the corrected heat addition which is defined as

$$QCORR = \frac{\dot{Q}}{P_{01} A_1 \sqrt{R T_{01} g_c}}$$

where A_1 is the inlet port area shown above, R is the real gas constant, P_{01} and T_{01} are the inlet stagnation pressure and temperature, \dot{Q} is the heat additions rate, and g_c is the Newton constant. The second column is the ratio of upper loop flow over throughflow. The third column is the corrected flow rate defined as

$$MFC = \frac{\dot{m} \sqrt{R T_{01}}}{P_{01} A_1 \sqrt{g_c}}$$

where \dot{m} is the mass flow rate. The values for PR and TR are the ratios of stagnation pressure and temperature across the entire machine (see Fig 3). OMEGA is the rotor non-dimensional rotor speed defined as

$$OMEGA = \frac{\omega L}{a_{01}}$$

where L is the rotor length, and a_{01} is the inlet stagnation speed of sound. P02 and T02 are the stagnation pressure and temperature coming from the burner (normalized by the inlet from the compressor-1). P05 and T05 represent the flow going to the combustor. EPSLON is the ratio of the exhaust port static pressure over the average pressure in the passage just before the exhaust port opens. The plots appearing in Figures 4-6 are reasonably self-explanatory. Leakage gaps of 0.005 in. were assumed since that is approximately where the NASA Phase 1 rotor is currently operating. The web blockage listed above should be used when calculating mass flows. That is, the mass flow obtained from the corrected flow rate above and the known area and inlet state should be reduced by 12.6% to get the true mass flow (this has worked well for the NASA experiment to date).

Note that Figures 4-6 are for a freewheeling wave rotor. It is not clear that this approach will work however, because it appears that as fuel flow is increased (i.e., increased heat addition) the corrected flow is reduced. This would seem to be precisely the opposite of what the surrounding turbomachinery requires. As such, maps and data which correspond to holding the rotor at fixed speeds are also included. The plots in Figures 7-10 show the performance on mass flow vs. pressure ratio curves for families of speed lines at 4 different fuel flow (heat addition) settings. Temperature ratio information can be found in the supplementary data. Note that the fixed speed supplementary data contains an extra column entitled WDOTIN. This is the ratio

$$WDOTIN = \frac{\dot{W}_{shaft}}{\dot{m} c_p T_{01}}$$

The speed labels on Figures 7-10 which have a (p) next to them indicate positive shaft work (i.e. a drive motor is required) all the rest show work is being extracted from the shaft.

Freewheel Performance Data

QCORR	MFRRAC	MFC	PR	TR	OMEGA	P02	T02	P05	T05
1.0775	0.9392	0.4992	0.9920	1.5654	0.4810	2.4442	2.4894	2.5980	1.8900
1.0775	0.9682	0.4941	1.0248	1.5704	0.4716	2.5107	2.4745	2.6630	1.8870
1.0775	0.9854	0.4780	1.0522	1.5863	0.4680	2.5327	2.5219	2.6840	1.9250
1.0775	1.0686	0.4468	1.0711	1.6259	0.4677	2.5298	2.5401	2.6880	1.9510
1.0775	1.2210	0.3993	1.0872	1.6997	0.4638	2.4959	2.5417	2.6610	1.9650
1.0775	1.2790	0.3755	1.0928	1.7437	0.4634	2.4630	2.5833	2.6280	1.9980
1.0775	1.3558	0.3352	1.0981	1.8317	0.4675	2.3895	2.7168	2.5490	2.0980
1.6163	1.0790	0.4960	1.0290	1.8532	0.5309	2.5607	2.7846	2.7780	1.9970
1.6163	1.1814	0.4935	1.0594	1.8574	0.5227	2.6452	2.6608	2.8750	1.9370
1.6163	1.2983	0.4906	1.0940	1.8624	0.5110	2.7581	2.5458	2.9980	1.8840
1.6163	1.3335	0.4856	1.1290	1.8701	0.5023	2.8280	2.5362	3.0650	1.8850
1.6163	1.3471	0.4648	1.1576	1.9048	0.4946	2.8501	2.6009	3.0810	1.9270
1.6163	1.3863	0.4497	1.1643	1.9341	0.4956	2.8374	2.6203	3.0700	1.9440
1.6163	1.4590	0.4282	1.1716	1.9812	0.4988	2.8138	2.6377	3.0520	1.9630
1.6163	1.5340	0.4054	1.1782	2.0365	0.5021	2.7844	2.6681	3.0270	1.9900
1.6163	1.5936	0.3847	1.1840	2.0920	0.5064	2.7513	2.7155	2.9960	2.0280
1.6163	1.6484	0.3633	1.1900	2.1561	0.5122	2.7123	2.7832	2.9570	2.0790
1.6163	1.6989	0.3416	1.1961	2.2297	0.5195	2.6696	2.8725	2.9120	2.1460
1.6163	1.7532	0.3189	1.2016	2.3165	0.5290	2.6221	2.9849	2.8610	2.2310
1.6163	1.8187	0.2939	1.2066	2.4281	0.5406	2.5712	3.1314	2.8030	2.3420
1.6163	1.9081	0.2647	1.2106	2.5846	0.5547	2.5188	3.3338	2.7390	2.4990
1.6163	2.0712	0.2203	1.2088	2.8990	0.5782	2.4331	3.7341	2.6330	2.8100
2.1550	1.1863	0.4834	1.0623	2.1613	0.5886	2.7533	3.1525	3.0140	2.1720
2.1550	1.2153	0.4814	1.0854	2.1673	0.5875	2.7763	3.1292	3.0400	2.1680
2.1550	1.2420	0.4783	1.1129	2.1749	0.5847	2.7952	3.1128	3.0610	2.1660
2.1550	1.2986	0.4744	1.1438	2.1881	0.5789	2.8311	3.0564	3.1030	2.1430
2.1550	1.3790	0.4695	1.1799	2.2013	0.5692	2.8758	2.9721	3.1560	2.1040
2.1550	1.4196	0.4677	1.1961	2.2063	0.5640	2.8994	2.9320	3.1840	2.0850
2.1550	1.5642	0.4650	1.2217	2.2122	0.5453	3.0184	2.8084	3.3230	2.0350
2.1550	1.6112	0.4490	1.2386	2.2504	0.5307	3.0752	2.8397	3.3800	2.0630
2.1550	1.6482	0.4342	1.2440	2.2913	0.5362	3.0480	2.8814	3.3540	2.0960
2.1550	1.6912	0.4182	1.2487	2.3410	0.5420	3.0199	2.9319	3.3280	2.1370
2.1550	1.7407	0.3998	1.2536	2.4026	0.5477	2.9908	2.9966	3.3010	2.1890
2.1550	1.7946	0.3799	1.2587	2.4760	0.5545	2.9577	3.0757	3.2680	2.2510
2.1550	1.8510	0.3595	1.2636	2.5600	0.5629	2.9190	3.1673	3.2280	2.3220
2.1550	1.9162	0.3367	1.2672	2.6651	0.5738	2.8702	3.2827	3.1780	2.4110
2.1550	1.9922	0.3113	1.2701	2.8000	0.5873	2.8124	3.4319	3.1170	2.5250
2.1550	2.0869	0.2826	1.2717	2.9822	0.6053	2.7433	3.6346	3.0420	2.6810
2.1550	2.2143	0.2485	1.2711	3.2524	0.6313	2.6576	3.9392	2.9460	2.9170
2.1550	2.3867	0.2016	1.2670	3.7692	0.6737	2.5371	4.5483	2.8030	3.3800
2.6937	1.3970	0.4721	1.1065	2.4854	0.6244	2.9928	3.3117	3.3110	2.2460
2.6937	1.4257	0.4705	1.1264	2.4932	0.6236	3.0178	3.2939	3.3400	2.2460
2.6937	1.4627	0.4673	1.1508	2.4997	0.6229	3.0446	3.2769	3.3710	2.2490
2.6937	1.5003	0.4639	1.1769	2.5124	0.6215	3.0705	3.2650	3.4010	2.2550
2.6937	1.5354	0.4592	1.2052	2.5298	0.6196	3.0888	3.2607	3.4230	2.2640
2.6937	1.5469	0.4569	1.2172	2.5375	0.6185	3.0922	3.2626	3.4280	2.2680
2.6937	1.5688	0.4533	1.2335	2.5484	0.6169	3.1010	3.2629	3.4370	2.2750
2.6937	1.5918	0.4498	1.2487	2.5608	0.6158	3.1093	3.2640	3.4480	2.2820
2.6937	1.6112	0.4464	1.2616	2.5727	0.6151	3.1148	3.2675	3.4550	2.2910
2.6937	1.6314	0.4425	1.2743	2.5864	0.6147	3.1186	3.2746	3.4590	2.3010
2.6937	1.6539	0.4384	1.2881	2.6009	0.6132	3.1238	3.2819	3.4650	2.3130
2.6937	1.6842	0.4305	1.3046	2.6304	0.6045	3.1314	3.2979	3.4720	2.3290
2.6937	1.7183	0.4125	1.3109	2.6995	0.6080	3.0926	3.3698	3.4340	2.3780
2.6937	1.7556	0.3944	1.3150	2.7785	0.6160	3.0529	3.4560	3.3950	2.4410
2.6937	1.8057	0.3742	1.3190	2.8746	0.6249	3.0125	3.5587	3.3550	2.5190
2.6937	1.8678	0.3509	1.3217	2.9975	0.6364	2.9652	3.6950	3.3090	2.6230
2.6937	1.9450	0.3246	1.3232	3.1594	0.6514	2.9099	3.8733	3.2540	2.7600
2.6937	2.0480	0.2935	1.3226	3.3881	0.6723	2.8435	4.1279	3.1850	2.9590
3.2325	1.5396	0.4619	1.1437	2.8261	0.6658	3.2029	3.6576	3.5710	2.4710
3.2325	1.5571	0.4583	1.1612	2.8349	0.6699	3.2098	3.6643	3.5800	2.4830
3.2325	1.5791	0.4565	1.1818	2.8441	0.6698	3.2308	3.6639	3.6030	2.4930
3.2325	1.6063	0.4538	1.2051	2.8575	0.6708	3.2530	3.6661	3.6290	2.5080
3.2325	1.6423	0.4491	1.2320	2.8749	0.6716	3.2758	3.6745	3.6560	2.5300
3.2325	1.6574	0.4468	1.2431	2.8834	0.6717	3.2838	3.6795	3.6660	2.5400
3.2325	1.6780	0.4435	1.2574	2.8986	0.6725	3.2929	3.6895	3.6770	2.5560
3.2325	1.6976	0.4400	1.2713	2.9124	0.6726	3.3003	3.6994	3.6870	2.5700
3.2325	1.7106	0.4371	1.2831	2.9262	0.6725	3.3025	3.7081	3.6910	2.5800

Freewheel Performance Data

3.2325	1.7225	0.4342	1.2959	2.9384	0.6709	3.3039	3.7161	3.6920	2.5880
3.2325	1.7375	0.4306	1.3087	2.9535	0.6701	3.3053	3.7273	3.6960	2.6000
3.2325	1.7544	0.4268	1.3211	2.9714	0.6697	3.3063	3.7414	3.6970	2.6150
3.2325	1.7737	0.4221	1.3335	2.9937	0.6693	3.3067	3.7610	3.6980	2.6340
3.2325	1.7947	0.4160	1.3454	3.0236	0.6685	3.3043	3.7894	3.6940	2.6590
3.2325	1.8164	0.4045	1.3547	3.0796	0.6697	3.2826	3.8486	3.6700	2.7010
3.2325	1.8401	0.3872	1.3590	3.1738	0.6774	3.2328	3.9503	3.6170	2.7670
3.2325	1.8716	0.3660	1.3610	3.2985	0.6896	3.1687	4.0890	3.5510	2.8580
3.2325	1.9093	0.3407	1.3619	3.4706	0.7047	3.0870	4.2811	3.4670	2.9850
3.2325	1.9597	0.3094	1.3597	3.7204	0.7282	2.9799	4.5679	3.3540	3.1770
3.2325	2.0391	0.2714	1.3558	4.0979	0.7614	2.8560	5.0090	3.2180	3.4850
3.2325	2.2180	0.2250	1.3516	4.7294	0.8048	2.7431	5.7203	3.0890	4.0310

Fixed Speed Performance Data

QCORR	MFFRAC	MFC	PR	TR	OMEGA	P02	T02	P05	T05	WDOTIN
1.616	1.179	0.521	1.037	1.804	0.440	2.892	2.455	3.124	1.768	-0.006
1.616	1.178	0.519	1.047	1.806	0.440	2.899	2.463	3.130	1.773	-0.006
1.616	1.180	0.515	1.067	1.811	0.440	2.911	2.479	3.140	1.786	-0.006
1.616	1.185	0.508	1.088	1.822	0.440	2.919	2.503	3.146	1.803	-0.006
1.616	1.199	0.495	1.109	1.842	0.440	2.915	2.535	3.144	1.825	-0.006
1.616	1.248	0.473	1.125	1.881	0.440	2.899	2.562	3.131	1.848	-0.006
1.616	1.276	0.506	1.013	1.834	0.495	2.748	2.466	2.985	1.812	-0.002
1.616	1.284	0.505	1.028	1.835	0.495	2.762	2.465	3.000	1.814	-0.002
1.616	1.297	0.502	1.050	1.838	0.495	2.785	2.468	3.023	1.820	-0.002
1.616	1.309	0.499	1.076	1.843	0.495	2.810	2.478	3.048	1.833	-0.002
1.616	1.319	0.494	1.104	1.850	0.495	2.834	2.498	3.071	1.851	-0.001
1.616	1.328	0.486	1.133	1.865	0.495	2.853	2.533	3.087	1.879	-0.001
1.616	1.348	0.465	1.158	1.904	0.495	2.850	2.600	3.081	1.927	0.000
1.616	1.389	0.449	1.164	1.937	0.495	2.838	2.620	3.071	1.943	0.000
1.616	1.476	0.422	1.171	1.994	0.495	2.813	2.637	3.053	1.961	-0.001
1.616	1.560	0.391	1.177	2.071	0.495	2.771	2.692	3.017	2.001	-0.002
1.616	1.617	0.360	1.182	2.162	0.495	2.717	2.796	2.963	2.071	-0.003
1.616	0.911	0.495	1.001	1.852	0.550	2.435	3.108	2.631	2.172	0.001
1.616	0.936	0.492	1.020	1.857	0.550	2.455	3.081	2.655	2.166	0.001
1.616	0.974	0.488	1.046	1.865	0.550	2.486	3.047	2.690	2.159	0.002
1.616	1.017	0.483	1.074	1.875	0.550	2.524	3.015	2.733	2.157	0.002
1.616	1.069	0.477	1.106	1.887	0.550	2.565	2.981	2.780	2.154	0.003
1.616	1.123	0.468	1.138	1.905	0.550	2.608	2.964	2.825	2.162	0.004
1.616	1.145	0.463	1.151	1.915	0.550	2.623	2.968	2.839	2.172	0.004
1.616	1.181	0.452	1.166	1.936	0.550	2.638	2.976	2.855	2.186	0.005
1.616	1.249	0.436	1.176	1.972	0.550	2.648	2.963	2.869	2.188	0.006
1.616	1.334	0.418	1.183	2.013	0.550	2.652	2.935	2.879	2.179	0.006
1.616	1.429	0.400	1.190	2.060	0.550	2.654	2.909	2.886	2.171	0.006
1.616	1.538	0.379	1.196	2.117	0.550	2.651	2.892	2.887	2.168	0.006
1.616	1.668	0.353	1.203	2.197	0.550	2.641	2.898	2.880	2.181	0.005
1.616	1.812	0.314	1.207	2.343	0.550	2.598	3.006	2.834	2.264	0.003
2.155	1.286	0.522	1.110	2.069	0.440	3.177	2.682	3.472	1.843	-0.009
2.155	1.288	0.521	1.117	2.071	0.440	3.182	2.684	3.475	1.845	-0.009
2.155	1.295	0.516	1.136	2.079	0.440	3.192	2.693	3.484	1.852	-0.008
2.155	1.305	0.509	1.155	2.094	0.440	3.197	2.710	3.488	1.864	-0.009
2.155	1.325	0.496	1.173	2.120	0.440	3.189	2.737	3.482	1.882	-0.009
2.155	1.372	0.472	1.186	2.176	0.440	3.158	2.783	3.458	1.914	-0.010
2.155	1.445	0.428	1.192	2.296	0.440	3.070	2.896	3.377	1.987	-0.010
2.155	1.430	0.506	1.090	2.106	0.495	3.087	2.709	3.384	1.932	-0.005
2.155	1.435	0.505	1.101	2.109	0.495	3.096	2.709	3.394	1.933	-0.005
2.155	1.444	0.504	1.121	2.114	0.495	3.112	2.709	3.412	1.935	-0.005
2.155	1.453	0.501	1.145	2.118	0.495	3.131	2.711	3.433	1.939	-0.005
2.155	1.463	0.496	1.172	2.128	0.495	3.148	2.722	3.450	1.947	-0.005
2.155	1.476	0.487	1.198	2.150	0.495	3.158	2.745	3.458	1.963	-0.004
2.155	1.510	0.463	1.219	2.205	0.495	3.136	2.806	3.438	2.001	-0.004
2.155	1.551	0.444	1.223	2.257	0.495	3.109	2.854	3.418	2.037	-0.006
2.155	1.611	0.416	1.228	2.341	0.495	3.065	2.937	3.382	2.098	-0.007
2.155	1.670	0.381	1.234	2.459	0.495	2.995	3.064	3.316	2.182	-0.009
2.155	1.708	0.351	1.235	2.586	0.495	2.921	3.203	3.234	2.264	-0.009
2.155	1.345	0.493	1.066	2.141	0.550	2.868	2.839	3.148	1.991	-0.003
2.155	1.355	0.491	1.084	2.145	0.550	2.877	2.840	3.158	1.995	-0.003
2.155	1.370	0.489	1.107	2.149	0.550	2.889	2.840	3.171	2.000	-0.003
2.155	1.393	0.485	1.133	2.157	0.550	2.905	2.838	3.189	2.006	-0.002
2.155	1.428	0.480	1.161	2.170	0.550	2.925	2.833	3.212	2.012	-0.001
2.155	1.481	0.473	1.191	2.187	0.550	2.955	2.824	3.248	2.021	-0.001
2.155	1.507	0.470	1.204	2.195	0.550	2.969	2.821	3.266	2.027	-0.001
2.155	1.541	0.465	1.220	2.208	0.550	2.988	2.822	3.289	2.037	0.000
2.155	1.570	0.458	1.234	2.226	0.550	3.003	2.834	3.305	2.052	0.001
2.155	1.603	0.448	1.244	2.254	0.550	3.009	2.856	3.312	2.073	0.002
2.155	1.663	0.428	1.249	2.313	0.550	3.003	2.907	3.309	2.116	0.001
2.155	1.734	0.403	1.254	2.393	0.550	2.989	2.986	3.298	2.181	0.000
2.155	1.806	0.372	1.258	2.505	0.550	2.955	3.108	3.267	2.272	-0.001
2.155	1.866	0.332	1.263	2.682	0.550	2.874	3.307	3.187	2.399	-0.004
2.155	1.053	0.482	1.054	2.166	0.605	2.653	3.434	2.897	2.326	0.002
2.155	1.084	0.479	1.077	2.175	0.605	2.676	3.406	2.923	2.322	0.002
2.155	1.094	0.474	1.103	2.186	0.605	2.682	3.429	2.929	2.345	0.002
2.155	1.107	0.469	1.132	2.200	0.605	2.686	3.458	2.934	2.373	0.002
2.155	1.136	0.462	1.164	2.219	0.605	2.699	3.466	2.950	2.394	0.002

Fixed Speed Performance Data

2.155	1.152	0.459	1.178	2.228	0.605	2.706	3.466	2.959	2.402	0.003
2.155	1.181	0.454	1.195	2.240	0.605	2.719	3.454	2.975	2.406	0.003
2.155	1.220	0.449	1.210	2.256	0.605	2.738	3.425	2.998	2.399	0.004
2.155	1.256	0.444	1.223	2.272	0.605	2.755	3.405	3.017	2.397	0.004
2.155	1.288	0.435	1.234	2.297	0.605	2.762	3.411	3.025	2.408	0.005
2.155	1.344	0.420	1.243	2.342	0.605	2.759	3.412	3.027	2.417	0.006
2.155	1.428	0.403	1.250	2.399	0.605	2.758	3.386	3.033	2.410	0.006
2.155	1.529	0.385	1.257	2.464	0.605	2.758	3.355	3.040	2.400	0.005
2.155	1.653	0.365	1.265	2.544	0.605	2.757	3.330	3.046	2.397	0.005
2.155	1.829	0.338	1.270	2.664	0.605	2.762	3.335	3.059	2.426	0.004
2.155	2.087	0.282	1.272	2.988	0.605	2.742	3.641	3.040	2.685	0.000
2.155	0.586	0.429	1.082	2.322	0.715	2.346	6.643	2.524	4.412	0.010
2.155	0.548	0.436	1.048	2.300	0.715	2.301	6.816	2.475	4.455	0.011
2.155	0.587	0.429	1.082	2.321	0.715	2.347	6.643	2.523	4.413	0.010
2.155	0.629	0.423	1.118	2.341	0.715	2.392	6.481	2.573	4.372	0.011
2.155	0.661	0.415	1.154	2.368	0.715	2.435	6.459	2.618	4.413	0.013
2.155	0.681	0.407	1.165	2.397	0.715	2.449	6.448	2.636	4.424	0.014
2.155	0.721	0.394	1.177	2.445	0.715	2.459	6.381	2.654	4.404	0.015
2.155	0.771	0.381	1.187	2.496	0.715	2.462	6.254	2.666	4.338	0.016
2.694	1.312	0.520	1.176	2.340	0.440	3.413	2.997	3.761	1.968	-0.011
2.694	1.316	0.519	1.182	2.342	0.440	3.417	2.999	3.765	1.969	-0.011
2.694	1.326	0.513	1.200	2.357	0.440	3.423	3.010	3.770	1.977	-0.011
2.694	1.341	0.503	1.217	2.381	0.440	3.419	3.032	3.767	1.991	-0.011
2.694	1.369	0.486	1.231	2.427	0.440	3.395	3.076	3.748	2.021	-0.012
2.694	1.474	0.507	1.157	2.377	0.495	3.359	3.056	3.709	2.116	-0.009
2.694	1.479	0.506	1.172	2.379	0.495	3.369	3.052	3.720	2.113	-0.009
2.694	1.485	0.505	1.193	2.384	0.495	3.383	3.049	3.737	2.111	-0.009
2.694	1.490	0.502	1.216	2.391	0.495	3.397	3.052	3.752	2.112	-0.009
2.694	1.499	0.495	1.240	2.409	0.495	3.406	3.064	3.761	2.118	-0.008
2.694	1.516	0.481	1.262	2.447	0.495	3.398	3.101	3.753	2.138	-0.008
2.694	1.582	0.446	1.273	2.559	0.495	3.348	3.220	3.716	2.225	-0.011
2.694	1.542	0.492	1.136	2.417	0.550	3.205	3.108	3.545	2.183	-0.007
2.694	1.558	0.491	1.149	2.421	0.550	3.223	3.108	3.566	2.190	-0.007
2.694	1.581	0.489	1.170	2.428	0.550	3.250	3.110	3.597	2.201	-0.006
2.694	1.608	0.487	1.194	2.437	0.550	3.281	3.113	3.632	2.215	-0.006
2.694	1.635	0.483	1.221	2.449	0.550	3.312	3.119	3.668	2.228	-0.005
2.694	1.659	0.478	1.251	2.464	0.550	3.337	3.128	3.697	2.242	-0.005
2.694	1.667	0.475	1.263	2.473	0.550	3.344	3.137	3.704	2.248	-0.004
2.694	1.677	0.469	1.278	2.492	0.550	3.348	3.153	3.708	2.260	-0.004
2.694	1.688	0.459	1.290	2.525	0.550	3.341	3.187	3.700	2.279	-0.003
2.694	1.712	0.440	1.295	2.588	0.550	3.313	3.256	3.675	2.323	-0.004
2.694	1.755	0.417	1.300	2.673	0.550	3.283	3.352	3.651	2.392	-0.006
2.694	1.800	0.390	1.305	2.789	0.550	3.236	3.480	3.608	2.478	-0.008
2.694	1.843	0.358	1.311	2.945	0.550	3.162	3.651	3.537	2.585	-0.011
2.694	1.883	0.304	1.308	3.282	0.550	3.004	4.023	3.362	2.796	-0.014
2.694	1.461	0.477	1.110	2.468	0.605	3.067	3.209	3.391	2.201	-0.003
2.694	1.467	0.477	1.116	2.470	0.605	3.072	3.208	3.396	2.203	-0.003
2.694	1.487	0.475	1.136	2.476	0.605	3.088	3.204	3.414	2.209	-0.003
2.694	1.507	0.472	1.159	2.484	0.605	3.102	3.204	3.433	2.217	-0.002
2.694	1.529	0.469	1.185	2.496	0.605	3.115	3.206	3.447	2.226	-0.002
2.694	1.553	0.464	1.213	2.514	0.605	3.121	3.214	3.456	2.238	-0.002
2.694	1.567	0.461	1.224	2.522	0.605	3.125	3.218	3.461	2.244	-0.002
2.694	1.587	0.457	1.240	2.534	0.605	3.131	3.223	3.468	2.254	-0.001
2.694	1.606	0.453	1.255	2.548	0.605	3.136	3.229	3.474	2.264	-0.001
2.694	1.624	0.450	1.268	2.558	0.605	3.139	3.236	3.479	2.273	-0.001
2.694	1.642	0.446	1.281	2.573	0.605	3.141	3.245	3.482	2.285	-0.001
2.694	1.664	0.441	1.293	2.591	0.605	3.145	3.260	3.487	2.302	-0.001
2.694	1.684	0.431	1.305	2.629	0.605	3.132	3.298	3.472	2.329	0.000
2.694	1.736	0.410	1.312	2.710	0.605	3.100	3.376	3.443	2.389	0.000
2.694	1.853	0.384	1.317	2.827	0.605	3.112	3.505	3.468	2.516	-0.002
2.694	1.962	0.351	1.321	2.994	0.605	3.107	3.703	3.471	2.683	-0.003
2.694	2.039	0.303	1.325	3.297	0.605	3.010	4.044	3.370	2.908	-0.009
2.694	1.177	0.467	1.097	2.505	0.660	2.816	3.772	3.111	2.494	0.004
2.694	1.189	0.467	1.106	2.512	0.660	2.827	3.758	3.123	2.491	0.004
2.694	1.245	0.463	1.131	2.524	0.660	2.867	3.692	3.171	2.471	0.005
2.694	1.314	0.458	1.160	2.543	0.660	2.912	3.616	3.225	2.448	0.005
2.694	1.391	0.451	1.189	2.567	0.660	2.956	3.548	3.276	2.427	0.005
2.694	1.424	0.447	1.201	2.579	0.660	2.971	3.525	3.295	2.422	0.005
2.694	1.463	0.443	1.217	2.595	0.660	2.988	3.503	3.316	2.418	0.005

Fixed Speed Performance Data

2.694	1.483	0.439	1.231	2.609	0.660	2.992	3.508	3.320	2.427	0.006
2.694	1.499	0.435	1.243	2.622	0.660	2.993	3.516	3.322	2.437	0.006
2.694	1.521	0.430	1.256	2.639	0.660	2.996	3.520	3.326	2.445	0.006
2.694	1.550	0.424	1.268	2.659	0.660	3.000	3.521	3.332	2.452	0.006
2.694	1.584	0.418	1.280	2.683	0.660	3.004	3.522	3.337	2.461	0.006
2.694	1.620	0.411	1.291	2.713	0.660	3.005	3.528	3.340	2.473	0.006
2.694	1.661	0.401	1.302	2.754	0.660	3.002	3.549	3.338	2.495	0.006
2.694	1.691	0.385	1.310	2.825	0.660	2.972	3.622	3.305	2.544	0.006
2.694	1.737	0.361	1.315	2.947	0.660	2.912	3.745	3.244	2.624	0.004
2.694	1.877	0.328	1.321	3.139	0.660	2.873	3.879	3.209	2.738	0.001
2.694	2.217	0.269	1.323	3.595	0.660	2.901	4.381	3.248	3.204	-0.005
3.233	1.313	0.517	1.240	2.616	0.440	3.614	3.334	4.010	2.091	-0.013
3.233	1.315	0.516	1.243	2.617	0.440	3.616	3.335	4.011	2.093	-0.013
3.233	1.328	0.509	1.261	2.638	0.440	3.620	3.351	4.016	2.104	-0.013
3.233	1.351	0.497	1.276	2.676	0.440	3.616	3.388	4.014	2.132	-0.014
3.233	1.390	0.476	1.288	2.748	0.440	3.590	3.464	3.998	2.190	-0.015
3.233	1.424	0.439	1.292	2.894	0.440	3.503	3.621	3.917	2.273	-0.015
3.233	1.319	0.371	1.282	3.231	0.440	3.266	4.096	3.624	2.374	-0.016
3.233	1.500	0.509	1.223	2.647	0.495	3.613	3.404	4.012	2.298	-0.013
3.233	1.503	0.508	1.234	2.648	0.495	3.620	3.399	4.020	2.295	-0.013
3.233	1.506	0.507	1.255	2.653	0.495	3.632	3.395	4.033	2.289	-0.013
3.233	1.510	0.503	1.277	2.663	0.495	3.641	3.399	4.044	2.289	-0.012
3.233	1.519	0.496	1.299	2.686	0.495	3.643	3.416	4.046	2.297	-0.012
3.233	1.541	0.480	1.317	2.739	0.495	3.625	3.467	4.031	2.327	-0.013
3.233	1.634	0.494	1.202	2.695	0.550	3.547	3.490	3.940	2.445	-0.010
3.233	1.641	0.493	1.216	2.699	0.550	3.557	3.488	3.952	2.445	-0.010
3.233	1.652	0.491	1.237	2.706	0.550	3.574	3.487	3.971	2.447	-0.010
3.233	1.663	0.488	1.260	2.715	0.550	3.593	3.487	3.993	2.449	-0.009
3.233	1.676	0.485	1.287	2.726	0.550	3.611	3.488	4.014	2.451	-0.009
3.233	1.685	0.479	1.315	2.748	0.550	3.619	3.503	4.025	2.459	-0.009
3.233	1.689	0.475	1.325	2.764	0.550	3.617	3.518	4.022	2.466	-0.008
3.233	1.697	0.464	1.337	2.806	0.550	3.601	3.559	4.007	2.487	-0.008
3.233	1.726	0.443	1.342	2.890	0.550	3.564	3.652	3.977	2.548	-0.010
3.233	1.759	0.423	1.346	2.976	0.550	3.530	3.747	3.948	2.614	-0.012
3.233	1.792	0.400	1.351	3.087	0.550	3.479	3.870	3.904	2.694	-0.014
3.233	1.827	0.374	1.354	3.229	0.550	3.412	4.023	3.840	2.790	-0.016
3.233	1.846	0.351	1.357	3.378	0.550	3.335	4.187	3.763	2.884	-0.018
3.233	1.573	0.479	1.175	2.748	0.605	3.331	3.542	3.703	2.423	-0.008
3.233	1.575	0.479	1.178	2.750	0.605	3.333	3.542	3.705	2.424	-0.008
3.233	1.588	0.477	1.196	2.756	0.605	3.343	3.542	3.717	2.428	-0.008
3.233	1.603	0.475	1.218	2.765	0.605	3.353	3.541	3.729	2.433	-0.008
3.233	1.621	0.472	1.243	2.777	0.605	3.363	3.543	3.741	2.440	-0.008
3.233	1.645	0.468	1.271	2.794	0.605	3.374	3.548	3.756	2.452	-0.007
3.233	1.656	0.466	1.283	2.801	0.605	3.378	3.551	3.761	2.457	-0.007
3.233	1.673	0.463	1.298	2.812	0.605	3.386	3.556	3.771	2.467	-0.007
3.233	1.694	0.460	1.313	2.823	0.605	3.399	3.564	3.787	2.482	-0.007
3.233	1.717	0.457	1.326	2.834	0.605	3.416	3.575	3.807	2.501	-0.006
3.233	1.741	0.454	1.338	2.850	0.605	3.433	3.592	3.826	2.524	-0.006
3.233	1.770	0.446	1.348	2.881	0.605	3.445	3.628	3.840	2.560	-0.005
3.233	1.820	0.430	1.355	2.952	0.605	3.450	3.713	3.852	2.635	-0.005
3.233	1.880	0.408	1.360	3.058	0.605	3.442	3.839	3.852	2.739	-0.007
3.233	1.936	0.379	1.365	3.210	0.605	3.409	4.016	3.824	2.868	-0.009
3.233	1.988	0.341	1.370	3.449	0.605	3.323	4.284	3.741	3.040	-0.014
3.233	1.553	0.463	1.150	2.816	0.660	3.222	3.641	3.592	2.467	-0.002
3.233	1.567	0.461	1.165	2.822	0.660	3.236	3.641	3.608	2.474	-0.002
3.233	1.589	0.460	1.186	2.830	0.660	3.257	3.640	3.631	2.485	-0.002
3.233	1.616	0.457	1.211	2.842	0.660	3.278	3.643	3.656	2.500	-0.002
3.233	1.648	0.453	1.237	2.859	0.660	3.299	3.651	3.682	2.520	-0.002
3.233	1.661	0.450	1.248	2.868	0.660	3.305	3.656	3.689	2.529	-0.002
3.233	1.679	0.447	1.263	2.881	0.660	3.314	3.664	3.699	2.541	-0.002
3.233	1.693	0.444	1.277	2.894	0.660	3.316	3.673	3.703	2.551	-0.002
3.233	1.705	0.441	1.289	2.907	0.660	3.317	3.681	3.705	2.560	-0.002
3.233	1.719	0.438	1.301	2.921	0.660	3.318	3.692	3.708	2.572	-0.001
3.233	1.735	0.434	1.314	2.937	0.660	3.320	3.704	3.709	2.585	-0.001
3.233	1.752	0.430	1.326	2.955	0.660	3.320	3.719	3.711	2.600	-0.001
3.233	1.771	0.425	1.339	2.978	0.660	3.320	3.740	3.710	2.620	-0.001
3.233	1.791	0.418	1.349	3.015	0.660	3.313	3.777	3.702	2.649	-0.001
3.233	1.811	0.403	1.358	3.088	0.660	3.276	3.853	3.661	2.697	-0.002
3.233	1.852	0.379	1.365	3.215	0.660	3.217	3.987	3.602	2.786	-0.004

Fixed Speed Performance Data

3.233	2.009	0.344	1.370	3.442	0.660	3.216	4.255	3.617	3.034	-0.007
3.233	2.148	0.302	1.374	3.776	0.660	3.189	4.655	3.594	3.353	-0.011

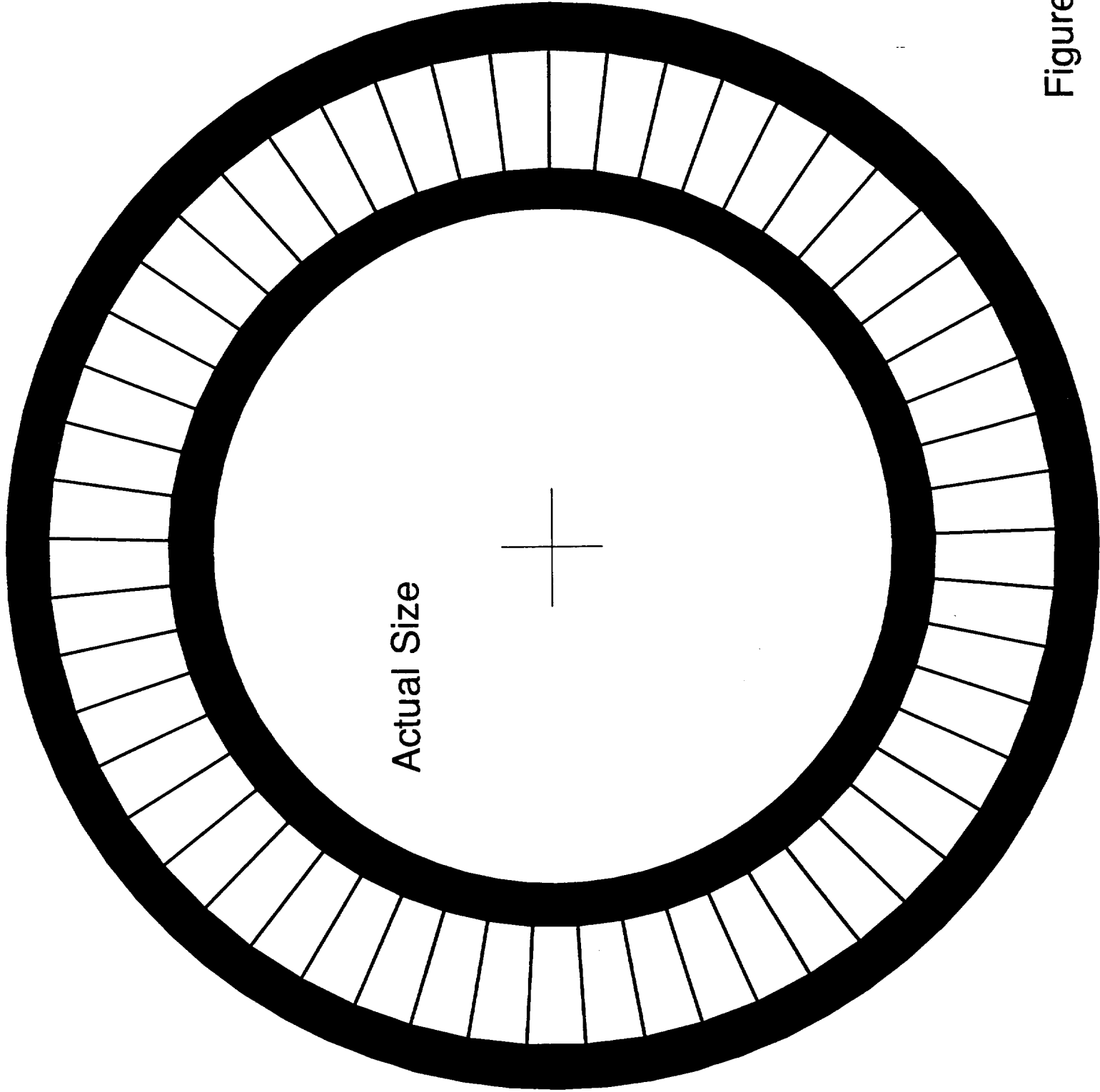


Figure 1

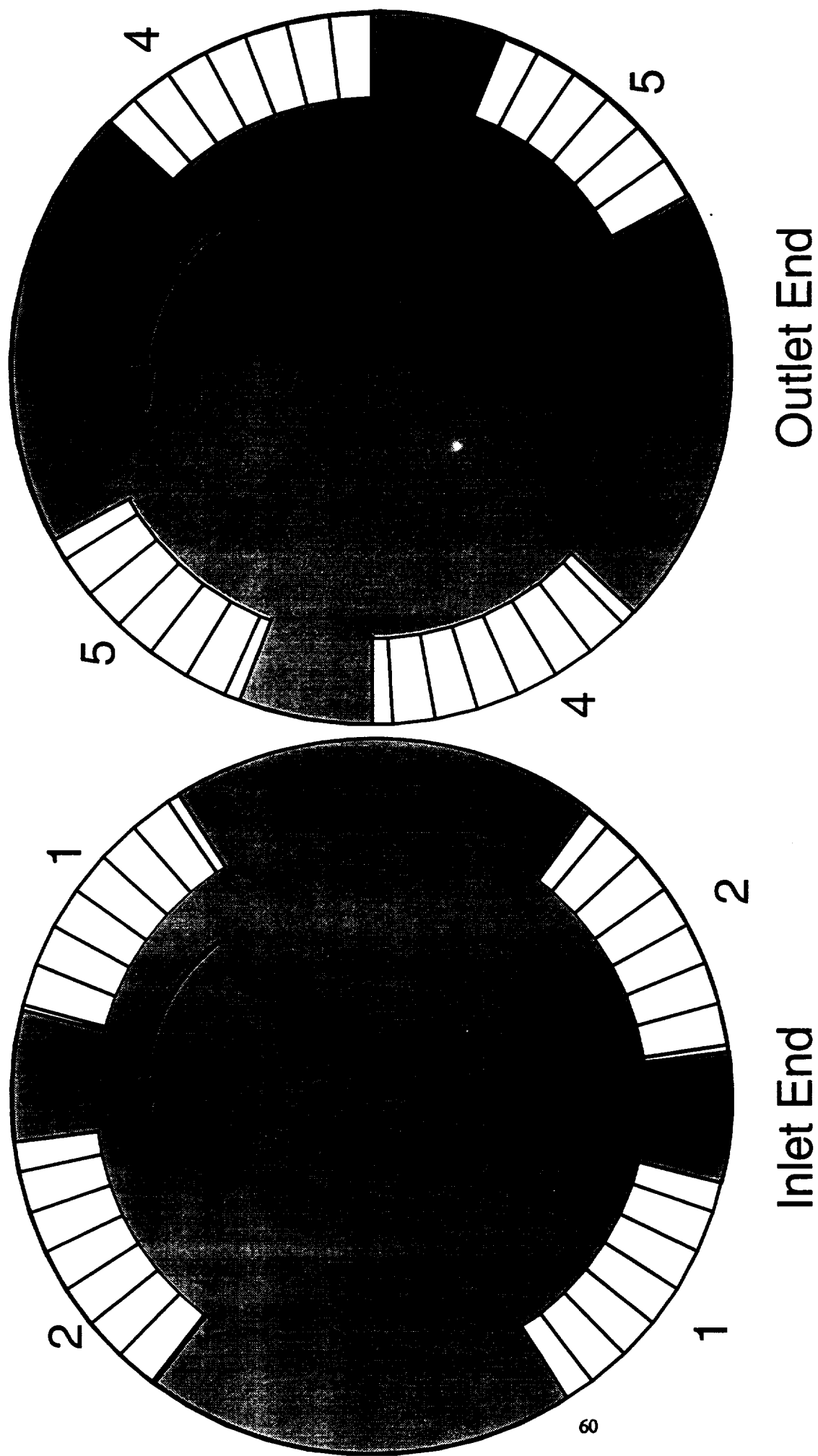


Figure 2

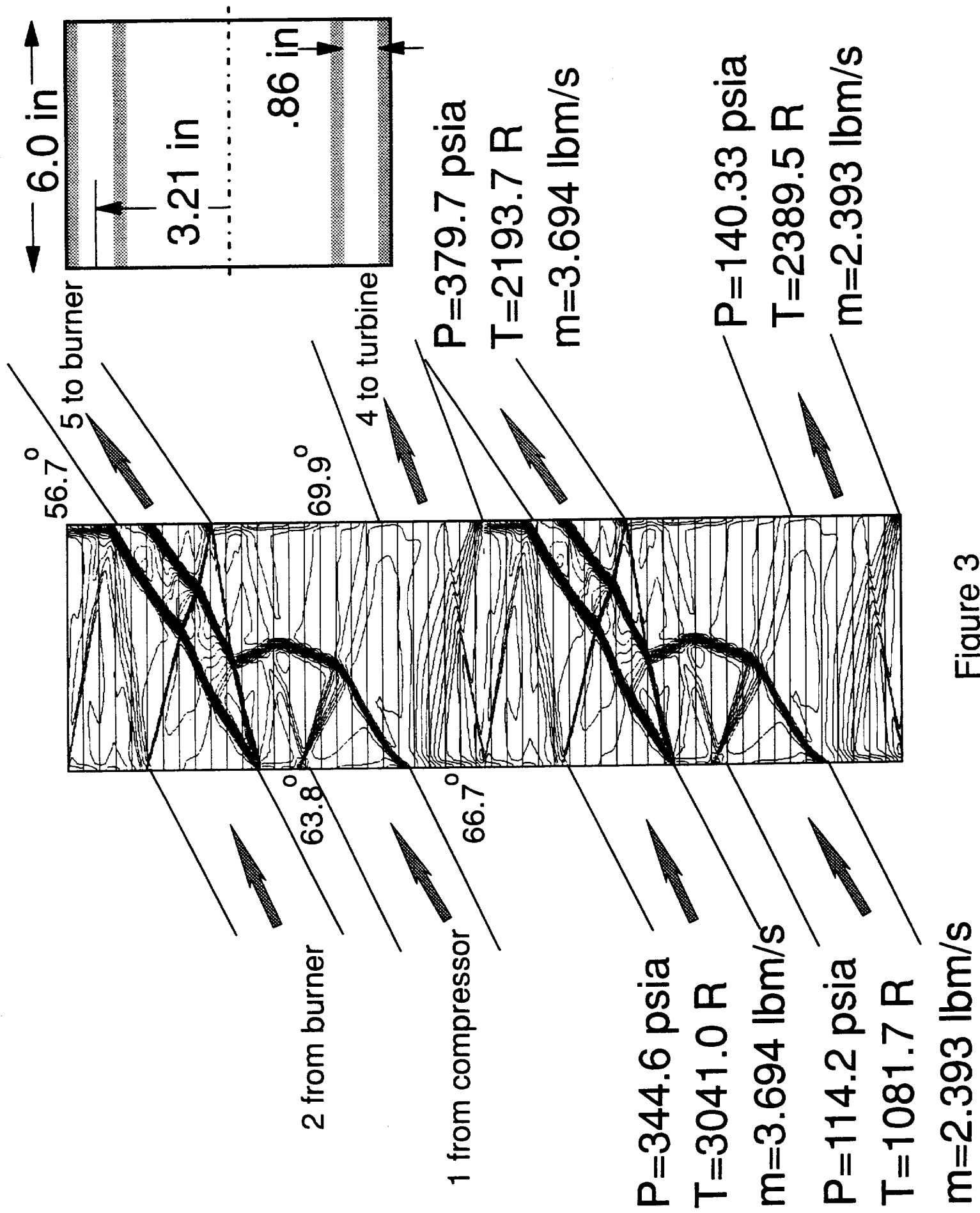


Figure 3

Allison 250 Rotor

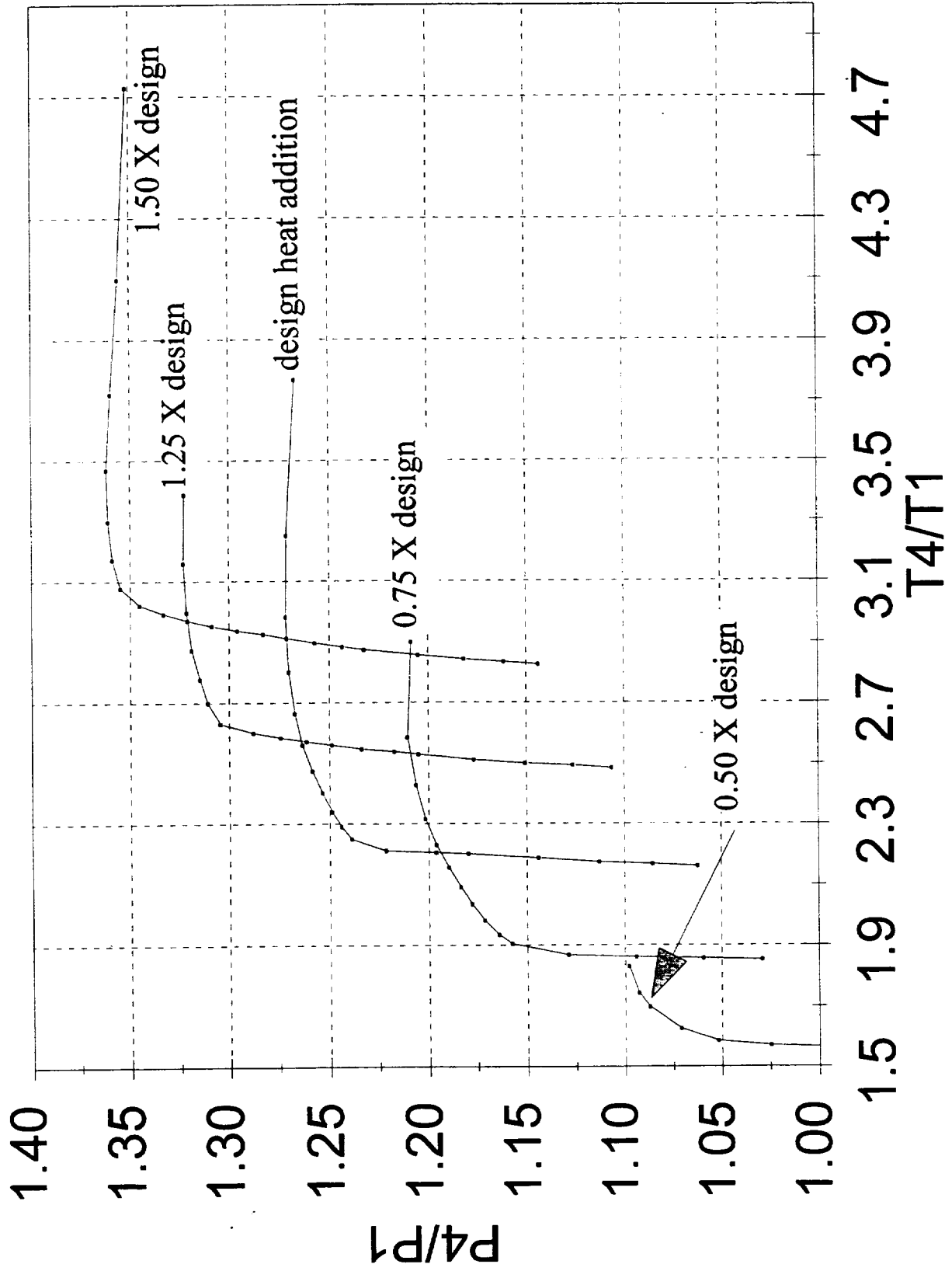


Figure 4

Allison 250 Rotor

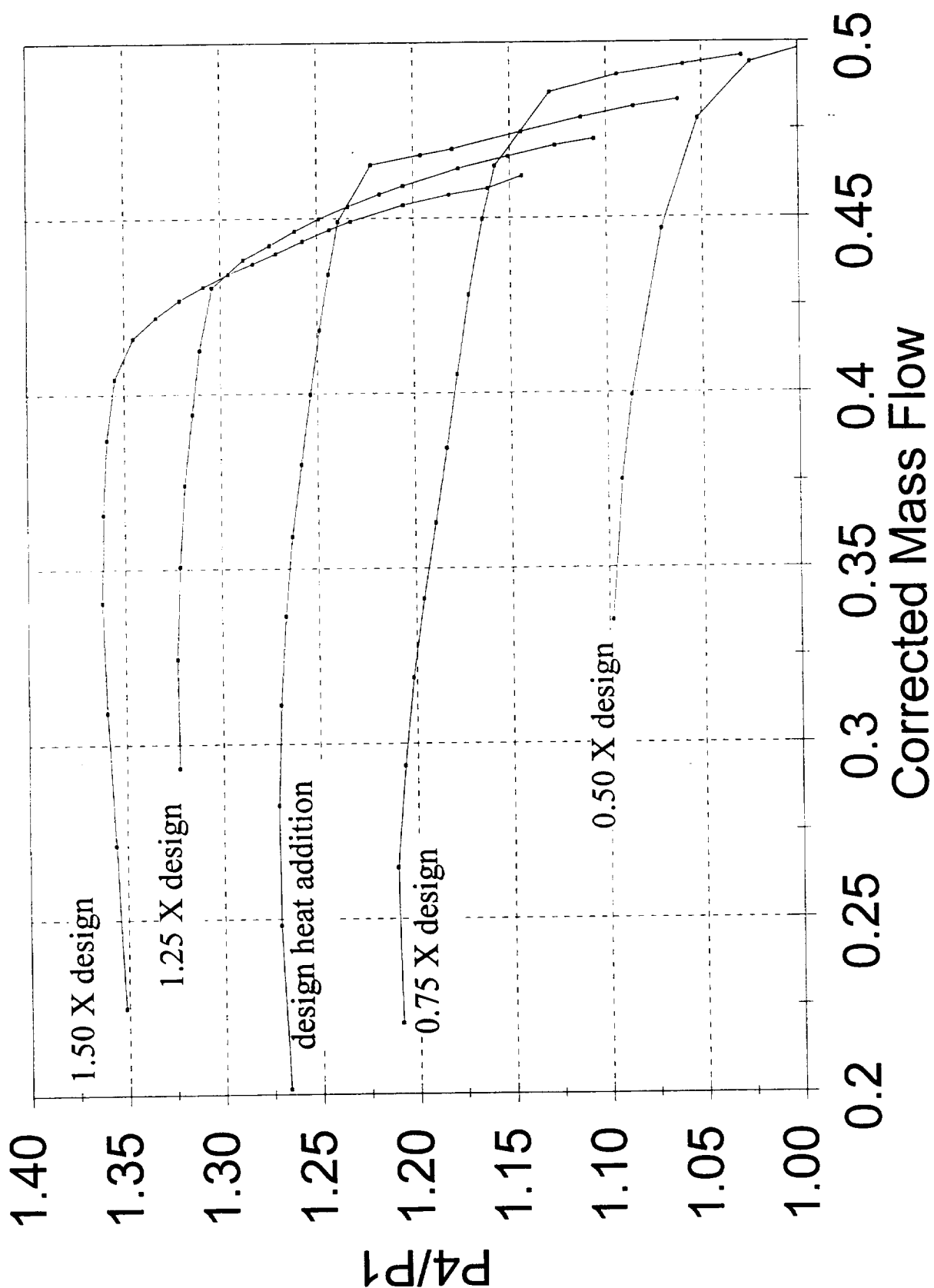


Figure 5

Allison 250 Rotor

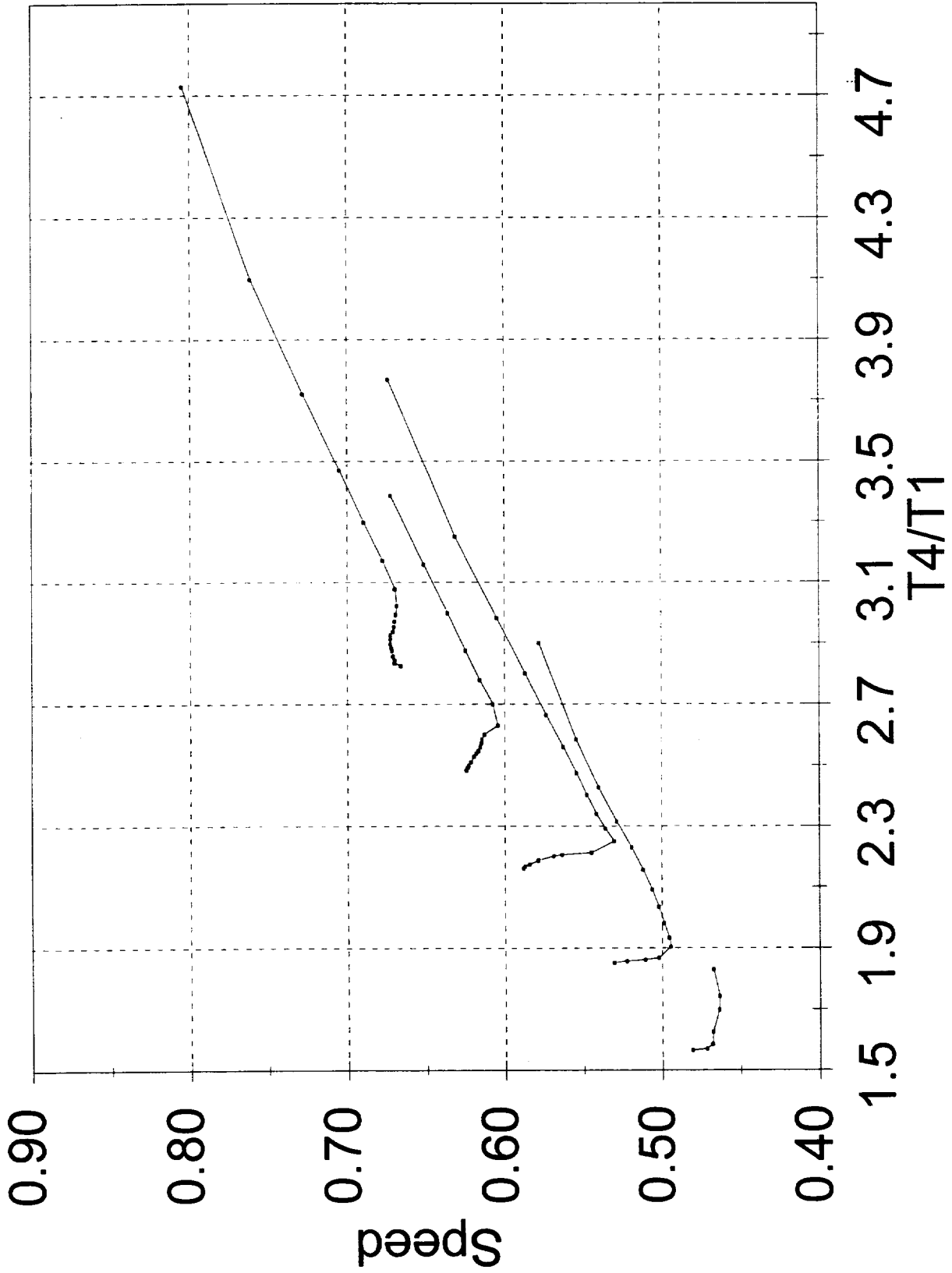


Figure 6

Allison 250 Rotor Design Q

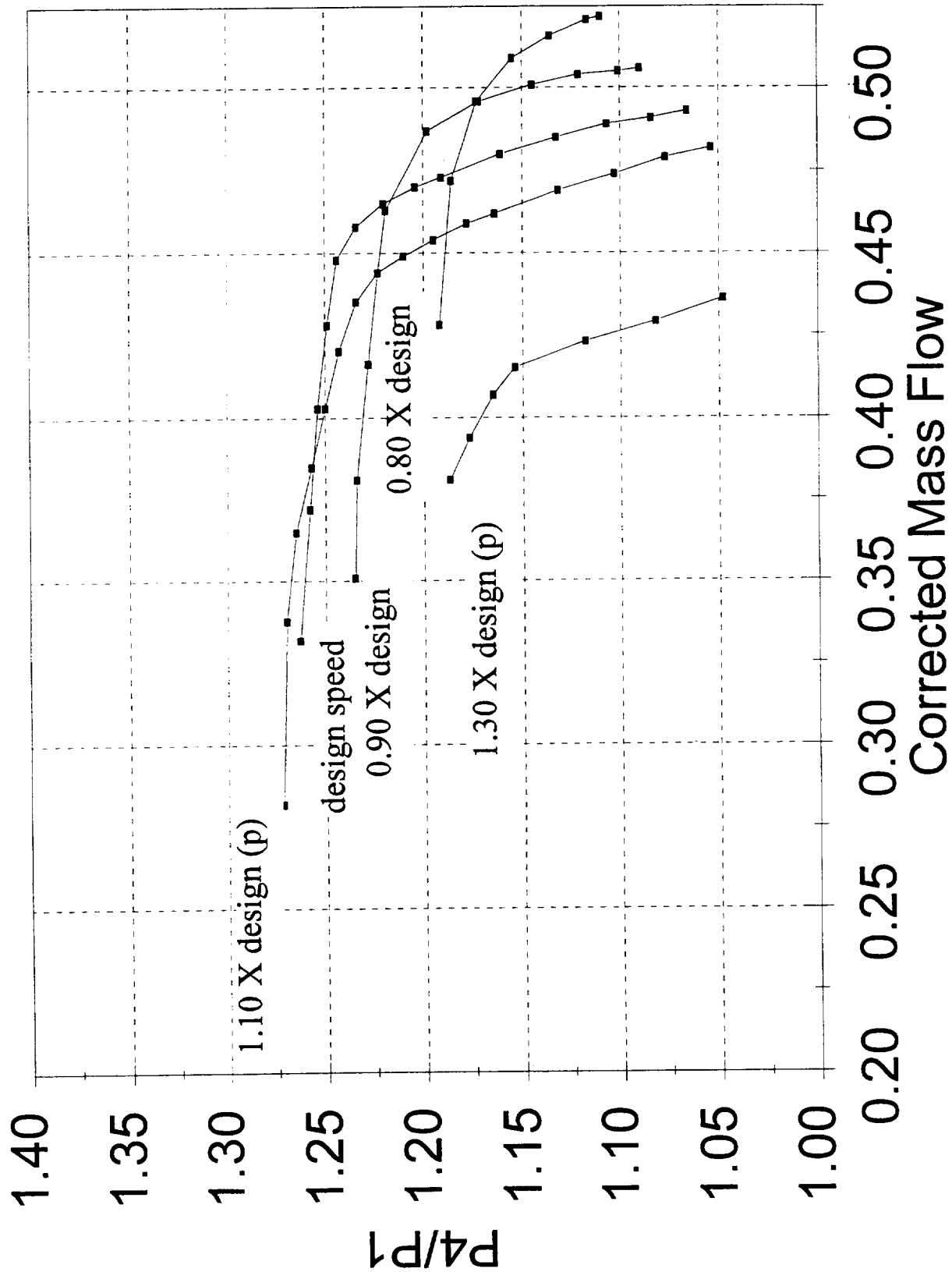


Figure 7

Allison 250 Rotor 1.25 X Design Q

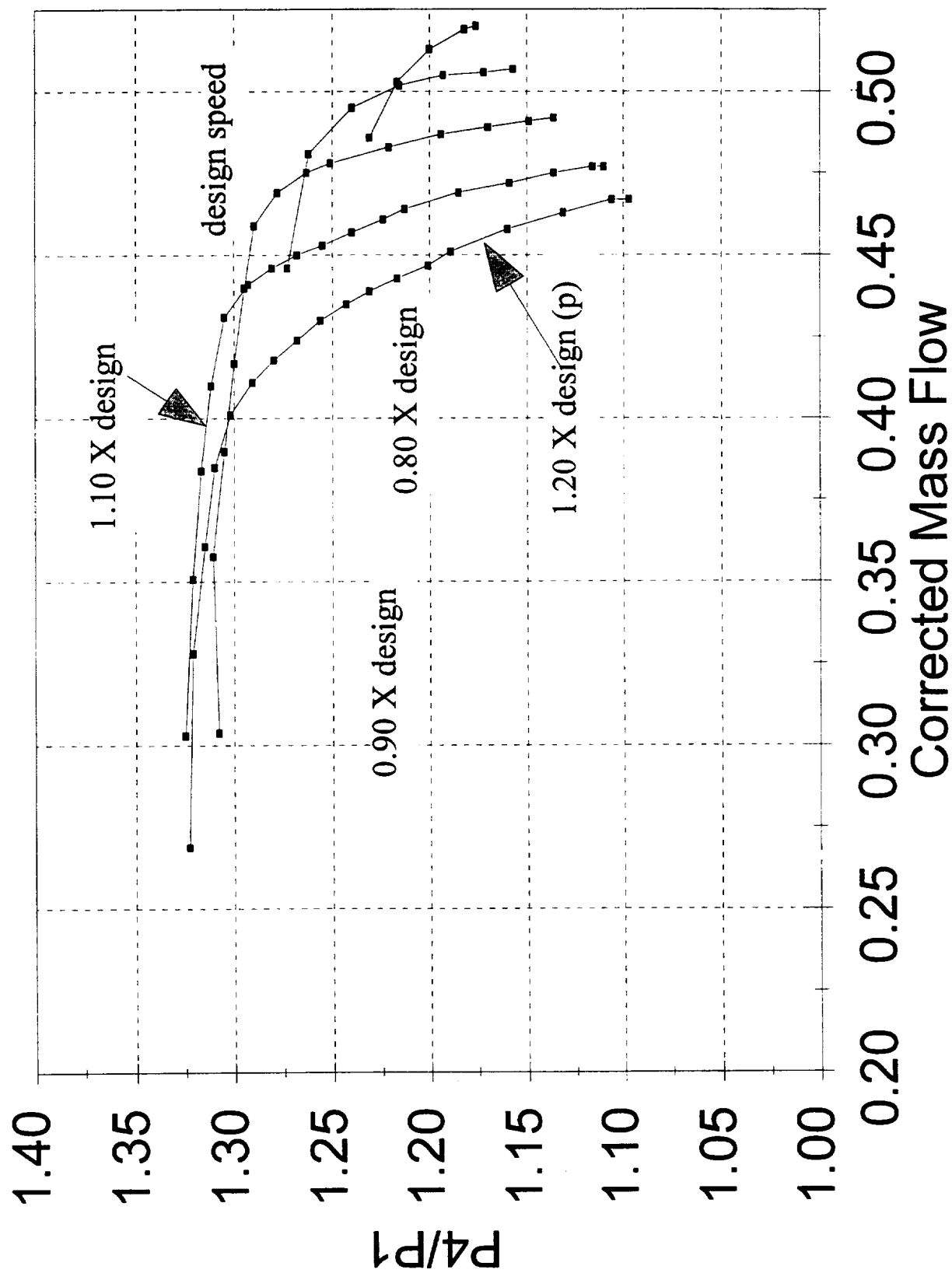


Figure 8

Allison 250 Rotor 1.50 X Design Q

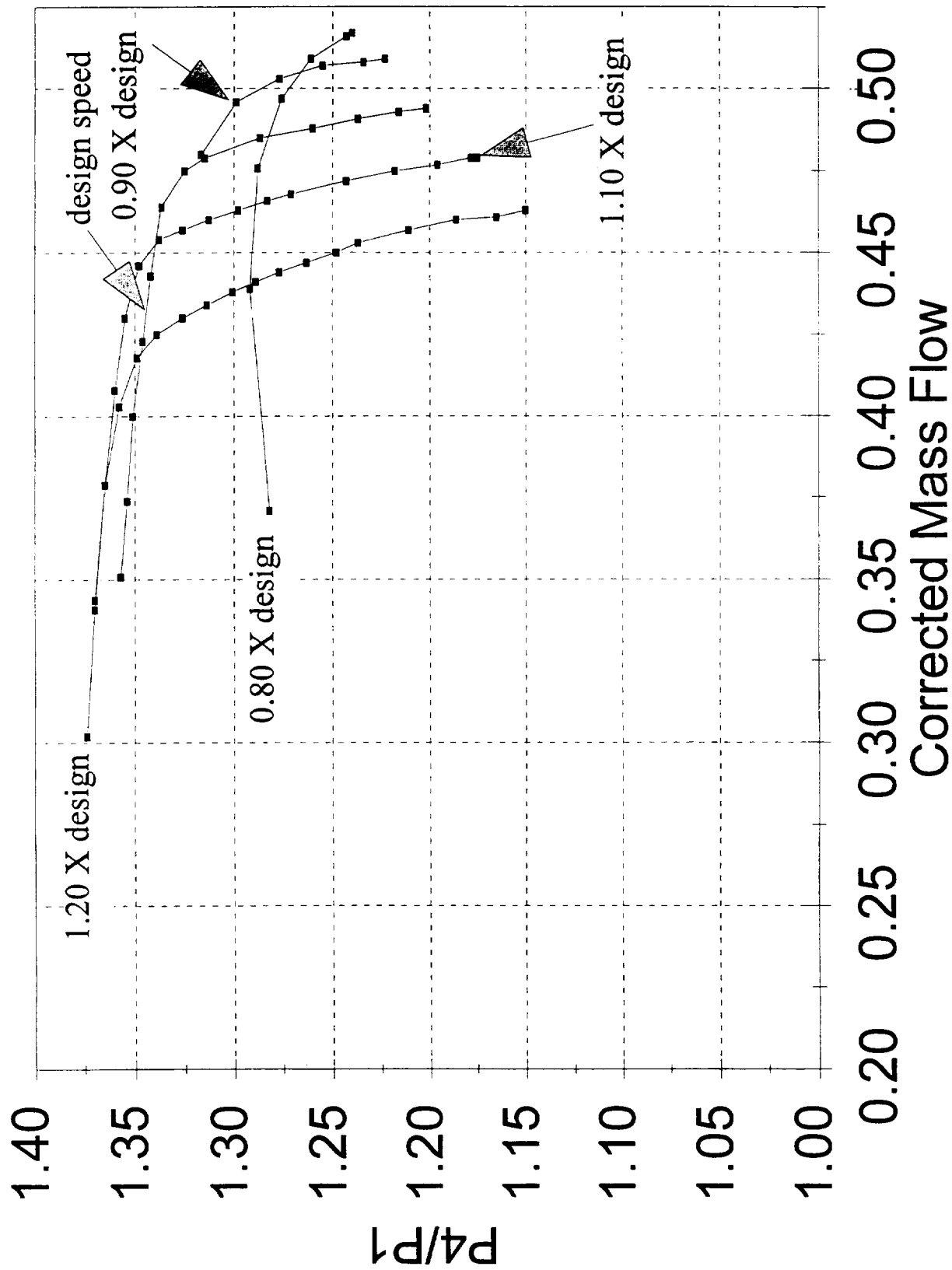


Figure 9

Allison 250 Rotor 0.75 X Design Q

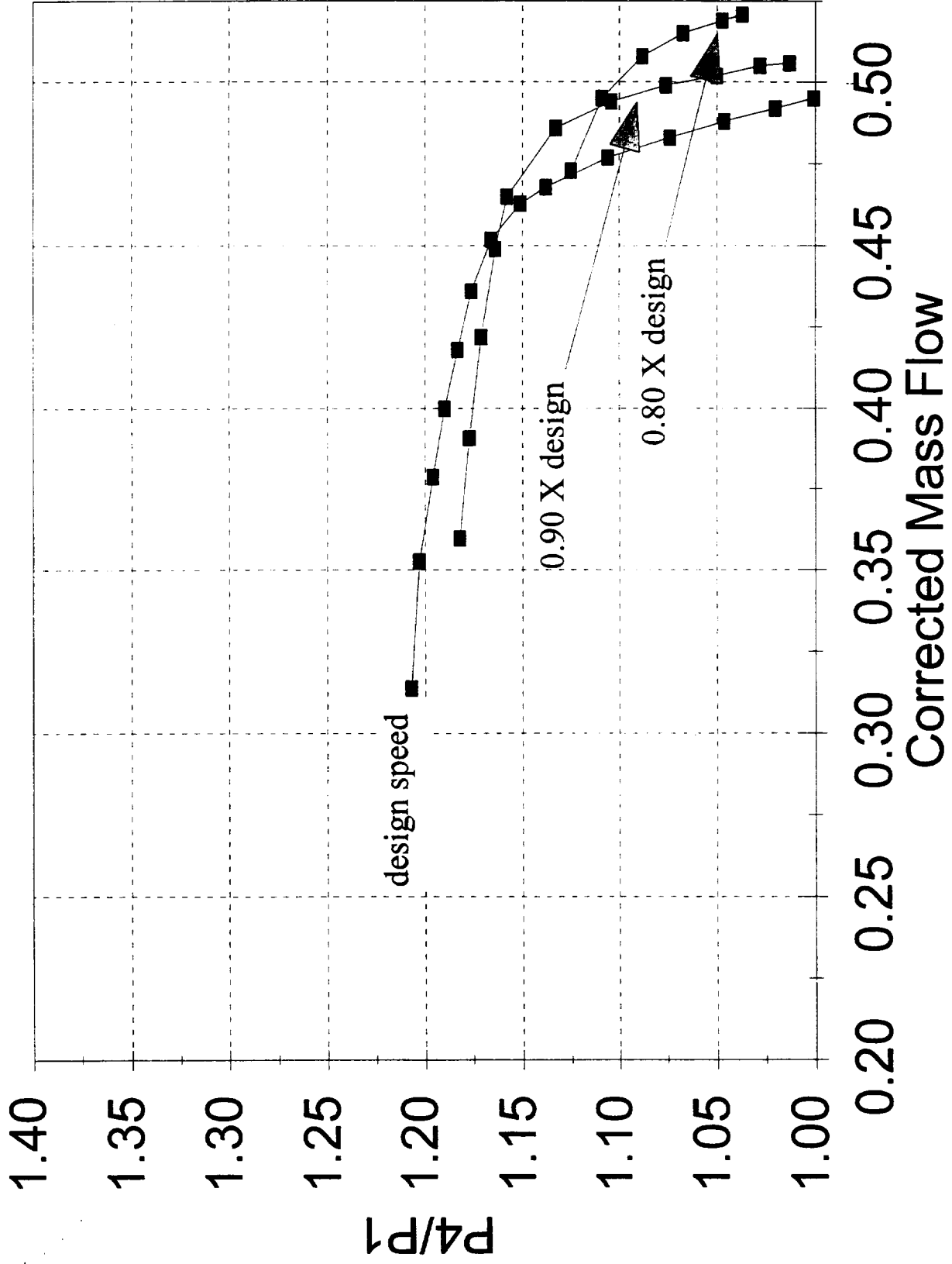


Figure 10

REPORT DOCUMENTATION PAGE			Form Approved OMB No. 0704-0188	
Public reporting burden for this collection of information is estimated to average 1 hour per response, including the time for reviewing instructions, searching existing data sources, gathering and maintaining the data needed, and completing and reviewing the collection of information. Send comments regarding this burden estimate or any other aspect of this collection of information, including suggestions for reducing this burden, to Washington Headquarters Services, Directorate for Information Operations and Reports, 1215 Jefferson Davis Highway, Suite 1204, Arlington, VA 22202-4302, and to the Office of Management and Budget, Paperwork Reduction Project (0704-0188), Washington, DC 20503.				
1. AGENCY USE ONLY (Leave blank)		2. REPORT DATE June 1996		3. REPORT TYPE AND DATES COVERED Final Contractor Report
4. TITLE AND SUBTITLE Wave Rotor Demonstrator Engine Assessment			5. FUNDING NUMBERS WU-505-62-10 C-NAS3-25950	
6. AUTHOR(S) Philip H. Snyder				
7. PERFORMING ORGANIZATION NAME(S) AND ADDRESS(ES) Allison Engine Company, Inc. P.O. Box 420 Indianapolis, Indiana			8. PERFORMING ORGANIZATION REPORT NUMBER E-10307	
9. SPONSORING/MONITORING AGENCY NAME(S) AND ADDRESS(ES) National Aeronautics and Space Administration Lewis Research Center Cleveland, Ohio 44135-3191			10. SPONSORING/MONITORING AGENCY REPORT NUMBER NASA CR-198496	
11. SUPPLEMENTARY NOTES Project Manager, Gary J. Skoch, Vehicle Technology Center, U.S. Army Research Laboratory, NASA Lewis Research Center, organization code 0300, (216) 433-3396.				
12a. DISTRIBUTION/AVAILABILITY STATEMENT Unclassified - Unlimited Subject Category 07 This publication is available from the NASA Center for AeroSpace Information, (301) 621-0390.			12b. DISTRIBUTION CODE	
13. ABSTRACT (Maximum 200 words) The objective of the program was to determine a wave rotor demonstrator engine concept using the Allison 250 series engine. The results of the NASA LeRC wave rotor effort were used as a basis for the wave rotor design. A wave rotor topped gas turbine engine was identified which incorporates five basic requirements of a successful demonstrator engine. Predicted performance maps of the wave rotor cycle were used along with maps of existing gas turbine hardware in a design point study. The effects of wave rotor topping on the engine cycle and the subsequent need to rematch compressor and turbine sections in the topped engine were addressed. Comparison of performance of the resulting engine is made on the basis of wave rotor topped engine versus an appropriate baseline engine using common shaft compressor hardware. The topped engine design clearly demonstrates an impressive improvement in shaft horsepower (+11.4%) and SFC (-22%). Off design part power engine performance for the wave rotor topped engine was similarly improved including that at engine idle conditions. Operation of the engine at off design was closely examined with wave rotor operation at less than design burner outlet temperatures and rotor speeds. Challenges identified in the development of a demonstrator engine are discussed. A preliminary design was made of the demonstrator engine including wave rotor to engine transition ducts. Program cost and schedule for a wave rotor demonstrator engine fabrication and test program were developed.				
14. SUBJECT TERMS Wave rotor; Compressor; Turbine			15. NUMBER OF PAGES 72	
			16. PRICE CODE A04	
17. SECURITY CLASSIFICATION OF REPORT Unclassified	18. SECURITY CLASSIFICATION OF THIS PAGE Unclassified	19. SECURITY CLASSIFICATION OF ABSTRACT Unclassified	20. LIMITATION OF ABSTRACT	

**National Aeronautics and
Space Administration
Lewis Research Center
21000 Brookpark Rd.
Cleveland, OH 44135-3191**

**Official Business
Penalty for Private Use \$300**

POSTMASTER: If Undeliverable — Do Not Return